Provided for non-commercial research and education use.
Not for reproduction, distribution or commercial use.

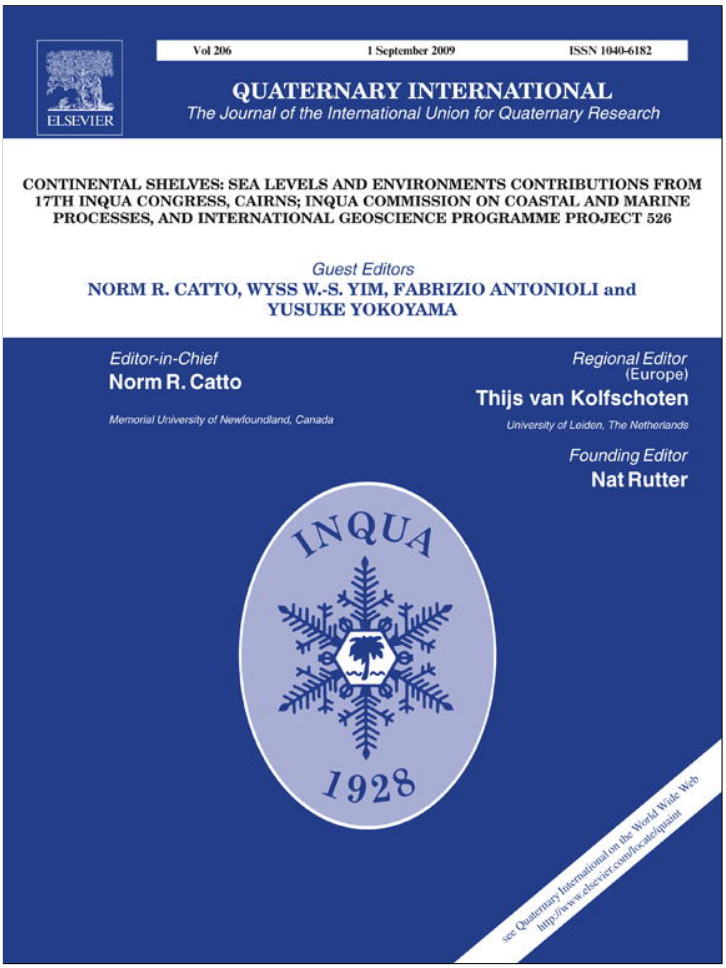

This article appeared in a journal published by Elsevier. The attached copy is furnished to the author for internal non-commercial research and education use, including for instruction at the authors institution and sharing with colleagues.

Other uses, including reproduction and distribution, or selling or licensing copies, or posting to personal, institutional or third party websites are prohibited.

In most cases authors are permitted to post their version of the article (e.g. in Word or Tex form) to their personal website or institutional repository. Authors requiring further information regarding Elsevier's archiving and manuscript policies are encouraged to visit:

http://www.elsevier.com/copyright

Author's personal copy

Quaternary International 206 (2009) 102–133

Contents lists available at ScienceDirect

Quaternary International

journal homepage: www.elsevier.com/locate/quaint

Holocene relative sea-level changes and vertical movements along the Italian and Istrian coastlines

F. Antonioli [a,*], L. Ferranti [b], A. Fontana [c], A. Amorosi [d], A. Bondesan [c], C. Braitenberg [e], A. Dutton [f], G. Fontolan [g], S. Furlani [g], K. Lambeck [f], G. Mastronuzzi [h], C. Monaco [i], G. Spada [j], P. Stocchi [j]

[a] *ENEA, cre Casaccia, via Anguillarese 301, 00123 Roma, Italy*
[b] *Dipartimento di Scienze della Terra, Università Federico II, Napoli, Italy*
[c] *Dipartimento di Geografia, Università degli Studi di Padova, Padova, Italy*
[d] *Dipartimento di Scienze della Terra e Geologico-Ambientali, Università di Bologna, Bologna, Italy*
[e] *Dipartimento di Scienze della Terra, Universita' di Trieste, Trieste, Italy*
[f] *Research School of Earth Sciences, Australian National University, Canberra ACT 0200, Australia*
[g] *Dipartimento di Scienze Geologiche Ambientali e Marine, Università di Trieste, Trieste, Italy*
[h] *Dipartimento di Geologia e Geofisica Università degli Studi "Aldo Moro", Bari, Italy*
[i] *Dipartimento di Scienze della Terra, Università di Catania, Catania, Italy*
[j] *Università degli Studi di Urbino "Carlo Bo", Urbino, Italy*

ARTICLE INFO

Article history:
Available online 11 December 2008

ABSTRACT

Published and new data exist for relative sea-level change for 105 locations (127 samples) during the late Holocene, along the Italian (and Istrian) coasts. These data, compared with predictions (derived from two different models associated with the last glacial cycle) allowed the calculation of the tectonic vertical movements. They are based on precise measures of geomorphological and archaeological markers between 0.4 and 12.6 ka cal. BP, sampled at elevations between +7 and −51 m. In order to decipher the broad pattern of Holocene tectonic vertical movements along the Italian coastline, these data were compared with predicted sea-level curves using the most recent models published for the Mediterranean sea. Tectonic rates varied from −4.85 mm/a, in a core at Sybaris, to 5 mm/a, in the volcanic areas of Pozzuoli and Pantelleria. New MIS 5.5 (125 ka) data, mostly from the Venetian plain, are reported. In particular the depth of the base of MIS 5.5 paralic deposits found in four cores near Venezia provides a mean subsidence of 0.62 mm/a. New, precise mass spectrometer U-Th analyses on *Cladocora* layers from the bottom of a long core (named ENEA), indicate older ages (195.7 ± 1.6 and 161.2 ± 1.2 ka, respectively), relative to the published MIS 5.5 ages, which were based on alpha-counting U-Th data.
Instrumental data obtained from tide gauges and repeated levelling measurements from the NE Adriatic and Sicily are also considered. These methods have one great advantage with respect to continuous GPS measurements and the satellite altimetric observations, in that a much greater time span is available. Although the altimetric measurements are available for 16 years, and the GPS for less than a decade, repeated levelling lines cover up to 50 years and tide gauge observations in some cases to 100 years or more. The greater time span allows for more stable differential rate estimates. The repeated levelling shows that the plain east of Mestre is subsiding (to −4 mm/a). The Messina tidal gauge demonstrates a total coseismic and post-seismic subsidence of 77 cm associated with the event of 1908, the post-seismic phase lasting for at least 13 years. The Reggio Calabria tidal station points to an uplift of this station relative to Palermo in the order of 1–2 mm/a.

© 2008 Elsevier Ltd and INQUA. All rights reserved.

1. Introduction

Sea-level change is the sum of eustatic, glacio-hydro-isostatic, and tectonic factors. The first is global and time-dependent, while the latter two vary with location, including sediment load, compaction and anthropogenic motions. Lambeck et al. (2004a) defined "tectonic factors" to include all movements that are not eustatic and isostatic. In Italy, the glacio-hydro-isostatic component of post-glacial sea-level rise has been recently predicted and compared with field data at several coastal sites (Lambeck et al., 2004a; Antonioli et al., 2007), and thus a framework for calculating vertical tectonic motions is available (Fig. 1). Italy is located in the

* Corresponding author. Tel.: +390630483955.
E-mail address: fabrizio.antonioli@enea.it (F. Antonioli).

1040-6182/$ – see front matter © 2008 Elsevier Ltd and INQUA. All rights reserved.
doi:10.1016/j.quaint.2008.11.008

Author's personal copy

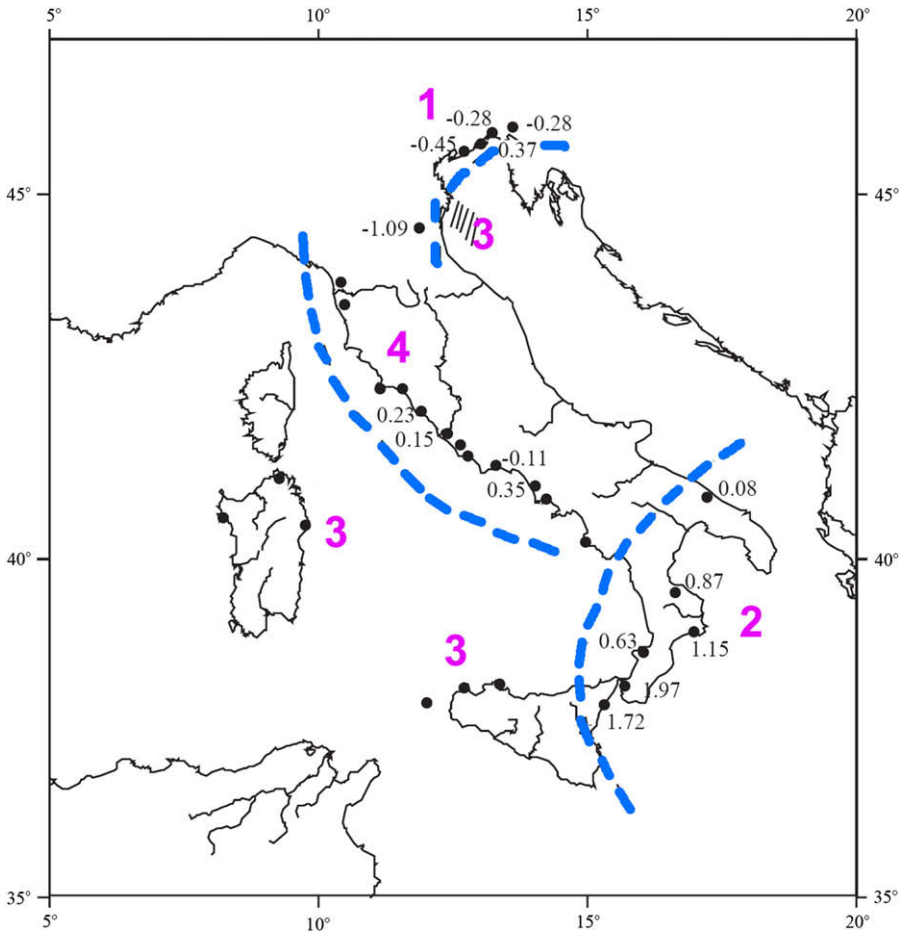

Fig. 1. Holocene tectonic movements along the Italian coastline (redrawn from Lambeck et al., 2004a). 1) Subsiding area with rates between 0.28 and 1.09 mm/a. 2) Uplifting area, with rates between 0.08 and 1.97 mm/a. 3) predominantly tectonic stability with local areas of subsidence or uplift. 4) Tectonic stability.

central Mediterranean Sea within the diffuse plate boundary between Europe and Africa, and active tectonic displacements are indicated by seismicity and geodetic velocities (Oldow et al., 2002; Pondrelli et al., 2004; Serpelloni et al., 2005; Ferranti et al., 2008a) (Fig. 2).

Lambeck et al. (2004a) published a comprehensive review of the last ~12 ka relative sea-level changes in Italy and used the elevation of the MIS 5.5 (Late Pleistocene) marker, aged at ~125 ka, as a benchmark to assess tectonic stability at individual coastal sites. Most of the sites investigated by Lambeck et al. (2004a) were located along tectonically stable coasts (Fig. 1).

The Holocene sites taken in consideration by Lambeck et al. (2004a) numbered 27. This paper compares more than 100 sites in stable, uplifting and subsiding areas with predicted sea level, covering the entire Italian coast. At sites where the MIS 5.5 shoreline occurs above or below its eustatic position (between 6 and 8 m a.s.l.), and where recent tectonic motion was independently identified, it was assumed that average rates of vertical crustal displacements for the past 125 ka and for the Holocene were comparable.

A recently published review of the MIS 5.5 marker along the whole coast of Italy (Ferranti et al., 2006) has shown dramatic differences in tectonic behaviour within adjacent coastline segments as a result of dominant tectonic signal over the long-term temporal scale (Fig. 3). Although in some cases the long- and short-term rates were comparable, in other sites the two rates had different magnitudes (Ferranti et al., 2006). Detailed studies in key sectors of the Italian coastline, and specifically in the rapidly uplifting Calabrian arc, found higher Holocene tectonic displacement rates (Antonioli et al., 2006), a pattern attributed to clustered seismic slip (Ferranti et al., 2007).

With the aim of deciphering the broad pattern of Holocene tectonic movements along the Italian coastline, this paper combines published and new data from materials that can be reliably linked to the coeval sea level. Then these data are compared with predicted sea-level curves using the model published by Lambeck et al. (2004a). Predictions are based on a recently published open-source numerical code that has been suitably adapted for Holocene relative sea-level computations in the Mediterranean (Spada and Stocchi, 2007). This approach allows to either document coastal stability or calculate rates of active tectonic movements. Knowledge of the relation between the Holocene and the long-term (125 ka BP) rates of tectonic movement is extended using the Ferranti et al. (2006) data set on the long-term history supplemented by new radiometric ages. Finally, understanding of the displacement pattern is extended into modern times by comparing the geologic rates with tide gauge and levelling data in a subsiding area (Trieste, in the northern Adriatic Sea) *vs* an uplifting coastal area (the Messina Straits, in the Calabrian arc).

The results achieved in this work refine and supplement the Lambeck et al. (2004a) investigation of the relative sea-level changes in Italy, providing a comprehensive picture of the relative sea-level history at sites significantly affected by tectonic displacements. The implemented database is of timely importance in light of the relevant flooding risk quoted by the 2007 IPCC report for the Mediterranean Sea. Any future planning regarding the Italian coastal area during the next century must rely on detailed estimation of relative sea-level changes.

Author's personal copy

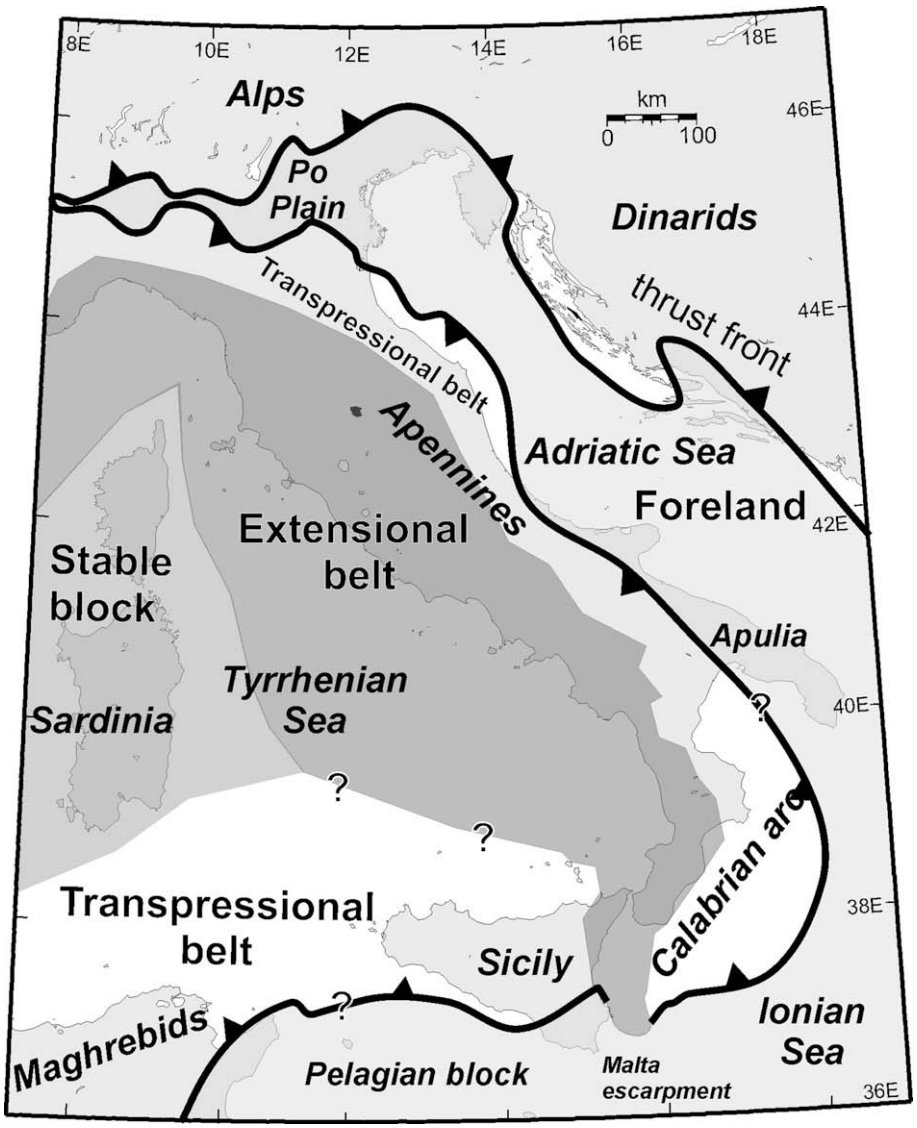

Fig. 2. Major tectonic domains of Italy: Adriatic foreland, contractional and extensional belts, and stable blocks, indicated by light grey, white, dark grey and medium grey (modified after Montone et al., 2004 and Ferranti et al., in press).

2. Tectonic setting

The Mediterranean region marks the broad collisional boundary between the African and the Eurasian plates. The geodynamic characteristics of this region are driven by lithospheric blocks showing different structural and kinematic interaction, including subduction, back-arc spreading, and fold-and-thrust belt development (Faccenna et al., 2001). The active dynamics of Italy within the central Mediterranean region is shown by the distribution of seismicity, which outlines the major deformation belts of the Alps, the Apennines and the Sicily Maghrebids (Fig. 2; Doglioni, 1991). The Adriatic Sea and surrounding promontories represent the remaining part of the Adriatic lithospheric block caught between Europe and Africa and serve as the foreland domain of the Alpine, Dinarid and Apenninic thrust belts (Oldow et al., 2002 and references therein). The Tyrrhenian back-arc basin opened behind the Apennines in the wake of the retreating Adriatic–Ionian slab and is partially floored by oceanic crust (Malinverno and Ryan, 1986; Doglioni, 1991).

Investigation focused on eight areas of the Italian coastline spanning specific tectonic domains (Fig. 4). Recent tectonic and sedimentary features of the individual sectors are summarized below.

2.1. The Northern Adriatic coast

The northernmost sector of the Adriatic Sea (Area 1 of Fig. 4) straddles the transition from the Adriatic foreland and Dinarid belt in Slovenija and Croatia to the east, to the Southern Alps and northern Apennines foredeep basin in the west (Fig. 2; Carminati et al., 2003). Active shortening and transpression occur in the Alps and in the frontal sector of the Apennines, as well as in the Dinaric belt to the east, as documented by seismicity and GPS observations (Pondrelli et al., 2004; D'Agostino and Selvaggi, 2004). A thick pre-orogenic carbonate succession crops out in Histria and Trieste, and is covered by Early-Mid Eocene turbidite flysch deposits (Cucchi et al., 1989; Velić et al., 2000). To the west, the activity of the northward migrating Apennine foredeep has affected the southern sector of the Venetian Plain since the Late Miocene. This has led to a regional south-westward tilting, indicated by the huge (up to 2 km) thickness of Quaternary deposits close to the Po River Delta (Fig. 4) and by their gradually pinching out eastwards (Carminati et al., 2003).

Several trangressive/regressive Pleistocene cycles are recorded in well-core stratigraphy, which consist of alternating shallow-marine and continental deposits. In the Late Quaternary, the

Author's personal copy

Fig. 3. MIS 5.5 uplift rates (redrawn from from Ferranti et al., 2006).

evolution of the Venetian–Friulian plain was strongly influenced by glacial cycles and a general regressive trend is recognisable (Massari et al., 2004). During the LGM and MIS 6, the glaciers hosted in the main Alpine valleys debouched into the plain, feeding large fluvial–glacial systems that led to the formation of alluvial megafans (Fontana et al., 2008). Due to the low gradient of the pre-existing alluvial plain, the post-LGM and the last interglacial sea-level highstands witnessed the sedimentation of wedge-shaped, deltaic-lagoonal sedimentary bodies.

A generalized subsiding trend during the Late Pleistocene, with increasing rates of downlift from the Friulian to the Venetian plain, was previously recognized on the basis of scant borehole data (Ferranti et al., 2006). In the eastern part of the Gulf of Trieste, archaeological remains of Roman age and geomorphological markers, mainly notches, were used to assess a similar pattern of subsidence during the Holocene, which was attributed to active shortening (Faivre and Fouache, 2003; Antonioli et al., 2004c, 2007). In addition, larger subsidence compared to the Gulf of Trieste was found on the Istrian coast. A contemporary tilt to the northwest between Trieste and the Friulian plain is indicated by long-base tiltmeters data (Braitenberg et al., 2005).

2.2. Northwestern Adriatic coast

The Po River Plain is a subsiding foreland basin, bounded by two fold-and-thrust belts, the Alps to the north and the Northern Apennines to the south (Fig. 2 and Area 2 of Fig. 4). The subsurface geology of the Po Basin has been widely described on the

Author's personal copy

Fig. 4. Areas discussed in the text with location of investigated Holocene and MIS 5.5 sites. In red are labelled harbours with tide gauges.

basis of seismic (Pieri and Groppi, 1981) and magnetostratigraphic (Muttoni et al., 2003) data, and basin geometry depicted through integration of seismic studies with well-log interpretations (Ori, 1993; Regione Emilia-Romagna, ENI – AGIP, 1998; Regione Lombardia, ENI Divisione AGIP, 2002). This has led to the subdivision of the Pliocene-Quaternary basin rocks into a series of unconformity-bounded stratigraphic units. Sequence boundaries were formed in response to episodes of drastic basin reorganization. Tectonic uplift led to the development of denudation surfaces in the marginal areas, while the depocentres experienced increased subsidence (Regione Emilia-Romagna, ENI – AGIP, 1998).

The dominant feature of the Quaternary alluvial to coastal basin stratigraphy is a prominent cyclic facies architecture, consisting of vertically stacked transgressive–regressive sequences (Amorosi and Colalongo, 2005; Amorosi, 2008). Close to the basin margin, the stratigraphic architecture is dominated by amalgamated alluvial-fan gravel bodies, passing at distal locations to mud-prone alluvial plain deposits. In contrast, the stratigraphic architecture in the Romagna coastal plain and in the subsurface of the modern Po River Delta (Fig. 4) includes a distinctive cyclic alternation of coastal and alluvial deposits, falling in the Milankovitch (100 ka) band (Amorosi et al., 2004). Basin sediments are progressively less deformed from bottom to top (Regione Emilia-Romagna, ENI – AGIP, 1998; Molinari et al., 2007), and lateral facies relationships within the uppermost cycles are well preserved.

The coastal to shallow-marine deposits assigned to MIS 5.5 can be tracked in borehole logs up to 30 km west of the present shoreline. South of the Po Delta, the base of the Tyrrhenian coastal deposits lies at about −125 m b.s.l., but its depth rapidly increases toward the south along the Romagna coastal plain (Amorosi et al.,

Author's personal copy

2004; Bondesan et al., 2006). This pattern may reflect the combined loading of the Apennines thrust belt to the south and the north-easterly retreat of the Adriatic slab to the east (Ferranti et al., 2006).

2.3. Central and southern Adriatic coast of Italy

The central and southern Adriatic Sea forms the foreland of both the east-verging Apennines and west-verging Dinaric fold-and-thrust belts (Fig. 2). On the western, Italian side, the southerly transition from the Apennines thrust belt to the foreland occurs moving from the Marche, Abruzzo and Molise regions to the Puglia region (Area 3 of Fig. 4). Historical and instrumental seismic activity mark the frontal thrust belt in the north, but contemporary deformation occurs also at the Gargano promontory, an uplifted foreland block in the south (CPTI, 2004; Pondrelli et al., 2004).

The coast from Termoli, in Molise, up to the southernmost limit of the Po Plain, in Northern Marche, is marked by a high cliff, which is generally shaped on poorly cemented sediments of the Apennines foredeep basin. In this area, the Apenninic thrust front, recognisable some hundred metres below the Adriatic Sea, is still active (Scrocca et al., 2007). Uplifted MIS 5.5 marine deposits in the Northern Marche area indicate slow differential uplift related to the segmented growth of anticline folds in the hanging-wall of the frontal thrust (Vannoli et al., 2004; Ferranti et al., 2006).

The boundary between Molise and Puglia is marked by the wide coastal plain formed by the deltaic system of the Fortore River, which to the south passes to the Gargano foreland high. The area is characterised by a long-term uplift (Doglioni et al., 1994; Ferranti and Oldow, 2005a,b), and Holocene coseismic vertical displacements were documented at the Fortore River coast (Mastronuzzi and Sansò, 2002a).

The Apulian foreland is characterised by three main uplifted structural blocks of Gargano, Murge and Salento separated by low plains. Whereas the highs are floored by a thick carbonate passive margin succession, the lows host thick Neogene synorogenic rocks. Vertical movements characterised this region since the Middle Pleistocene as a consequence of the buckling of the entire Apulian foreland and/or due to folds and thrust faults localised in the basement (Doglioni et al., 1994; Ferranti and Oldow, 2005a,b). The structural highs are marked by a staircase of depositional or abrasive marine surfaces, but few geo-chronological constraints are available. Regional reconstructions of the MIS 5.5 marker elevation point to differential and discontinuous uplift rates from north to south. On the western, Ionian coast of Salento, uplift decreases from 0.18 mm/a in the Taranto area to zero at Leuca Cape (Ferranti et al., 2006; Mastronuzzi et al., 2007).

2.4. North-eastern Calabria coast

The Ionian coast of Northern Calabria lies behind the thrust front of the Southern Apennines (Fig. 1, Area 4 of Fig. 4). In this region, the geological architecture consists of Paleozoic crystalline rocks and related Cenozoic forearc sediments of the Calabrid units and of Mesozoic–Cenozoic sedimentary rocks of the Apennines, which underwent a complex Oligocene–Pliocene thrust history (Bonardi et al., 2001). Rapid uplift commenced in the Middle Pleistocene and led to the formation of a stepped flight of terraces (Westaway, 1993; Cucci and Cinti, 1998; Cucci, 2004). Coeval activity on high-angle faults helped shaping the Sybaris coastal plain intervening between the Pollino and Sila mountain ranges to the north and south, respectively (Fig. 4). The plain is floored by Upper Pliocene–Lower Pleistocene marine clays, sands, and fanglomerates, in turn covered by the Middle Pleistocene terraced coastal deposits. The plain and the adjacent mountain ranges are drained by several ephemeral streams which provide a huge clastic supply.

The coast-parallel profile of Middle Pleistocene–Holocene terraces records small-wavelength (~2–10 km) and amplitude undulations superposed on the regional uplift (~100 km scale). The MIS 5.5 terrace is by far the widest within the terrace flight (Cucci, 2004; Santoro et al., 2009), and rises southward from ~110 to ~130 m along the Pollino coast. In the Sybaris plain, the terrace is placed at a ~20-m lower elevation, but in Sila it rises again to ~130 m.

At the local-scale, pervasive undulations in the deformation profile of marine terraces have been attributed to shallow-crustal folds related to a still active transpressional field, which is jointly recorded by fluvial anomalies, marine geological data, local seismicity and broad geodetic networks (Ferranti et al., in press). Whereas the Pollino and Sila mountain ranges represent two structural culminations, the Sybaris Plain forms a local structural depression within the general uplift context. Historical subsidence in the plain is testified by the vertical stacking of three ancient towns in the Sybaris Archeological park along the Crati river (Paladino and Troiano, 1989), the old town founded by the Acheans (1230–1440 ka), the Hellenistic town of Thurii (1506–1757 ka) and later the Roman town of Copiae (1757–1350 ka). A longer (Latest Pleistocene–Holocene) subsidence record was obtained through borehole drillings in the Archeological park (Pagliarulo, 2006).

2.5. Southern Calabria and eastern Sicily coast

The Calabrian arc and eastern Sicily (Area 5 of Fig. 4) connect the Apennines and the Sicilian–Maghrebian orogens. The Calabrian Arc was emplaced to the south-east during north-westerly subduction and roll-back of the Ionian oceanic slab (Malinverno and Ryan, 1986). In the western Ionian Sea, along the Sicily offshore, a Mesozoic boundary (the Malta Escarpment; Sartori et al., 1991) separates the oceanic crust of the Ionian Basin from the continental domain of the Pelagian Block (Burollet et al., 1978), which represents the foreland of the Sicilian–Maghrebian south-verging thrust-and-fold system. Between Sicily and northern Africa, along the Sicily Channel (Figs. 1 and 4), the Pelagian Block is stretched by three main WNW–ESE striking tectonic depressions (Pantelleria, Linosa and Malta basins), developed since the Late Miocene-Early Pliocene (Finetti and Morelli, 1973) and characterised by widespread volcanism. These are interpreted as the result of dextral oblique rifting processes in a collisional context (Boccaletti et al., 1987).

During the Late Pliocene-Quaternary, the contractional structures of the hinterland part of the orogen were superseded by extensional faults, which form an active belt characterised by strong seismicity and volcanism along the western coast of Calabria and the eastern coast of Sicily (Monaco and Tortorici, 2000, 2007). Active WNW–ESE extension is documented by focal mechanisms of crustal earthquakes (Pondrelli et al., 2004; CMT catalogue, 1976–2006; RCMT Catalogue, 1976–2006), structural studies (Tortorici et al., 1995; Monaco et al., 1997; Monaco and Tortorici, 2000; Jacques et al., 2001; Ferranti et al., 2007), and geodetic velocities (D'Agostino and Selvaggi, 2004).

Since the Middle Pleistocene, extensional tectonics coupled with strong regional uplift developed spectacular flights of marine terraces (Dumas et al., 1988; Ghisetti, 1992; Westaway, 1993; Miyauchi et al., 1994; Bianca et al., 1999; Catalano and De Guidi, 2003; Tortorici et al., 2003). Uplift and attendant extension are interpreted as a response to stalling of slab retreat and consequent asthenospheric flow into the gap resulting from slab detachment (e.g. Westaway, 1993; Wortel and Spakman, 2000; Goes et al., 2004), or as being supported by asthenosphere wedging beneath the decoupled crust (Doglioni et al., 2001; Gvirtzman and Nur, 2001).

The elevation of marine terraces and their offset across the main faults has been used to establish the relative contribution of regional and fault-related sources to uplift. According to Westaway

Author's personal copy

(1993), 1.67 mm/a of post-Middle Pleistocene uplift of southern Calabria was partitioned into ~1 mm/a due to regional processes and the residual to displacement on major faults. Shorter-term uplift rate estimates are provided by raised Holocene beaches, terraces and tidal notches (Firth et al., 1996; Stewart et al., 1997; Pirazzoli et al., 1997; Rust and Kershaw, 2000; De Guidi et al., 2003; Antonioli et al., 2006; Ferranti et al., 2007).

2.6. Central Tyrrhenian coast

Most areas of the eastern Tyrrhenian coast experienced extension in a back-arc setting (Fig. 1), which was accompanied by volcanism on the young continental margin and in the basin (Beccaluva et al., 1989). Fault displacement articulated the coastal region (Area 6 of Fig. 4) in a complex alternation of subsiding basins and uplifting rocky promontories (Mariani and Prato, 1992). The southern part of this coastal extensional belt from Borgo Sabotino to the Garigliano River mouth (Area 6 of Fig. 4) is characterised by a series of distinct plains (Pontina Plain, Fondi Plain, Garigliano Plain, Volturno Plain) that occupy the major structural depressions. These plains are separated by promontories where Mesozoic carbonate rocks crop out. In the north, the coastal belt extending from the Argentario Promontory to the northern margin of the Pontina Plain mainly suffered the effects of the eruptions of the Vulsini, Sabatini and Colli Albani volcanoes which were active between 600 and 20 kyr (Barberi et al., 1994). Likewise, in the southern belt of Campania tectonic displacements were accompanied by volcanic processes in the Phlegrean Fields and Vesuvius volcanic area (Scandone et al., 1991). The pattern of subsidence in the plains and stability of promontories is confirmed by the elevation of the MIS 5.5 marker (Ferranti et al., 2006).

2.7. Northern Tyrrhenian coast

The coast stretching between eastern Liguria and northern Tuscany hosts the Viareggio Basin (Area 7 of Fig. 4), a prominent extensional half-graben formed in response to stretching in the Ligurian and northern Tyrrhenian back-arc basins (Argnani et al., 1997; Martini et al., 2001). Five unconformity-bounded stratigraphic units, ranging in age from Late Miocene to Holocene, have been recognized within the Viareggio Basin fill on the basis of seismic studies (Pascucci, 2005). Detailed facies analysis of late Quaternary deposits of the Arno coastal plain in the southern part of the basin has been recently carried out by Aguzzi et al. (2006, 2007), who documented a cyclic pattern of continental, paralic and shallow-marine deposits that can be grouped into a series of vertically stacked transgressive–regressive sequences. Long-term subsidence is apparent in this record, but no detailed information exists for recent movements.

In the northern sector of the half-graben, the Versilia Plain was bordered by normal faults active since the Early Miocene, and recent activity along these faults was inferred through geophysical exploration (Carminati et al., 1999; Cantini et al., 2001). A moderate subsidence of the plain during the last 125 ka was documented from borehole data (Nisi et al., 2003) and attributed to the bordering fault to the south (Ferranti et al., 2006). However, Holocene stability was noted at the same location (Lambeck et al., 2004a).

2.8. Sardinia coast

The island of Sardinia (Area 8 of Fig. 4) is a detached fragment of the Alpine foreland (Fig. 2). The western and eastern side of Sardinia have been effected by intense extensional tectonics related to the Oligocene–Miocene Ligurian–Balearic and Miocene–Pliocene Tyrrhenian sea rifting, respectively (Fig. 2; Cherchi and Montandert, 1982; Burrus, 1984).

The very low seismicity and geodetic deformation in Sardinia indicate that this block is at present quasi-stable (Serpelloni et al., 2005). Nevertheless, detailed studies of the MIS 5.5 marker indicate subtle displacements attributed to residual subsidence on the northwestern side of the island, or to isostatic uplift related to lava flow emplacement on the eastern side (Ferranti et al., 2006; Mariani et al., in press). Dense GPS measurements in southern Sardinia suggest that residual horizontal motions occur across the Campidano basin where the bounding faults are reactivated in strike-slip (Ferranti et al., 2008a).

3. Material and methods

A collection of 127 published Holocene (geomorphological and archaeological markers) and 11 new MIS 5.5 datapoints is used to compute the recent movements along the whole Italian coast (Tables 1 and 2). The listed uncertainties on Holocene material elevations (column H of Table 1) are derived from corrections discussed in the quoted references (column O); standard values adopted for bathymetric corrections for the Holocene and Late Pleistocene markers followed Table 1 of Lambeck et al. (2004a) and Ferranti et al. (2006). Additionally, precise measurements of the height of some Holocene cores in Area 1 (sites 16, 17, 18, 19, 21, 22, 23, 24, 25) were performed using a differential GPS.

Heights of the selected archaeological markers were measured and compared with the present sea level, applying corrections for tide, pressure and wind at the time of the surveys. Errors for the elevations and ages of the archaeological markers are estimated and functional heights evaluated on the basis of accurate archaeological interpretations provided by maritime archaeologists. Antonioli et al. (2007) defined the "functional height" of the archaeological benchmarks, in order to estimate the sea-level change at each location, and compare the observed results at different locations. This parameter is defined as the elevation of specific architectural parts of an archaeological structure with respect to an estimated mean sea level at the time of their construction. It depends on the type of structure, on its use and on the local tide amplitudes. Functional heights also define the minimum elevation of the structure above the local highest tides.

The functionality adopted on some sites with archaeological markers used in the present paper was previously discussed by Antonioli et al. (2007) and Scicchitano et al. (2008). For some new sites used here as sea-level markers, the functional height was defined. For sites 49, 50, 53 in Area 3 (Puglia), a 1-m functional height was considered for tombs, water cisterns, and hut holes. A similar value was used for the spring water well of Etruscan age and hut holes of Bronze age at sites 106 and 107 in Area 5 (Latium). For sites 51 and 52 (quarries) of Area 3 (Puglia) and site 115 of Area 7 (Liguria), the functional height was defined by the Italian mean tide of 0.44 m. The published ages were recalibrated (column G), but the original, noncalibrated ages are listed in column F for future improved calibration.

The tectonic movements (columns M and N) were computed ages of the different prediction on sea-level position listed in columns I and L from the Spada and Stocchi (SS) and Lambeck (KL) models, respectively. Errors on tectonic motions were stipulated using an error propagation strategy and provide an upper boundary to the absolute error. For the SS model, the uncertainty on the tectonic rate $\Delta(M)$ is:

$$\Delta(M) = \Delta(H)/G + (H - I/G)(\Delta(G)/G,$$

with $\Delta(H)$ and $\Delta(G)$ being the errors on the corrected heights and calibrated ages, respectively. A similar calculation is made for the KL model using the notations I and M.

Author's personal copy

Table 1
Holocene data. Column A: site number; B: site name; C: type of marker (geomorphological or archaeological) used for the chronological attribution; D: centesimal coordinates; E: laboratory number or core code; F: uncalibrated ages; G: calibrated ages 1 sigma used CALIB 5.01 program, marine entry; samples from sites 13, 14, 22 were calibrated as continental using the Intcal entry because of a peat immediately above lagoonal deposit; H: corrected (measure, water table, pressure and tide, functionality) height, see also Cap 3; I: predicted sea-level points using the Spada and Stocchi model; L: predicted sea-level points using the Lambeck model; M: tectonic rate using the Spada and Stocchi model – (H−I)/G for the error bar calculation see Cap. 3; N: tectonic rate using the Lambeck model – (H−L)/G for the error bar calculation see Cap. 3; O: references for original ages and corrections.

A, no.	B, site name	C, kind of marker and stratigrapy	D, centesimal coordinates	E, lab. and core number	F, age (^{14}C uncal. BP)	G, age cal. BP 1 σ archaeological	H, corrected height (m a.s.l.)	I, predicted values with SS model	L, predicted values Lambeck model	M, tectonic movements (H−I)/G (mm\y)	N, tectonic movements (H−L)/G (mm\y)	O, reference
1	Brijuni	Pavement	44.91111, 13.77472	/		1950 ± 50	−1.80 ± 0.6	−0.78	−0.31	−0.52 ± 0.32	−0.76 ± 0.33	Degrassi, 1957; Antonioli et al., 2007
2	Brijuni	Dock/pier	44.91083, 13.77639	/		1950 ± 50	−1.60 ± 0.6	−0.78	−0.31	−0.42 ± 0.32	−0.66 ± 0.32	Degrassi, 1957; Antonioli et al., 2007
3	Savudrija	Pavement	45.49972, 13.50361	/		1950 ± 50	−1.50 ± 0.6	−0.61	−0.06	−0.46 ± 0.32	−0.74 ± 0.33	Antonioli et al., 2007
4	Savudrija	Pier	45.49972, 13.50361	/		1950 ± 50	−1.50 ± 0.6	−0.61	−0.06	−0.46 ± 0.32	−0.74 ± 0.33	Fouache et al., 2000; Antonioli et al., 2007
5	Secovlje	Lagoonal fossils	45.52361, 13.52667	Core V6	9180 ± 120	9975.5 ± 175	−26.5 ± 0.5	−28.72	−30.2	0.22 ± 0.05	0.37 ± 0.06	Ogorelec et al., 1997
6	Sv. Simon	Pier	45.5325, 13.64472	/		1950 ± 50	−1.60 ± 0.6	−0.62	−0.06	−0.50 ± 0.32	−0.79 ± 0.33	Degrassi, 1957
7	Capodistria Bay	Lagoonal fossils	45.5415, 13.7224	/	1367 ± 83	900 ± 95	−1.24 ± 0.5	−0.24	0.16	−1.11 ± 0.67	−1.53 ± 0.72	Ogorelec et al., 1997
8	Jernejeva Draga	Vivaria dock	45.59278, 13.7224	/		1900 ± 100	−1.40 ± 0.6	−0.57	−0.06	−0.44 ± 0.34	−0.71 ± 0.35	Antonioli et al., 2007
9	Punta Sottile	Pier	45.60222, 13.71944	/		1950 ± 50	−1.60 ± 0.6	−0.59	−0.06	−0.52 ± 0.07	−0.79 ± 0.33	Antonioli et al., 2007
10	Stramare	Walking surface	45.60194, 13.79	/		1900 ± 100	−1.60 ± 0.6	−0.58	−0.06	−0.54 ± 0.07	−0.81 ± 0.36	Antonioli et al., 2007
11	Trieste town	Lagoonal fossils	45.64861, 13.7675	Poz-15855	2020 ± 30	1576.5 ± 47.5	+0.10 ± 0.1	−0.47	0.25	0.36 ± 0.05	−0.09 ± 0.07	Furlani et al., 2007
12	Trieste town	Lagoonal fossils	45.64861, 13.7675	Poz-15854	2065 ± 30	1639 ± 48	0.00 ± 0.1	−0.49	0.23	0.30 ± 0.05	−0.14 ± 0.07	Furlani et al., 2007
13	Trieste gulf	Lagoonal fossils	45.67, 13.67972	Core GT1	9140 ± 40	9928.5 ± 104	−25 ± 0.5	−27.60	−30.7	0.26 ± 0.08	0.57 ± 0.06	Covelli et al., 2006
14	Trieste gulf	Lagoonal fossils	45.6075, 13.55278	Core GT3	8810 ± 40	9479.5 ± 32.5	−26 ± 0.5	−23.02	−23.07	−0.3 ± 0.05	−0.31 ± 0.05	Covelli et al., 2006
15	Lagoon of Caorle. Palude Rocca (VE)	Organic silt base of lagoon	45.64722, 12.92778	Ua-24876	5730 ± 45	6153 ± 67	−5.15 ± 0.5	−4.75	−4.2	−0.07 ± 0.08	−0.18 ± 0.08	Fontana, 2006
16	Sepolcreto Concordia, Sagittaria (VE)	Peat swamp	45.75667, 12.85	Beta-173013	1800 ± 70	1755 ± 66	−2.85 ± 0.05	−0.43	−0.33	−1.38 ± 0.08	−1.44 ± 0.07	This work
17	Sepolcreto. Concordia, Sagittaria (VE)	Peat salt marsh	45.75639, 12.85194	Beta-184247	4080 ± 70	4115 ± 109	−5.0 ± 0.05	−1.61	−1.95	−0.82 ± 0.03	−0.74 ± 0.03	This work
18	Sepolcreto. Concordia, Sagittaria (VE)	Peat base of lagoon	45.75639, 12.85194	Beta-184248	5700 ± 70	6186 ± 88.5	−6.87 ± 0.05	−4.40	−4.45	−0.40 ± 0.01	−0.40 ± 0.01	This work
19	Paludetto. Concordia, Sagittaria (VE)	Loamy peat swamp	45.7575, 12.82861	Beta-184249	1920 ± 60	1880 ± 66	−3.79 ± 0.05	−0.46	−0.49	−1.77 ± 0.09	−1.76 ± 0.09	Fontana, 2006
20	Paludetto. Concordia, Sagittaria (VE)	Loamy peat base of lagoon	45.7575, 12.82861	Beta-184250	5910 ± 70	6330 ± 68	−8.63 ± 0.05	−4.80	−4.9	−0.61 ± 0.01	−0.59 ± 0.01	Fontana, 2006
21	Casa Zucca. Caorle (VE)	Loamy peat base of lagoon	45.63611, 12.88722	Beta-184251	6080 ± 80	6507 ± 95	−8.59 ± 0.05	−5.43	−5.6	−0.49 ± 0.01	−0.46 ± 0.01	Fontana, 2006
22	Fiorentina. San Donà di Piave (VE)	Organic silt base of lagoon	45.65222, 12.64028	Beta-170844	3570 ± 70	2917.5 ± 62.5	−2.6 ± 0.05	−0.93	−1.3	−0.58 ± 0.03	−0.45 ± 0.03	Bondesan et al., 2003
23	Torre di Mosto (VE)	Peat base of lagoon	45.62167, 12.75611	Ua-24049	6580 ± 55	7090 ± 75	−9.2 ± 0.05	−6.58	−7.8	−0.37 ± 0.03	−0.20 ± 0.01	Fontana, 2006
24	Fossetta (VE)	Peaty silt base of lagoon	45.58528, 12.47472	Beta-157974	3140 ± 40	3146.5 ± 67.5	−3.9 ± 0.5	−1.08	−1.48	−0.90 ± 0.18	−0.77 ± 0.18	Bondesan et al., 2002
25	Ca' Tron. Roncade (TV)	Lagoon sediment base of lagoon	45.57167, 12.44639	/		1950 ± 50	−1.6 ± 0.5	−0.38	−0.62	−0.63 ± 0.27	−0.50 ± 0.27	Bondesan et al., 2003

(*continued on next page*)

Author's personal copy

Table 1 (*continued*)

A, no.	B, site name	C, kind of marker and stratigrapy	D, centesimal coordinates	E, lab. and core number	F, age (^{14}C uncal. BP)	G, age cal. BP 1 σ archaeological	H, corrected height (m a.s.l.)	I, predicted values with SS model	L, predicted values Lambeck model	M, tectonic movements (H−I)/G (mm\y)	N, tectonic movements (H−L)/G (mm\y)	O, reference
26	Venice Lagoon BH2	Shells base of lagoon	45.52222, 12.53056	Beta-206482	6740 ± 50	7270 ± 57	−10.15 + 0.5–2	−7.09	−9.1	−0.42 ± 0.18	−0.14 ± 0.17	Canali et al., 2007; Tosi et al., 2007
27	Burano, Venezia	Peat base of lagoon	45.48528, 12.41722	GX-26939	4120 ± 40	4171 ± 66	−4.2 ± 0.5	−1.74	−2.02	−0.58 ± 0.13	−0.52 ± 0.13	Lezziero, 2002
28	Venice Lagoon BH1	Shells base of lagoon	45.48333, 12.54583	Beta-169857	6840 ± 40	7364 ± 42	−12.9 + 0.5–2	−7.35	−10.4	−0.75 ± 0.17	−0.17 ± 0.17	Canali et al., 2007; Tosi et al., 2007
29	Marghera, Venezia	Peat base of lagoon	45.47556, 12.23917	Rome-1206	1095 ± 55	1007 ± 50	−1.57 ± 0.5	−0.49	−0.28	−1.07 ± 0.55	−1.28 ± 0.56	Mozzi et al., 2003
30	Piazza S. Marco. Venezia	Shells base of lagoon	45.43417, 12.33889	OZD-608	4670 ± 70	4900 ± 84	−5.8 + 0.5–2	−2.67	−3.31	−0.64 ± 0.27	−0.51 ± 0.26	Serandrei-Barbero et al., 2001
31	Boccasette – Core 3 (Delta Po)	Organic swamp	45.0099, 12.4369	CEDAD	8495 ± 55	9110.5 ± 84.5	−29.8 + 0.5–2	−19.66	−26.4	−1.11 ± 0.15	−0.37 ± 0.14	Amorosi et al., 2008b
32	Barricata – Core 1 (Delta Po)	Organic swamp	44.84794, 12.46263	CEDAD	8404 ± 100	9004.6 ± 150	−29.9 ± 0.5	−18.79	−25.6	−1.22 ± 0.08	−0.48 ± 0.06	Amorosi et al., 2008b
33	Pomposa – Core 187-S1 (FE)	Organic swamp	44.84089, 12.20108	Beta	8220 ± 60	8736.5 ± 110	−25.5 ± 0.5	−16.28	−22.6	−1.06 ± 0.07	−0.33 ± 0.06	Bondesan et al., 2006; Amorosi et al., 2007
34	Ostellato, Core 204-S6 (FE)	Organic lagoon	44.73333, 11.88333	LLNL Livermore	6895 ± 80	7400.5 ± 76.5	−14.2 ± 0.5	−7.64	−13.6	−0.89 ± 0.08	−0.08 ± 0.07	Amorosi et al., 2005
35	Portomaggiore, Core 204-S5 (FE)	Organic swamp	44.7, 11.85	LLNL, Livermore-	7735 ± 50	8217 ± 62	−15.8 ± 0.5	−7.53	−18.1	−1.01 ± 0.07	−0.28 ± 0.06	Amorosi et al., 2005
36	Conselice	Cerastoderma	45.478, 11.845			5924 ± 50	−9.0 + 0.5–2	−5.1	−4.6	−0.66 ± 0.22	−0.74 ± 0.22	Preti, 1999
37	Ravenna, core 223-S1	Organic swamp	44.43333, 12.21667	LODYC (Paris)	8170 ± 50	8657.5 ± 82	−25.5 ± 0.5	−15.99	−22.5	−1.17 ± 0.07	−0.35 ± 0.06	Amorosi et al., 2005
38	Ancona	Fish tank	43.5667, 13.56667	/		1950 ± 50	−1.1 ± 0.2	−0.95	−0.94	−0.08 ± 0.10	−0.08 ± 0.10	Profumo, 2007
39	Vomano river	Continental Peat	42.65056, 14.03389	/	10,250 ± 50	12,024.5 ± 74.5	−18 ± 0.5	−60.23	−62.9	–	–	Parlagreco et al., in press
40	Punta Pietre Nere	Cladocora	41.91488, 15.34431	GX-28709	5950 ± 110	6373.5 ± 114	0.5 ± 0.2	−7.67	−8.2	1.28 ± 0.05	1.37 ± 0.06	Mastronuzzi and Sansò, 2002a
41	Punta Pietre Nere	*Lithophaga* sp.	41.91488, 15.34431	GX-6369	880 ± 40	497.5 ± 27.5	0.93 ± 0.2	−0.31	−0.27	2.49 ± 0.54	−442.41 ± 0.54	Mastronuzzi and Sansò, 2002a
42	Punta Pietre Nere	*Dendropoma* sp.	41.91488, 15.34431	GX-27061	1210 ± 70	748.5 ± 72.5	0.77–0.88	−0.46	−0.42	1.71 ± 0.23	1.66 ± 0.23	Mastronuzzi and Sansò, 2002a
43	Punta Pietre Nere	*Vermetid* sp.	41.91488, 15.34431	GX-26368	1520 ± 110	1066.5 ± 115	0.95 ± 0.1	−0.66	−0.61	1.51 ± 0.26	1.46 ± 0.25	Mastronuzzi and Sansò, 2002a
44	Palude Frattarolo/ Coppa nevigata	*Cerastoderma glaucum*	41.557222, 15.833333	?	2870 ± 40	2654.5 ± 61.5	−1.4 ± 0.5	−1.92	−1.96	0.20 ± 0.19	0.21 ± 0.19	Caldara et al., 2002
45	Palude Frattarolo/ Coppa nevigata	*C. glaucum*	41.557222, 15.833333	?	3180 ± 70	2856.5 ± 58.5	−2.25 ± 0.5	−2.10	−2.1	−0.05 ± 0.18	−0.05 ± 0.18	Caldara et al., 2002
46	Palude Frattarolo/ Coppa nevigata	*C. glaucum*	41.557222, 15.833333	?	3195 ± 80	2999 ± 116	−2.25 ± 0.5	−2.23	−2.35	−0.01 ± 0.17	0.03 ± 0.17	Caldara et al., 2002
47	Palude Frattarolo/ Coppa nevigata	*C. glaucum*	41.557222, 15.833333	GX28575AMS	4950 ± 40	5286 ± 47.5	−3.48 ± 0.5	−5.45	−4.4	0.37 ± 0.10	0.17 ± 0.10	Caldara and Simone, 2005
48	Palude Frattarolo/ Coppa nevigata	*C. glaucum*	41.557222, 15.833333	GX28576AMS	5580 ± 40	5953.5 ± 53.6	−6.6 + 0.5–2	−6.86	−7.3	0.04 ± 0.21	0.12 ± 0.21	Caldara and Simone, 2005
49	Egnatia	Tumb	40.8886, 17.3928			2450 ± 100	−1.7 ± 0.5	−1.68	−1.8	−0.01 ± 0.20	0.03 ± 0.21	Auriemma et al., 2004; Milella et al., 2006
50	Egnatia	Cistern/sewer	40.8886, 17.3928			1900 ± 100	−1.36 ± 0.5	−1.22	−1.15	−0.07 ± 0.27	−0.11 ± 0.27	Auriemma et al., 2004; Milella et al., 2006
51	Egnatia	Quarries	40.8886, 17.3928			1500 ± 100	−1.04 ± 0.5	−0.96	−0.9	−0.05 ± 0.34	−0.09 ± 0.34	Auriemma et al., 2004
52	Santa Sabina	Quarries	40.8222, 17.6086			1500 ± 100	1.04 ± 0.5	−0.95	−0.9	−0.06 ± 0.42	−0.09 ± 0.42	Auriemma et al., 2004; Auriemma et al., 2005

Author's personal copy

53	Torre Guaceto	Hut holes	40.7161, 17.7986			3500 ± 500	−3.5 ± 1	−2.57	−3.03	−0.27 ± 0.32	−0.13 ± 0.30	Auriemma et al., 2004
54	Sibari. Parco Archeologico Nazionale	Marsh	39.72533, 16.46598	S1	4685 ± 69	4913 ± 86	−3.0 ± 03	−4.65	−5.3	0.34 ± 0.07	−0.47 ± 0.07	Pagliarulo, 2006
55	Sibari. Parco Archeologico Nazionale	Marsh	39.72533, 16.46598	S1	8410 ± 70	9401 ± 135	−38.0 ± 03	−26.13	−35.6	−1.26 ± 0.05	−0.28 ± 0.04	Randisi, 2007
56	Sibari. Parco Archeologico Nazionale	Organic mud with lagoonal fossils	39.71749, 16.48802	S15	6310 ± 70	6769 ± 88	−49.4 + 0.5–2	−8.73	−10.6	−6.01 ± 0.26	−5.73 ± 0.26	Randisi, 2007
57	Sibari. Parco Archeologico Nazionale	Marsh	39.71401, 16.49279	S16	3140 ± 50	2920 ± 74	−6.8 + 0.5–2	−2.15	−2.5	−1.59 ± 0.47	−1.47 ± 0.47	Randisi, 2007
58	Sibari. Parco Archeologico Nazionale	Organic mud	39.71401, 16.49279	S16	6540 ± 70	7059 ± 88	−57.4 + 0.5–2	−9.46	−12.2	−6.79 ± 0.26	−6.4 ± 0.26	Randisi, 2007
59	Sibari. Parco Archeologico Nazionale	Organic mud with lagoonal fossils	39.71401, 16.49279	S16	7160 ± 110	7639 ± 106	−59.8 + 0.5–2	−11.39	−18.7	−7.72 ± 0.25	−5.37 ± 0.24	Randisi, 2007
60	Sibari. Parco Archeologico Nazionale	Organic mud	39.7174, 16.49579	S18	2900 ± 45	2692 ± 47	−1.0 + 0.5–2	−1.95	−2.4	0.35 ± 0.47	0.41 ± 0.47	Randisi, 2007
61	Sibari. Parco Archeologico Nazionale	Peat	39.7174, 16.49579	S18	3285 ± 50	3129 ± 80	−6.0 + 0.5–2	−2.35	−2.7	−0.83 ± 0.43	−1.05 ± 0.43	Randisi, 2007
62	Sibari. Parco Archeologico Nazionale	Organic mud	39.7174, 16.49579	S18	4470 ± 65	4673.5 ± 98.5	−17.0 + 0.5–2	−4.27	−5.1	−2.72 ± 0.32	−2.57 ± 0.32	Randisi, 2007
63	Sibari. Parco Archeologico Nazionale	Organic mud	39.7174, 16.49579	S18	4945 ± 50	5313 ± 102	−21.1 + 0.5–2	−5.45	−6.4	−2.95 ± 0.29	−2.80 ± 0.29	Randisi, 2007
64	Sibari. Parco Archeologico Nazionale	Organic mud	39.7174, 16.49579	S18	5775 ± 55	6209.5 ± 60.5	−38.9 + 0.5–2	−7.41	−8.8	−5.07 ± 0.25	−4.85 ± 0.25	Randisi, 2007
65	Sibari. Parco Archeologico Nazionale	Organic mud	39.7174, 16.49579	S18	6510 ± 55	7025.5 ± 79.5	−40.9 + 0.5–2	−9.35	−12.8	−4.49 ± 0.23	−4.00 ± 0.29	Randisi, 2007
66	Sibari. Casa Bianca	*Donax* sp.	39.71796, 16.498	184-1	1415 ± 23	1314.5 ± 15	−1.14 ± 0.5	−0.86	−0.82	−0.21 ± 0.38	−0.25 ± 0.38	Randisi, 2007
67	Punta Carace. Pantelleria Island	*Dendropoma petraeum*	36.80917, 12.03306	Poz 21913	1360 ± 30	912 ± 36	4.2 ± 0.3	−0.58	−0.5	5.24 ± 0.54	5.15 ± 0.53	De Guidi and Monaco, 2009
68	Cala di Levante., Pantelleria Island	*D. petraeum*	36.79583, 12.05	Poz 17750	1155 ± 30	694 ± 29	2.2 ± 0.3	−0.45	−0.5	3.82 ± 0.59	3.89 ± 0.59	De Guidi and Monaco, 2009
69	Vendicari (Syracuse)	*C. glaucum*	36,481325, 15,05 53	Poz 17907	4610 ± 40	4830 ± 118	−5.40 + 0.5–2	−5.18	−5.5	−0.05 ± 0.26	0.02 ± 0.26	Scicchitano et al., 2007
70	Vendicari (Syracuse)	*Cerithium vulgatum*	36.4637, 15.0540	Poz 17906	4890 ± 40	5176 ± 128	−6.90 + 0.5–2	−5.91	−6.28	−0.19 ± 0.25	−0.12 ± 0.24	Scicchitano et al., 2007
71	Plemmirio cave (Syracuse)	*Serpulid* overgrowth on stalagmite	36.97997, 15.25642	C2	7780 ± 230	8229 ± 242	−20.22 ± 0.5	−16.34	−26.6	−0.47 ± 0.07	0.78 ± 0.08	Scicchitano et al., 2008
72	Ognina (Syracuse)	Tomb floor (*dromos*)	37.04125, 15.30708	/		3500 ± 300	−1.81 ± 0.3	−3.09	−3.5	0.57 ± 0.14	0.49 ± 0.13	Scicchitano et al., 2008
73	Ognina (Syracuse)	Channel sea-bottom	36.97933, 15.26303	/		3500 ± 300	−1.97 ± 0.3	−3.09	−3.5	0.32 ± 0.12	0.44 ± 0.12	Scicchitano et al., 2008
74	Punta della Mola (Syracuse)	Quarries	37.15892, 15.232	/		2600 ± 100	−0.98 ± 0.3	−2.11	−2.25	0.43 ± 0.13	0.49 ± 0.13	Scicchitano et al., 2008
75	Thapsos (Syracuse)	Tomb floor	37.20578, 15.18433	/		3350 ± 150	−1.03 ± 0.3	−2.87	−3.29	0.55 ± 0.11	0.68 ± 0.12	Scicchitano et al., 2008
76	Megara Iblea (Syracuse)	Dock/pier	37.36944, 15.08056	/		2600 ± 100	−1.48 ± 0.3	−2.08	−2.25	0.23 ± 0.13	0.30 ± 0.13	Scicchitano et al., 2008
77	Catania Plain	Bivalve fragments	37.35833, 15.06111	Utc 11546	6343 ± 41	6759 ± 98	−7.2 + 0.5–2	−9.50	−11.6	0.34 ± 0.19	0.65 ± 0.19	Monaco et al., 2004
78	Catania Plain	*Cerastoderma* sp.	37.34444, 15.05833	Utc 11548	9110 ± 50	9699 ± 100	−37.9 + 0.5–2	−31.57	−43.3	−0.65 ± 0.13	0.56 ± 0.13	Monaco et al., 2004
79	Ganzirri	*Serpulids*	38.26556, 15.62889	UTC 12275	5557 ± 47	5954 ± 99	0.70 ± 0.3	−7.14	−7.6	1.32 ± 0.07	1.39 ± 0.07	Antonioli et al., 2006
80	Milazzo Peninsula	*Patella* sp.	38.23306, 15.25056	UTC 11356	5665 ± 36	6065 ± 35	2 ± 0.3	−7.41	−7.9	1.55 ± 0.07	1.63 ± 0.06	Gringeri et al., 2004
81	Scilla, Marina S. Gregorio	*Chthamalus depressus*	38.24933, 15.68957	UTC 12274	3501 ± 35	3386 ± 42	1.79 ± 0.07	−2.79	−3.01	1.35 ± 0.05	1.42 ± 0.04	Ferranti et al., 2007

(*continued on next page*)

Author's personal copy

Table 1 (*continued*)

A, no.	B, site name	C, kind of marker and stratigrapy	D, centesimal coordinates	E, lab. and core number	F, age (^{14}C uncal. BP)	G, age cal. BP 1 σ archaeological	H, corrected height (m a.s.l.)	I, predicted values with SS model	L, predicted values Lambeck model	M, tectonic movements (H−I)/G (mm\y)	N, tectonic movements (H−L)/G (mm\y)	O, reference
82	Scilla	*C. depressus*	38.24933, 15.68957	UTC 12273	3530 ± 39	3409 ± 47	1.80 ± 0.07	−2.81	−3.2	1.35 ± 0.04	1.47 ± 0.04	Ferranti et al., 2007
83	Marina S. Gregorio	*Spondylus* sp.	38.24933, 15.68957	UTC 12656	3610 ± 49	3504 ± 65	3.65 ± 0.07	−2.91	−3.5	1.87 ± 0.07	2.04 ± 0.06	Ferranti et al., 2007
84	Scilla	*Hexaplex* sp.	38.24933, 15.68957	Gx 28331	3930 ± 40	3909 ± 60	3.00 ± 0.07	−3.34	−4.2	1.62 ± 0.05	1.84 ± 0.05	Ferranti et al., 2007
85	Marina S. Gregorio	*Spondylus* sp.	38.24933, 15.68957	R 3717	4497 ± 69	4746 ± 51	2.30 ± 0.07	−4.68	−5.5	1.47 ± 0.07	1.64 ± 0.07	Ferranti et al., 2007
86	Scilla, Punta Paci	*C. depressus*	38.2522, 15.70053	UTC 12271	2274 ± 34	1881 ± 47	1.91 ± 0.17	−1.33	−1.27	1.72 ± 0.13	1.69 ± 0.13	Antonioli et al., 2006
87	Scilla, Punta Paci	*C. depressus*	38.2522, 15.70053	UTC 12654	2549 ± 38	2230 ± 58	0.99 ± 0.17	−1.63	−1.85	1.17 ± 0.12	1.27 ± 0.11	Antonioli et al., 2006
88	Scilla, Punta Paci	*Spondylus* sp.	38.2522, 15.70053	R 2625	2683 ± 45	2376 ± 60	2.12 ± 0.17	−1.77	−1.76	1.64 ± 0.07	1.63 ± 0.07	Antonioli et al., 2006
89	Scilla, Punta Paci	*C. depressus*	38.2522, 15.70053	UTC 12272	2744 ± 34	2427 ± 73	1.92 ± 0.17	−1.82	−2.02	1.54 ± 0.12	1.62 ± 0.12	Antonioli et al., 2006
90	Scilla, Punta Paci	*C. depressus*	38.2522, 15.70053	Poz 13000	3410 ± 40	3290 ± 52	2.87 ± 0.21	−2.66	−3.1	1.68 ± 0.07	1.81 ± 0.09	Antonioli et al., 2006
91	Scilla, Punta Paci	*C. depressus*	38.2522, 15.70053	UTC 12652	3609 ± 42	3500 ± 58	1.92 ± 0.17	−2.88	−3.5	1.37 ± 0.07	1.55 ± 0.07	Antonioli et al., 2006
92	Scilla, Punta Paci	*Conus* sp.	38.2522, 15.70053	Poz 13005	4760 ± 40	4933 ± 84	2.59 ± 0.22	−4.95	−6.0	1.53 ± 0.07	1.76 ± 0.07	Antonioli et al., 2006
93	Palmi, Pietra Galera	*C. depressus*	38.34049, 15.83149	Poz 13010	2785 ± 35	2529 ± 80	2.20 ± 0.18	−1.92	−2.1	1.63 ± 0.12	1.70 ± 0.12	Antonioli et al., 2006
94	Marina di Palmi	*Gastrana fragilis*	38.35264, 15.83579	Poz 13011	4430 ± 40	4587 ± 68	1.75 ± 0.19	−4.37	−5.2	1.28 ± 0.07	1.52 ± 0.06	Antonioli et al., 2006
95	Ioppolo (Capo Vaticano)	*Dendropoma*	38.56556, 15.90111	GX 28045	5120 ± 50	5501.5 ± 58	1.8 ± 0.3	−6.09	−7.2	1.43 ± 0.07	1.64 ± 0.07	Antonioli et al., 2006
96	Ioppolo (Capo Vaticano)	Columella	38.56556, 15.90111	GX 28332	5380 ± 40	5762 ± 66	1.8 ± 0.3	−6.66	−7.7	1.47 ± 0.07	1.65 ± 0.07	Antonioli et al., 2006
97	S. Maria Ricadi (Capo Vaticano)	*Monodonta articulata*	38.60635, 15.85058	CV3	3885 ± 35	3863 ± 55	0.60 ± 0.3	−3.22	−3.9	0.99 ± 0.09	1.22 ± 0.09	This paper
98	S. Maria Ricadi (Capo Vaticano)	Bivalve shell	38.60581, 15.85298	CV5	5330 ± 40	5681 ± 52	1.55 ± 0.3	−6.49	−7.5	1.42 ± 0.07	1.59 ± 0.07	This paper
99	Pozzuoli	*Lithophaga*	40. 862, 14.1204	–	1235 ± 55	580 ± 70	7 ± 0.10	−0.38	−0.34	12.72 ± 1.71	12.66 ± 1.7	Morhange et al., 2006
100	Pozzuoli	*Lithophaga*	40. 862, 14.1204	–	2250 ± 35	1570 ± 110	7 ± 0.10	−1.06	−1.02	5.13 ± 0.43	5.11 ± 0.42	Morhange et al., 2006
101	Sarinola	Fish tank	41.25527 13.60833			2000 ± 50	−1.28 ± 0.22	−1.28	−1.40	0.05 ± 0.11	0.06 ± 0.11	Lambeck et al. (2004a)
102	Ventotene	Fish tank, harbour	40.79916, 13.43305			2000 ± 50	−1.30 ± 0.22	−1.38	−1.41	0.04 ± 0.11	−0.05 ± 0.11	Lambeck et al. (2004a)
103	Ponza	Fish tank	40.89361, 12.96916			2000 ± 50	−1.30 ± 0.22	−1.28	−1.40	−0.01 ± 0.11	−0.14 ± 0.11	Lambeck et al. (2004a)
104	Torre Astura, La Banca	Fish tank	41.41736, 12.7495			2000 ± 50	−1.15 ± 0.22	−1.24	−1.32	0.05 ± 0.11	0.09 ± 0.11	Lambeck et al. (2004a)
105	S.Marinella, Le Grottacce	Fish tank	42.03888, 11.90138			2000 ± 50	−1.37 ± 0.22	−1.28	−1.23	−0.05 ± 0.11	−0.07 ± 0.11	Lambeck et al. (2004a)
106	Pyrgi	Spring water well	42.015, 11.95806			2400 ± 50	−1.2 ± 0.5	−1.39	−1.48	0.08 ± 0.11	0.12 ± 0.21	Enei, 2008
107	Pyrgi	Hut holes	42.015, 11.95806			4700 ± 100	−4.5 ± 0.5	−3.72	−4.3	−0.17 ± 0.11	−0.04 ± 0.11	Enei, 2008
108	P.Ta della Vipera	Fish tank	42.04888, 11.82			2000 ± 50	−1.28 ± 0.22	−1.28	−1.23	0.00 ± 0.11	−0.03 ± 0.11	Lambeck et al., 2004b

Author's personal copy

109	Santa Liberata	Fish tank	42.43589, 11.15261			2000 ± 50	−1.04 ± 0.22	−1.03	−1.2	−0.01 ± 0.11	0.08 ± 0.11	Lambeck et al., 2004b
110	Core M1	Organic estuary	43.62978, 10.28872	CEDAD	10004 ± 50	11012 ± 98	−51.1 ± 3	−41.49	−53.2	−0.87 ± 0.26	0.19 ± 0.27	Aguzzi et al., 2007; Amorosi et al., 2008a
111	Core M1	Organic estuary	43.62978, 10.28872	CEDAD	8840 ± 75	9495 ± 72	−39.4 ± 3	−24.53	−32.0	−1.57 ± 0.32	−0.78 ± 0.32	Aguzzi et al., 2007; Amorosi et al., 2008a
112	Core S1	Organic estuary	43.72781, 10.43431	Beta	11,034 ± 63	12,668 ± 130	−45.4 ± 3	−67.21	−65.8	1.72 ± 0.25	0.82 ± 0.25	This work
113	Core S1	Organic lagoon	43.72781, 10.43431	Beta	7370 ± 60 BP	7845 ± 67	−13.5 + 0.5–2	−9.87	−15.4	−0.46 ± 0.16	0.24 ± 0.16	This work
114	Core CC	Organic swamp	43.67123, 10.67064	CEDAD	10,106 ± 60	11,136.5 ± 53	−54.7 ± 3	−43.19	−55.8	−1.03 ± 0.26	1 ± 0.27	Aguzzi et al., 2006
115	La Spezia	Canne on pier	44.34278, 9.240278	–	–	2000 ± 50	−0.85 ± 0.4	−0.75	−0.78	−0.05 ± 0.20	−0.035 ± 0.20	Chelli et al., 2005
116	Capo Malfatano	Breakwater dock	38.891670, 8.803056	–	–	2400 + 100	−2.10 ± 0.22	−1.99	−2.3	−0.046 ± 0.09	0.08 ± 0.10	Antonioli et al., 2007
117	Nora *molo Schmiedt*	Pier	38.984720, 9.012850	–	–	1900 ± 300	−1.42 ± 0.22	−1.30	−1.68	−0.06 ± 0.13	0.14 ± 0.14	Antonioli et al., 2007
118	Nora *Basilica*	Pavement	39.021940, 9.025278	–	–	1650 ± 50	−1.02 ± 0.22	−1.13	−1.38	0.07 ± 0.13	0.22 ± 0.14	Antonioli et al., 2007
119	Perd'e Sali	Quarry	39.02194, 9.025278	–	–	2000 ± 300	−1.32 ± 0.30	−1.40	−1.78	0.05 ± 0.18	0.24 ± 0.18	Antonioli et al., 2007
120	Cagliari core	*C. vulgatum*	39.2161, 9.0939	GX-30098	4090 ± 70	4129 ± 109	−7.80 + 0.5–2	−3.87	−5.9	−0.95 ± 0.31	−0.46 ± 0.31	Antonioli et al., 2007
121	Cagliari core	*Hinia reticulata mamillata*	39.2161, 9.0939	GX-30097	6930 ± 80	7345.5 ± 71	−14.90 + 0.5–2	−12.35	−17.1	−0.35 ± 0.17	0.30 ± 0.17	Antonioli et al., 2007
122	Cagliari core	*C. vulgatum*	39.2161, 9.0939	GX-30096	7010 ± 80	7493 ± 61	−19.20 + 0.5–2	−12.94	−21.3	−0.84 ± 0.17	0.28 ± 0.17	Antonioli et al., 2007
123	Cagliari core	*Hinia reticulata mamillata*	39.2161, 9.0939	GX-30100-	7270 ± 80	7737 ± 83	−25.20 + 0.5–2	−13.92	−23.4	−1.46 ± 0.16	−0.23 ± 0.16	Antonioli et al., 2007
124	Cagliari core	*Hinia reticulata mamillata*	39.2161, 9.0939	GX-29077-	9050 ± 30	9753 ± 74	−30.56 + 0.5–2	−34.05	−42.8	0.36 ± 0.15	1.25 ± 0.14	Antonioli et al., 2007
125	Santa Gilla	Insitu Anphorae	39.26333, 9.031944	–	–	2450 ± 40	−2.0 ± 0.22	−1.90	−2.3	−0.04 ± 0.08	0.12 ± 0.09	Antonioli et al., 2007
126	Tharros	Thombs Quarry	39.879230, 8.435920	–	–	2200 ± 200	−1.35 ± 0.30	−1.63	−1.75	0.13 ± 0.15	0.27 ± 0.15	Antonioli et al., 2007
127	Capo Testa	Quarry. −70, Pier	41.24031, 9.16118	–	–	2000 ± 200	−1.20 ± 0.30	−1.60	−1.70	0.2 ± 0.17	0.25 ± 0.18	Antonioli et al., 2007

Author's personal copy

Table 2
MIS 5.5 data.

Site no.	Locality	Coordinates	Kind of marker	Tecnique of chronological attribuition and age	Shoreline elevation m a.s.l. base	Vertical displacement rate mm\a	Error bar		Reference
200	Piancada	45.783750, 13.084250	Base of lagoonal deposits	Stratigraphic correlation	−57.5	−0.49	+1	−5	Feruglio, 1936
201	CNC4 Concordia	45.759333, 12.840972	Lagoonal deposits	Pollen correlation stratigraphic correlation	−48.8	−0.5	+1	−5	This paper
202	Belfiore PRA	45.774417, 12.713000	Base of lagoonal deposits	Pollen correlation stratigraphic correlation	−52.5	−0.48	±2		This paper
203	Torre di Mosto TdM	45.621667, 12.756111	Base of prodelta-inner platform	Pollen correlation stratigraphic correlation	−70.5	−0.54	+1	−5	This paper
204	Portegrandi	45.549028, 12.433833	Base of neritic to lagoonal deposits	Stratigraphic correlation	−71.0	−0.58	+1	−5	Tosi et al., 2007
205	Malamocco	45.336544, 12.326236	Base of interdistributary bay deposits	Stratigraphic correlation	−86 m	−0.69	±5		This paper
206	Valle Averto	45.352278, 12.137500	Base of lagoonal deposits	Stratigraphic correlation	−63.6	−0.57	±2		Donnici and Serandrei-Barbero, 2004
207	Tirrenia, Core M1	43.629775, 10.288722	Base of lagoonal deposits	Pollen correlation stratigraphical correlation supposed MIS 5.5	−102 m	0.77	±10		Aguzzi et al., 2007
208-209	Versilia	43.800, 10.317	*Cladocora coespitosa* in core	MC-ICP-MS U-Th age: 195.7 ± 1.6 ka, MIS 7.1	−72.8	−0.22		−10	This paper
210	Tavolara	40.921111, 9.733889	Notches	Stratigraphic correlation	6.8–7.2	Stable	±0.1		This paper

Comparison of the current elevations of the markers (i.e., the relative sea-level change at each location) with the sea-level elevation predicted by two models at each location readily identifies stable sites from sites affected by deformation. Tectonic stability is inferred at sites where the elevations of the markers are in agreement with the predicted sea-level curve. Conversely, tectonic subsidence or uplift is indicated where the elevations of the markers are below or above those of the predicted sea-level curve, respectively. Concerning the new MIS 5.5 markers, the base of paralic sediments retrieved in cores is used as altitude reference.

4. Data analysis

4.1. Istrian, Friulian and Venetian Plain

4.1.1. Holocene

Late Holocene sea-level indicators in the NE Adriatic coast (Italy, Slovenia and Croatia) are submerged because of tectonic subsidence. In Istria and Trieste coast, sea-level data have been obtained using precise measurements of six submerged Roman archaeological sites dated ~2.0 ka (Antonioli et al., 2007) and five ^{14}C dates of lagoon fossils and organic carbon from marine cores or outcrops in urban archaeological surveys (Ogorelec et al., 1997; Covelli et al., 2006; Furlani et al., 2007) (Figs. 5 and 6).

On the Brijuni islands (Croatia, Fig. 6), archaeological excavations performed during the 1990s documented the architecture of the underwater structures and determined the period of use. Measurements indicate a relative sea-level rise of 1.80 ± 0.60 m for the foundation and 1.60 ± 0.60 m for the pier's upper surface (Table 1, sites 1 and 2).

In Sicciole (Croatia) (Table 1, sites 3 and 4, Fig. 6), two large piers and an underwater terrace suggest a sea-level change of 1.50 ± 0.60 m. In San Simone (Izola, Slovenija) (site 5), a Roman pier is the best sea-level indicator of the area. The pier shows three layers of large stone blocks. The presence on the upper layer of large mooring rings suggests a relative sea-level rise of 1.60 ± 0.60 m. In S. Bartolomeo (Slovenija) (site 8), the preservation of the ancient walking surface on the eastern side of a large fish-pond at −0.8 m indicates a sea-level rise of 1.40 ± 0.60 m. At Punta Sottile (site 9) the Roman sea level has been obtained from a pier. The structure suggests a relative sea-level rise of 1.60 ± 0.60 m. At Stramare (Italy, site 10, Fig. 6), an anthropogenic terrace suggests a sea-level rise since Roman time of 1.60 ± 0.60 m. In the Bay of Koper, during an engineering excavation (Župančič, 1985), a sample of *Cardium* sp. was collected at −1.24 m (Table 1, site 7) and was dated at 1367 ± 83 BP (Ogorelec et al., 1997).

The following sedimentological indicators from cores and coastal deposits when compared with predicted sea level curve would suggest the absence of tectonics in some areas of the Gulf of Trieste: wood in a peat layer from core V6 in the Sečovljie Plain, (Koper Bay) (site 5), which provided a ^{14}C age of 9180 ± 120 BP at −26.5 m; two samples of *Bittium reticulatum* aged 2065 ± 120 BP at 0 m a.s.l. and 2020 ± 120 BP at +0.10 m (Table 1, sites 11 and 12); a ^{14}C age of mottled peat at –25 m (9140 ± 40 BP) in core GT1 (site 13); and a *Cerastoderma glaucum* lagoonal shell at −26 m (8810 ± 40 BP) in core GT3 (site 14).

In the Venetian-Friulian plain new stratigraphic information about the Holocene sea-level position were obtained from lagoonal deposits found in boreholes between Tagliamento River and the city of Venice (Fig. 6). Other data are derived from the abundant literature available for the Venice lagoon and its mainland (Serandrei-Barbero et al., 2001; Bondesan et al., 2002, 2003, 2004; Donnici and Serandrei-Barbero, 2004; Canali et al., 2007). Most of the dated samples correspond to the base of the Holocene lagoonal deposits, which generally overlie the Last Glacial Maximum alluvial plain deposits (Mozzi et al., 2003; Fontana et al., 2008). The stratigraphic features considered as sea-level markers are the top of the organic or peaty horizon representing transgressive swamp or salt marsh deposits or shells embedded in fine-grained lagoonal deposits.

A particular setting characterizes the area of sites Concordia-Sepolcreto (samples 16–18 from a single core, Fig. 6) and Concordia-Paludetto (samples 19–20 from a single core), where two fluvial incisions were developed and abandoned by the Tagliamento River between the Lateglacial and the early Holocene. Sea-level rise caused the lagoon to submerge these pre-existing valleys (Fontana, 2006; Fontana et al., 2008). The base of lagoonal deposits is recorded at −6.85 m in Sepolcreto (sample 17), with a radiocarbon age of 5700 ± 70 BP, and at −8.59 m in Paludetto (sample 20) with an age of

Author's personal copy

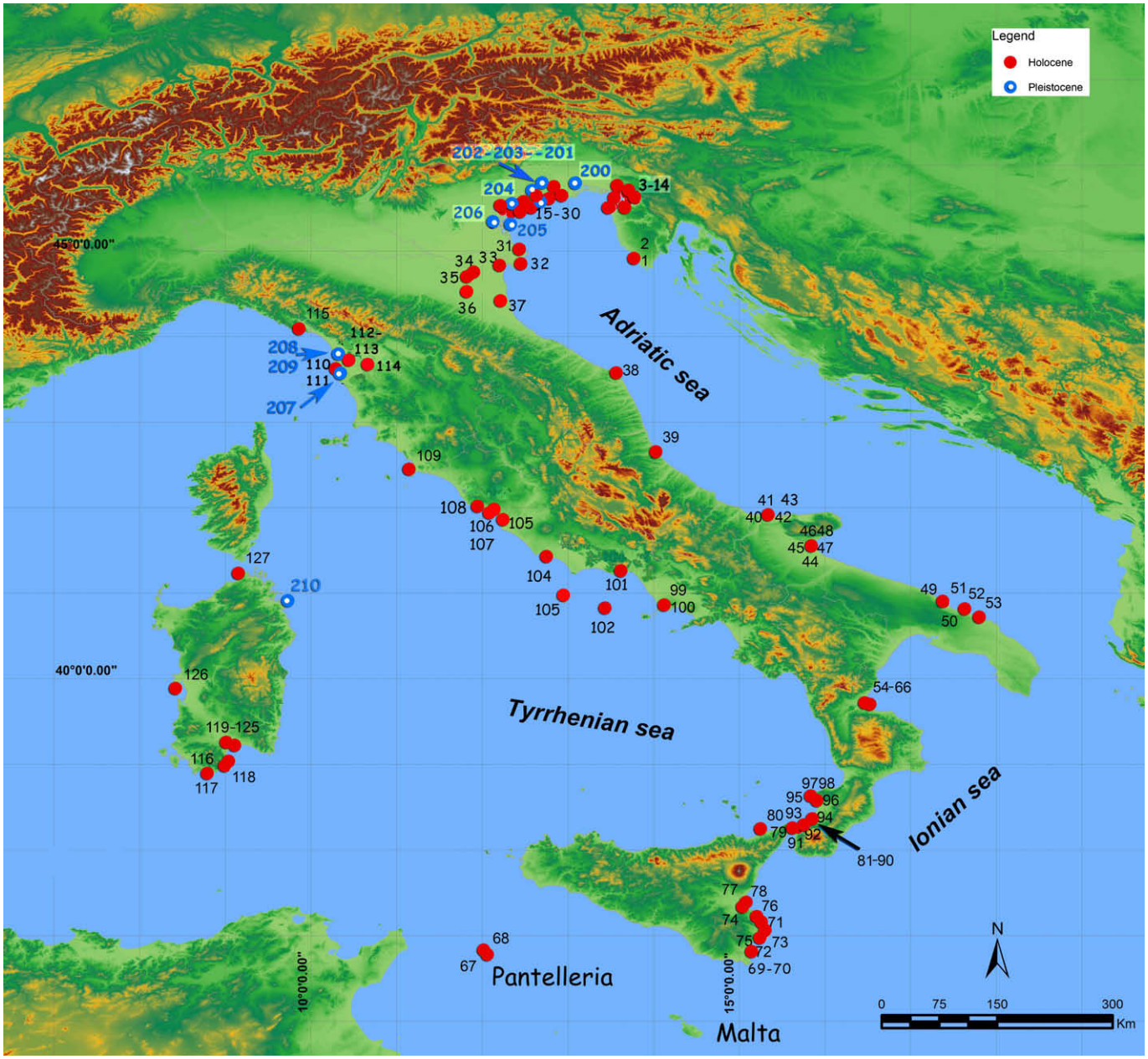

Fig. 5. Map of the Holocene and MIS 5.5 sites discussed in this paper with site numbers.

5910 ± 70 BP (Fontana, 2006). In Sepolcreto (sample 16) a salt marsh peaty horizon dated to 4080 ± 70 ^{14}C years is found at −5.0–5.05 m and a base-level swamp peat dating to 1800 ± 60 BP at −2.8–2.9 (sample 18). In Paludetto a similar stratigraphy has been described, with minor differences in age and vertical position; the base of the coastal swamp horizon has an elevation of −3.79 m and dates to 1920 ± 60 BP (sample 19), whereas the salt marsh peaty horizon at −5.60–5.80 m has not been dated yet (Fontana, 2006).

In the present lagoon of Caorle the base of Holocene lagoonal deposits was observed at −5.15 m (site 15) and at −8.55 m in the adjacent reclaimed area of site 21, with an age estimate of 5730 ± 45 and 6080 ± 80 BP, respectively (Fontana, 2006). Between Livenza River and the north-eastern fringe of the lagoon of Venice the boundary between LGM alluvialplain and lagoonal deposits has been found at −9.2 m in site 23, with a ^{14}C age of 6580 ± 55 BP, and at a shallower depth for the younger dated levels of site 22 (3570 ± 70 BP at −2.5 m) and site 24 (3140 ± 40 BP at −3.8 m) (Bondesan et al., 2002, 2003).

At site 25 the ingression of the lagoon along a little groundwater-fed river submerged the wooden bridge crossing the channel and the adjacent path of the Roman road named via Annia. The lagoonal sediments cover artifacts dating to the first half of the 1st century BC and at their top some remains of the 1st century AD are present (Bondesan et al., 2004). Moreover, damage to the road forced building of a new pathway 200 m landward in the first part of the 1st century AD. This setting indicates a sea-level rise of 1.6 ± 0.60 m since that period.

In the eastern sector of the Venice lagoon, Canali et al. (2007) found the base of lagoonal deposits at −10.15 m and −12.9 m in cores BH2 and BH1, which gave ages of 6740 ± 50 BP (site 26) and 6840 ± 40 BP (site 28), respectively. On the island of Burano (site 27) the lagoonal deposits overlie the LGM alluvial plain deposits at

Author's personal copy

Fig. 6. Map of the Northern Adriatic Sea with the distribution of the sites considered in the research. a) Alluvial and coastal sediments; b) pre-Quaternary bedrock; c) area of cores from Correggiari et al., 1996; d) main cities; e) sites with Holocene sea-level marker (Refs. Table 1); f) sites with MIS 5.5 sea-level marker (Refs. Table 2; sites from southern delta Po are from Ferranti et al., 2006); g) core with continental deposits during MIS 5.5, A: Azzano, B: Faenza, C: Imola; h) isobath line; i) most inner margin of Holocene lagoon; l) most landward position reached by the Holocene coast; m) inner margin of MIS 5.5 lagoon (A from Zanferrari et al., in press; (i, l and m from Amorosi et al., 2008c). The color of the circles refers to the subsidence rate, expressed in mm/a. In grey, the area studied by Correggiari et al., 1996.

−4.2 m, with an age of 4120 ± 40 BP (Lezziero, 2002). In the subsurface of Venice, the base of lagoonal deposits in San Marco square (site 30) has a depth of −5.8 m and an age of 4670 ± 70 BP (Serandrei-Barbero et al., 2001). Along the inner margin of the lagoon of Venice, one of the youngest datings of the base of lagoonal deposits has been detected in the industrial area of Marghera (site 29), where the boundary with alluvial plain deposits dates to 1095 ± 55 BP and lies at −1.50–1.65 m.

4.1.2. MIS 5.5

Several new sites related with sea-level position during MIS 5.5 are presented. These have a fairly good W–E distribution along

Author's personal copy

the distal sector of the plain. Some are introduced in this paper (Fig. 6, Table 2, sites 201, 202, 203, 205), whereas other data were obtained from published deep boreholes (Table 2, sites 200, 204, 206). The new stratigraphic data were obtained from boreholes mainly drilled for the Geological Map of Italy (CARG-Veneto Region) (Fontana, 2006; Fontana et al., 2008) as well as for the MOSE Project by Venice Water Authority (Fontolan et al., 2007). Due to the recent stratigraphic drilling carried out in the Friulian plain, the base of the lagoonal sediments intercepted in the core of Piancada between −38 and −58 m (Feruglio, 1936) could be correlated to MIS 5.5.

Lagoonal sediments between −37 and −49 m have been found on the borehole carried out in in the area of the Roman theatre (Table 2, site 201) inside the Roman city of Concordia Sagittaria, between Sepolcreto and Paludetto (samples 16–18 and 19–20, Table 1); although the drilling did not reach the boundary with the underlying alluvial plain deposits, stratigraphic and pollen correlation, with an error bar of ±5 m, allow assignment of these deposits to MIS 5.5.

One of the most important sites to determine sea-level position during the peak of MIS 5.5 transgression in the western Friulian plain is the Belfiore core, which is characterised by lagoonal sediments between −46 and −51 m. These deposits overlie a fairly developed palaeosol formed on top of the MIS 6 alluvial plain. In the Azzano core (site A in Fig. 5; Zanferrari et al., in press) 6 km north of Belfiore, only continental deposits have been found since the end of middle Pleistocene, but pollen analyses support chronostratigraphic correlation between MIS 5.5 alluvial deposits found in Azzano and the lagoon sediments of Belfiore. This allows tracing of the inner margin of the MIS 5.5 lagoon, which marks the peak of the transgression (Fig. 6).

About 20 km south of Belfiore, in borehole Torre di Mosto, a succession of prodelta to lagoonal deposits, with an erosional lower boundary on the MIS 6 alluvial plain deposits, lies between −72 and −44 m. A similar succession has been described in Portegrandi (Tosi et al., 2007), where the boundary between alluvial plain and neritic deposits has a depth of −71 m; from −71 to −65 m the transition to lagoonal facies is observed, followed by delta-front sediments up to −55 m (Tosi et al., 2007). In core Valle Averto lagoonal deposits of MIS 5.5 have been recognized between −63.3 and −60.45 m, overlying the alluvial plain deposits of MIS 6 (Donnici and Serandrei-Barbero, 2004).

Borehole CVN-CH1 M, located within the Malamocco Inlet (Venice, Fontolan et al., 2007), reached −100 m below m.s.l. The core lacks the Holocene sedimentary succession, due to the erosional effect of the inlet, but recovered the complete transgressive–regressive MIS 5.5 cycle between 86 and 69 m below m.s.l. The base consists of a bioturbated mud facies (interdistributary bay), overlain by laminated inner prodelta silts, which represent the maximum flooding deposits, settled slightly below the local closure depth (−6 to −7 m). The overlying coarsening-upward succession testifies the terminal phase of MIS 5.5 regression, culminated with coastal medium sand deposits at −69 m below m.s.l. A subsequent 18-m-thick sand without any marine fossils may represent a phase of subaerial deltaic progradation. The depth of the base of the MIS 5.5 paralic deposits found in the cores Portegrandi (Table 2, Fig. 5, site 204, Tosi et al., 2007), Valle Averto (site 206, Donnici and Serandrei, 2004), Venezia Malamocco (site 205) and Venezia (Kent et al., 2002; Massari et al., 2004), shows considerably different elevations between −63.6 and −86 m.

Between cores Valle Averto and Venice a difference of about 15 m exists, while their planimetric distance is only 10 km. A similar difference is apparent between the core Venezia Malamocco (site 205) with Portegrandi (site 204) which are also 10 km apart. These differences in depth could be explained according to the erosive morphology which shaped the pre-existing alluvial plain before or during the trasgression.

4.2. Romagna and the Po River Delta

Despite the abundant literature on the Holocene stratigraphy of the Adriatic coastal plain south of Po River Delta (Romagna coastal plain), the stratigraphic architecture in the subsurface of the present delta system is poorly known. New stratigraphic data in this area are derived from two continuously cored boreholes, about 35 m deep, that were recently drilled at Boccasette (Core 3, site 31) and Barricata (Core 1, site 32), beneath the modern delta plain (Amorosi et al., 2007, 2008b) At these locations, two ^{14}C ages of 8495 ± 55 BP and 8404 ± 100 BP, respectively, were obtained from transgressive swamp deposits collected at about 30 m depth (Table 1, sites 31–32).

In a relatively landward position (Romagna coastal plain), the Holocene transgression is recorded at comparatively shallower depths (about −25 m), within similar paludal deposits dated to 8220 ± 60 BP at Pomposa (Core 187-S1, site 33, in Bondesan et al., 2006), and 8170 ± 50 BP at Ravenna (Core 223-S1, site 37, in Amorosi et al., 2005). At all these sites, early transgressive deposits invariably overlie an alluvial plain succession assigned to the Last Glacial Maximum. The boundary between these two facies associations is an unconformable surface, corresponding to an indurated and locally pedogenized horizon.

Recent correlation of millennial-scale depositional cycles from the subsurface of Romagna coastal plain has enabled identification of the Holocene transgressive deposits up to 30 km landward of present shoreline position (Amorosi et al., 2005). In this case, lagoonal and swamp clays collected at an approximate depth of 15 m provide ages of 6895 ± 80 and 7735 ± 50 BP, respectively (sites 34–35). A lagoonal deposit with fossils *Cerastoderma* was sampled in a core at −9 m 27 km inland (site 36): its age is 5600 ± 50 BP.

In the Adriatic Sea east of the Po Delta, Lambeck et al. (2004a) compared the predicted sea-level curve to many data (Correggiari et al., 1996) from sediment cores that have yielded 23 depth–age datapoints within the depth interval from 26 to 52 m with radiocarbon-based ages of 9.3–12.9 ka cal. BP. The analyses carried out on lagoonal-marsh deposits, compared with the predicted sea-level curve indicate tectonic stability for the entire area (Figs. 1 and 6).

Concerning the position of the MIS 5.5 highstand body, the linkage between coastal and lagoonal deposits is well established on the basis of stratigraphic correlation of long-cored sedimentary successions, up to 200 m thickness, from the Romagna coastal plain (Amorosi et al., 2004). Two new deep boreholes (S1 and S2) from Imola and Faenza areas, drilled by Regione Emilia-Romagna, as part of Geological Mapping project of Italy at 1:50,000 scale (Sheet 239), display the vertical stacking of alluvial (fluvial-channel and floodplain) facies, with no intervening brackish-water deposits (A. Amorosi, unpublished data). This allows tracing the 5.5 shoreline north of these cores.

4.3. Central and southern Adriatic coast of Italy

Different kinds of markers tracking the Holocene sea-level history are found in this wide coastal area. However, large stretches of coast lack accurate sea-level markers and reliable chronological constraints (see for instance: Mastronuzzi and Sansò, 2002b, 2003). Data derived from geomorphologic and archaeological surveys performed in five different sites in Marche (site 38), Abruzzo (site 39) at the boundary between Molise and Puglia (sites 40–43), central (sites 44–48) and southern Puglia (49–53) were used. These data include both sea-level and less specific coastal markers (Antonioli and Leoni, 1998; Auriemma et al., 2004).

A Roman age fishtank (2 ka BP) in site 38 was recently measured at an altitude of −1 m b.s.l. (Profumo, 2007). Further south, in site 39, earliest Holocene continental peat has been encountered in borehole at ∼18 m b.s.l. (Parlagreco et al., in press), thus limiting the coeval sea-level rise landward.

Author's personal copy

At the boundary between Molise and Puglia, the Fortore River built its coastal plain around the Punta delle Pietre Nere headland. Here, a columnar bioconstuction some hundred metres wide and characterised mainly by calcareous algae and globular colonies of *Cladocora coespitosa* is found up to ~1 m a.s.l. (sites 40–43). Samples of *C. coespitosa* collected at 0.50 m a.s.l. yielded a ^{14}C age of 5950 ± 110 years (Table 1). Moreover, the same bioconstruction is colonised by sparse vermetids and *Lithophaga* sp.; in their lowest part a continuous band of *Dendropoma* sp. is at about 0.30 m a.s.l. ^{14}C dating of the superposed *Lithophaga*, vermetid and *Dendropoma* yields different yet more recent ages than the *Cladocora* bioconstruction. These relations can be interpreted with different phases of coseismic emersion (Mastronuzzi and Sansò, 2002a), consistent with active thrusting in the Gargano area. Along the Tavoliere coastal plain different archaeological and palaeontological data coming from sites 44 to 48 in Palude Frattarolo (Table 1) are consistent with a Late Holocene relative sea-level rise; in particular, the finding of lagoonal deposits characterised by *C. glaucum* indicate different phases of transgression (Caldara et al., 2002; Caldara and Simone, 2005).

Along the coast of the Murge block three archaeological sites preserve land indicators used to constrain the coeval shoreline location (Auriemma et al., 2004, 2005; Milella et al., 2006). In the Egnatia harbour area (sites 49–51), tombs and quarries of Messapic age (2450 ± 50 BP), cisterns, sewers and harbour structures of Roman age (2000 ± 100 BP) and quarries of Medieval age (500 ± 100) are at present at a few cm b.s.l. (Table 1). These findings are confirmed in the Santa Sabina harbour area, ~40 km to the south (site 52) (Auriemma et al., 2005). Finally, in site 53, pile holes of huts belonging to a settlement ascribed to the Bronze Age (3750 ± 250 BP) have been found between 0.5 and 2.5 m b.s.l.

4.4. North-eastern Calabria coast

Few data on the Holocene relative sea-level change are available in Northern Calabria, and they all come from a spatially limited area of subsidence on the Ionian Sea coast. Dated Holocene markers are located in the area of the archaeological site of Sybaris, where historical subsidence is documented by the vertical stacking of three archaeological levels (Pagliarulo et al., 1995).

The historical subsidence has been traced to the Latest Pleistocene-Early Holocene by means of several boreholes, which crossed lagoonal deposits grading downward to littoral deposits, including several peat levels. Ages published by Pagliarulo (2006) from peat, organic-rich mud or shell sampled within four different boreholes (three in the archaeological area along the Crati River and the fourth ~1 km to the northwest, sites 54–65) were recalibrated (Table 1). These ages established a pattern of near equilibrium between the competing effects of sea-level rise, regional uplift and local subsidence due to compaction of the peat layers and backshore lagoonal mud. However, a locally intense difference is found between boreholes located either away (samples 54 and 55, from a single core) or close to (samples 56–65, with the exception of site 60, coming from the remaining three cores) the ancient town and the Crati River course. In general, whereas data from the ancient town document a larger subsidence, the site away from the backshore/floodplain environment has a lesser downlift or even a small uplift (datapoints 54–55). Similar results were obtained by Cucci (2004) using these four plus two additional published boreholes. The large subsidence in the archaeological site is attributed to differential compaction (Cucci, 2004; Pagliarulo, 2006). However, the very large subsidence reported from many boreholes may result from the drilled mud reflecting a floodplain rather than a coastal envirnment.

A new age was obtained from a shell of *Donax* sp. which was attached at −1.14 m b.s.l. on the external wall of Casa Bianca (Randisi, 2007), the more seaward section of the ancient town (site 66). This wall, during the 1st century B.C., enclosed a small settlement abutting the ancient coastline (Greco and Luppino, 1999). The wall was sitting on a previous basement, but accurate archaeological age constraints are lacking. This settlement includes a paved towpath which probably hosted small boats when not used, in a manner similar to the present-day usage. The shell calibrated age of ~1.3 ka confirms ongoing subsidence after abandonement of the settlement.

4.5. Sicily Channel, Eastern Sicily and Southern Calabria coast

In the Sicily Channel (Fig. 5), according to historical reports, the north-eastern coastal sector of the volcanic Pantelleria Island was strongly uplifted up to 1 m a.s.l. since one year before the onset of the October 1891 offshore eruptive event. In order to verify the occurrence of uplifted coastal sectors, detailed mapping of morphological and biological indicators of raised palaeo-shorelines was carried out all over the island coastlines (see also De Guidi and Monaco, 2009). This survey confirmed the occurrence of the observed raised shoreline and allowed to identify two additional palaeo-shorelines located at elevations of 1.5–2.7 m a.s.l. and 2.5–4.3 m a.s.l., respectively. Radiocarbon dating on samples of corals and vermetids placed tight time constraints on the uplifting of the raised shorelines. In particular, two samples of *Dendropoma petraeum* collected at elevations of 4.2 m (site 67) and 2.2 m (site 68) yielded ages of 1360 ± 30 and 1155 ± 30 BP, respectively.

In south-eastern Sicily (Fig. 7), data on relative sea-level change have been obtained by analysis of boreholes from lagoonal deposits (see also Monaco et al., 2004; Scicchitano et al., 2007) and by measures of submerged archaeological markers and of speleothems collected in submerged karstic caves (see also Scicchitano et al., 2008). In the south-eastern corner of Sicily (Vendicari lagoon) the ^{14}C AMS dates for a *C. glaucum* sampled in a borehole at −5.40 m b.s.l. and a *Cerithium vulgatum* sampled at −6.90 m b.s.l. gave ages of 4610 ± 40 and 4890 ± 40 BP, respectively (sites 69 and 70).

A submerged speleothem was collected at site 71, located along the Syracuse coast, at about −22 m depth. Numerical age determination of the last marine encrustation on this speleothem was carried out on a sample taken from the base of the Serpulid crust coating the stalagmite at −20.22 m corrected depth, and yielded an age of 7780 ± 230 BP (Schiccitano et al., 2008). As Serpulids colonize quite quickly after a cave becomes inundated (Antonioli et al., 2001), this age represents a precise time estimate of cave submergence during the last transgression.

A partially submerged Bronze Age tomb located at site 72 shows its floor at −1.21 m below the present sea level. Taking into account that the palaeo-sea level was at least 0.60 m lower than the original floor, the relative sea level should have been at −1.81 m depth 3.5 ± 0.3 ka ago. This value can be compared to that obtained by the palaeo-topography of the Ognina bay site 73, which is characterised by sea-bottom maximum depths of −2.97 m (corrected for tide and pressure). In the Bronze age (3.5 ka ago), the sea level was 3.5 m lower than the present (Lambeck et al., 2004a). The channel bottom should have been emergent, unless tectonic uplift has occurred in the intervening time. Taking into account that the ships that used these coastal structures could have had a possible draught of about 1.0 m (Antonioli et al., 2007) and assuming negligible sediment accumulation since the Bronze Age, the relative sea level should have been not more than 1.97 m lower than the present, which might fit with the maritime topography analyzed. Another important marker for identifying sea level comes from old Greek quarries located in the site 74. Their floor is at a corrected maximum depth of 0.38 m below sea level and considering that the palaeo-sea level was at least 0.60 m lower than the anthropogenic platform (0.30 m above high tide to be always dry), the relative sea level should have

Author's personal copy

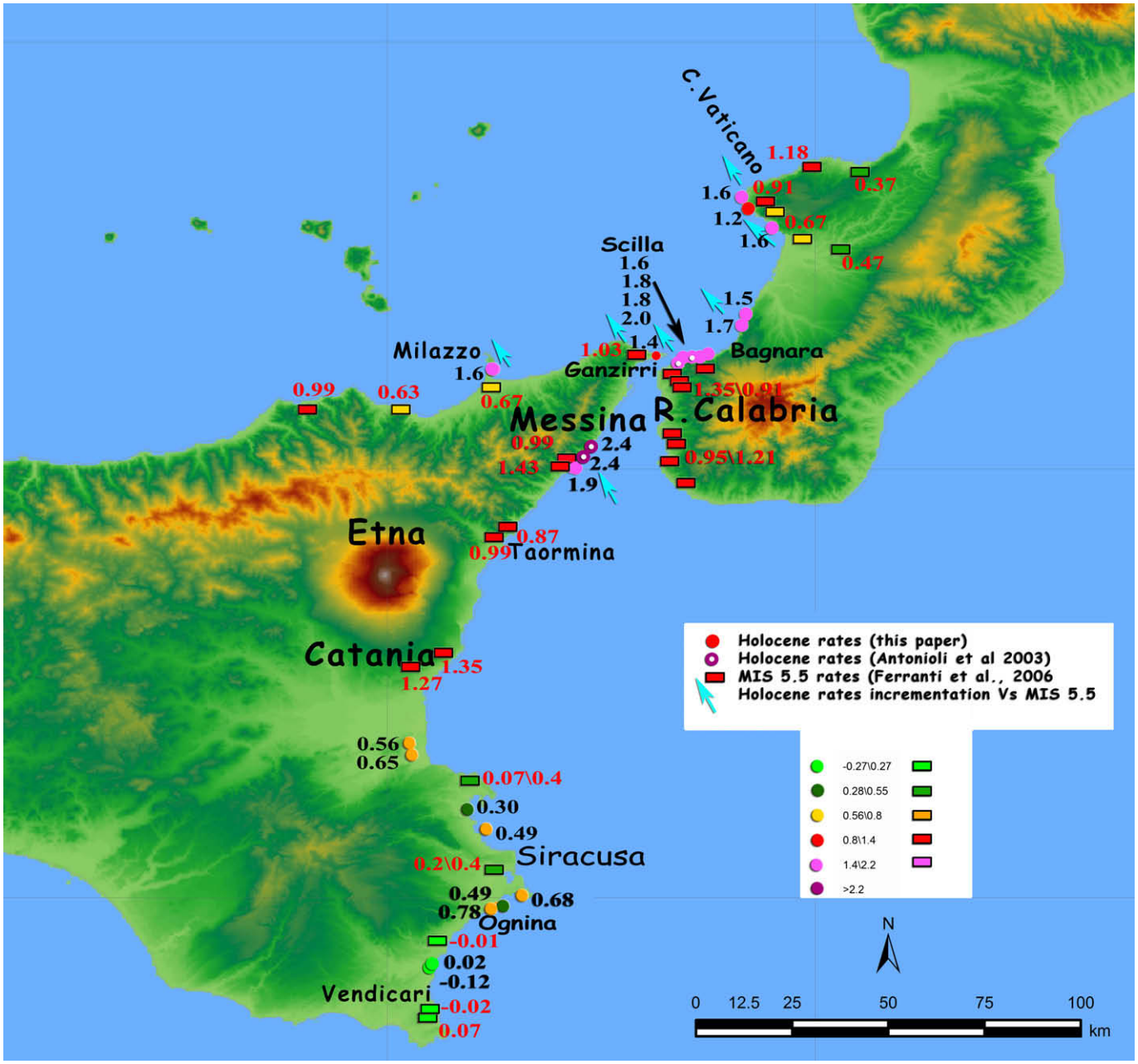

Fig. 7. A Detailed map of Eastern Sicily and southern Calabria showing Late Pleistocene and Holocene site uplift rates.

been at −0.98 m depth 2.6 ± 0.1 ka ago. For the ground-plan of a partially submerged Bronze Age tomb at Thapsos site 75, a corrected value of −0.43 m has been estimated. Considering a functional height of 0.60 m, the palaeo-sea level should have been at ≤−1.03 m depth. A significant marker is represented by the old Greek archaeological site 76 of Megara Iblea. The pier head is located at −0.88 m and considering a functional height of 0.60 m, that is 0.30 m above high tide (+0.30 m) to be always dry, the relative sea level should have been at −1.48 m depth 2.6 ± 0.1 ka ago.

In the Catania Plain, the ^{14}C AMS dating of a bivalve fragment sampled in a borehole at −7.20 m b.s.l. and a *Cerastoderma* sp. sampled at −37.90 m b.s.l. yielded ages of 6343 ± 41 and 9110 ± 50 BP, respectively (sites 77 and 78).

In north-eastern Sicily (Figs. 5 and 7), new data on relative sea-level change have been recently obtained on the eastern side of Capo Peloro facing the Messina Straits (Ganzirri, site 79, Table 1), Here, uplifted conglomerates crop out at elevations from −2 m to +0.70 m relative to present sea level. Serpulids encrusting the conglomerate were sampled close to the maximum elevation of the deposit and yielded an age of 5557 ± 47 BP. This age is confirmed by archaeological remains younger than 5 ka (Antonioli et al., 2004a) associated with the sand that covers the conglomerate. Not far from this site, uplifted upper infralittoral gravel deposits occur in the Milazzo peninsula (site 80, Table 1), where ^{14}C dating on a specimen of *Patella* sp. sampled at 2 m. a.s.l. showed an age of 5665 ± 36 BP (Gringeri et al., 2004).

In southern Calabria (Fig. 7) new data derive from the Scilla–Palmi coast and the Capo Vaticano area. Along the Scilla–Palmi coast two Holocene uplifted shorelines have been identified (Antonioli et al., 2004a; Ferranti et al., 2007). The upper shoreline is represented by a wave-cut platform locally covered by fossiliferous beach deposits including intact or fragmented bioclasts. At Marina di San Gregorio (site 81–85), the upper shoreline is conservatively estimated at 3.65 m a.s.l. halfway between the upper limit of the

Author's personal copy

beach sands and the upper limit of fossil shells observed in the deposit. Conversely, the availability of several elevation constraints allows a robust elevation estimate at ~2.9 m a.s.l. for the upper shoreline at Punta Paci (site 86–92; Table 1), although the nominal uncertainty is large. On the coastline between Palmi and Bagnara, the upper shoreline elevation sharply decreases to ~2.2 m a.s.l. at site 93 (Table 1).

The lower shoreline is characterised by a prominent barnacle band, and locally by a wave-cut platform. The band lies at different elevations ranging between ~0.8 and ~1.8 m a.s.l. This variability reflects both differences in environmental energy and lateral variations in tectonic displacement. In the Scilla area (sites 81–92), the elevation markedly changes across a few tens of metres from ~0.8–1.9 m a.s.l. on a relatively sheltered platform to ~1.7–2.9 m a.s.l. within a surge channel. At the platform site, an algal rim bored by *Lithophaga* holes is found at ~1.4 m a.s.l. below the denser patch of the barnacle band, and only isolated individuals are found beneath. Similarly, in the Palmi area (site 94) the band varies in elevation from ~0.9–1.8 to 1.5–2.5 m a.s.l. across a short distance. Duration of the lower shoreline is tightly constrained by ages of barnacles between 3.5 and 1.9 ka, and its inception is in good agreement with cessation of the older shoreline (Ferranti et al., 2007).

At Capo Vaticano, two ages of 5.5 and 5.8 ka from shells sampled at about 1.6–1.8 m (sites 95 and 96) published by Antonioli et al. (2006) were supplemented by two new radiometric determination from shells sampled at 0.6 and 1.6 m, which yielded ages of 3.9 and 5.7 ka, respectively (sites 97 and 98).

4.6. Central Tyrrhenian coast (Area 6)

Sites 99 and 100 are located in a famous and very unstable area of the Campania region. Here during the past 2 ka yrs, vertical movements (bradysism) of several metres have occurred in the active volcanic caldera of the Phlegrean Fields in Pozzuoli Bay. Morhange et al. (2006) sampled and dated (1235 and 2250 BP) some fossil shells, on marble columns of Roman age at an elevation of about 7 m a.s.l.

In the north, along the Latium coast, several Roman age fish tanks were accurately measured at a depth of between −1.04 and −1.35 m b.s.l. (Lambeck et al., 2004b). This archaeological marker is considered one of the most reliable sea-level indicators with a very low error bar, and a selection of seven sites is considered in this paper (Figs. 4 and 5, sites 101–106 and 109). In southern Tuscany, at the Etruscan site of Pyrgi, two novel data are represented by a water cistern whose opening presently lies at −0.25 m b.s.l., and a terrace hosting hut holes found at −3.5 m b.s.l. (sites 106–107). The cistern and hut holes have been assigned an early Roman (2400 yrs BP, site 107) and Early Bronze (~4700 BP) age, respectively (Enei, 2008). A functional height of 1 m is assigned to both sea-level markers.

4.7. Northern Tuscany and southernmost Liguria coast (Area 7)

New stratigraphic data from the subsurface of the Arno coastal plain have recently documented the presence of an incised-valley fill of Holocene age, 30–40 m thickness. The valley body, which is recognized approximately beneath the present Arno River, can be physically traced landward of the Tyrrhenian coast in the subsurface of Pisa and Pontedera (Aguzzi et al., 2007; Amorosi et al., 2008a). A huge thickness (50–55 m) of Holocene deposits is the diagnostic stratigraphic feature of the valley fill, while less than 20 m of Holocene sediments are generally recorded on the interfluves.

A radiocarbon date of 10,004 ± 50 BP has been recorded at a depth of about 51 m at the base of the Holocene transgressive succession within the 105 m long Core M1 (Figs. 4 and 5, Table 1, site 110). Higher up in the stratigraphic column (Table 1, site 111), an age of 8840 ± 75 BP has been obtained from estuarine deposits (Aguzzi et al., 2007).

Transgressive deposits flooring the palaeovalley can be traced a few tens of km upstream, in the Pontedera area (Core CC in Aguzzi et al., 2006), where a radiocarbon age of 10.106 ± 60 years BP is recorded at about 55 m depth within swamp deposits (Table 1, site 114). Close the town of Pisa (Core S1, 56 m thickness), lower estuarine deposits at about 45 m depth have been dated to 11,034 ± 63 BP (Amorosi et al., 2009), while lagoonal deposits above the incised-valley fill, at 13.5 m depth, have provided an age of 7370 ± 60 BP (Table 1, sites 112 and 113). Concerning the position of MIS 5.5 deposits in the Arno plain, Aguzzi et al. (2007) have documented from Core M1, at about 102 m depth, the presence of a transgressive *suite* of lagoonal and transgressive barrier sands, overlain by prograding, highstand delta-front deposits. This transgressive–regressive succession, which is separated from the Holocene marine deposits by about 40 m of continental deposits, is assigned to MIS 5.5 on the basis of integrated stratigraphic and pollen data (Table 2, site 207).

Lambeck et al. (2004a) found an excellent agreement between the model-predicted sea level and the observational evidence (mainly lagoonal shells) in the ENEA core located in the Versilian Plain, indicating tectonic stability in this area during the Holocene. Hence, this core has become a regional reference for the marine Holocene transgression in the Mediterranean Sea. However, MIS 5 ages for some corals found lower in the core suggest subsidence over this longer timescale, but the available ages are imprecise.

To better understand the older marine trasgressions and the tectonic assesment, new U-Th analyses using a multi-collector inductively coupled mass spectrometer (MC-ICP-MS) on two different Cladocora layers from the ENEA core: at −72.8 and −68.5 m are presented. These samples were analyzed following the procedure described in McCulloch and Mortimer (in press). Results indicate older ages (195.7 ± 1.6 and 161.2 ± 1.2 ka, respectively) relative to the MIS 5.5 ages published in Nisi et al. (2003), which were based on alpha-counting U-Th data. However, the shallower (and younger sample) has a very low initial δ234U value (~108 permil) compared to that of modern seawater, indicating that it may be altered. The other sample, which gave the MIS 7.1 age, has a slightly low δ234U value (~140 permil). However, this value is within an acceptable range of the modern composition and hence is regarded as reliable. Given the absence of evidence for a regression between these two samples in the core, it is likely that the shallower sample is also from MIS 7.1 (see Table 2, sites 208 and 209).

At La Spezia (Liguria), the channel of a pier was recently measured at −0.41 m (Chelli et al., 2005). A functionality of 44 cm (mean of the Italian tide) was added (Table 1, site 115).

4.8. Sardinia coast (Area 8)

Antonioli et al. (2007) recently provided new data on relative sea-level change during the late Holocene from twelve locations in Sardinia. These are based on precise measures (applying corrections for tide and atmospheric pressure values at the time of surveys) of submerged markers, such as piers, thombs, and quarries, aged between 2450 and 1600 BP, located along the coast.

The following markers were studied and measured *in situ*: amphorae at Santa Gilla at −2.00 m (site 125); a quarry at Perdesali at −1.32 m (site 119); the pavement of a Basilica and a pier at Nora, at −1.02 and −1.42 m, respectively (sites 117 and 118); a 400-m long breakwater dock at Capo Malfatano (site 116) at −2.10 m; a tumb at Tharros at −1.35 m (site 126) and a pier at Capo Testa (site 127) at −1.20 m.

Author's personal copy

A core was recovered near the town of Cagliari (Orrù et al., 2004). The core crossed Holocene marine deposits containing lagoonal fossils. Five samples were sampled at a height between −34 and −7.8 m. ^{14}C analyses provided ages between 4090 and 9050 BP (sites 120–124). For MIS 5.5, 11 new measures were determined from a well-developed tidal notch carved on the limestones at Tavolara island (eastern side of the island), which lies at an elevation between 6.9 and 7.8 m (Table 2, site 210).

5. Isostatic model, and comparison of predicted and observed RSL data

In a dynamic Earth, sea-level variations driven by the melting of large continental ice sheets depart from eustasy because of solid Earth deformations and geoid height variations, which result from time-dependent variations of ice and water loads on the Earth surface. The description of the interaction between the solid Earth, gravity field and the cryosphere, has been given in the seminal work of Farrell and Clark (1976), who provided a self-consistent theory of glacio and hydro-isostasy also taking into account for the effects of the delayed response of the mantle due to delayed visco-elastic effects. Solving the resulting fundamental equation (the so-called "Sea-Level Equation") shows a large spatial and temporal variability of relative sea-level variations in various parts of the globe, which is an integrated effect of mantle rheology, the complexity of the ocean-continents distribution, and of the deglaciation time-history. A review of the physics behind the Sea Level Equation and of applications to the interpretations of post-glacial sea level change is beyond this paper. For a discussion of the history of Holocene sea level in the Mediterranean, the reader is referred to Lambeck et al. (2004a) and references therein, while an in-depth investigation of the role of remote ice sheets has been given in Stocchi and Spada (in press) by an analysis and an interpretation of the shape of relative sea-level curves.

Here, two different sets of relative sea-level predictions for the Mediterranean are provided, based on two distinct approaches. The first set, labelled by "L" in Table 1, is based on the recent study of Lambeck et al. (2004a), while the second set, reported in column "I" of Table 1, has been obtained by independent solutions of the Sea-Level Equation by an open-source program (SELEN, a Sea-Level Equation solver) recently published by Spada and Stocchi (2007), which can provide predictions of various geophysical quantities related with glacial isostasy. The prediction of Spada and Stocchi assumes an *a-priori* ice sheet chronology (in this case model ICE5G of Peltier, 2004) instead of deriving the surface load distribution by an iterative trial-and-error comparison with global relative sea-level observations. The second set of solutions is based on further simplifying assumptions, i.e., mantle incompressibility, and fixed shorelines approximation. All the computations by Stocchi and Spada and Lambeck, have assumed viscosity values of 10, and 0.3×10^{21} Pa.s in the lower and upper mantle, respectively, a spatial resolution corresponding to a maximum harmonic degree of 96, and PREM-averaged values of density and shear moduli. The solution method has been recently described by Spada and Stocchi (2006, 2007), to which the reader is referred for further details.

Columns "I" and "L" of Table 1 show predictions of relative sea level at the ages "G" according to the glacio-isostatic models SS (Spada and Stocchi, 2007) and KL (Lambeck et al., 2004a), whose basic features and differences have been discussed above. The two sets of predictions are compared in Fig. 8. Frame (a), in which predictions for individual stations are shown, qualitatively demonstrates the overall agreement between the two sets of predictions. These are somewhat more clearly represented in the bottom frame (b), where each point corresponds to the epoch when an RSL observation is available (see entry "G" in Table 1). Despite differences between the two isostatic models, their predictions qualitatively agree both in sign and in amplitude on the whole range of RSL variations considered here. We observe that the fit visually improves for relatively small RSL variations, in the range approximately between −10 and 0 m. These RSL values, which correspond to relatively short ages BP subsequent to the end of melting of the largest ice sheets, are mostly controlled by mantle viscosity, which is the same in the two sets of calculations. During the melting phase, when RSL amounts generally exceeds ~10 m, differences in the deglaciation chronologies of ICE5 G and the ice model of Lambeck et al. (2004a) are responsible for larger discrepancies between the two sets of predictions. It is apparent that calculations based on model SS are found systematically below the KL values, which can be explained by the larger equivalent sea level that the latter exhibits in comparison to ICE5G during the time span considered in this study. As a final remark, we observe that because the two ice chronologies considered here differ in their northern Europe components, we expect that predictions for the

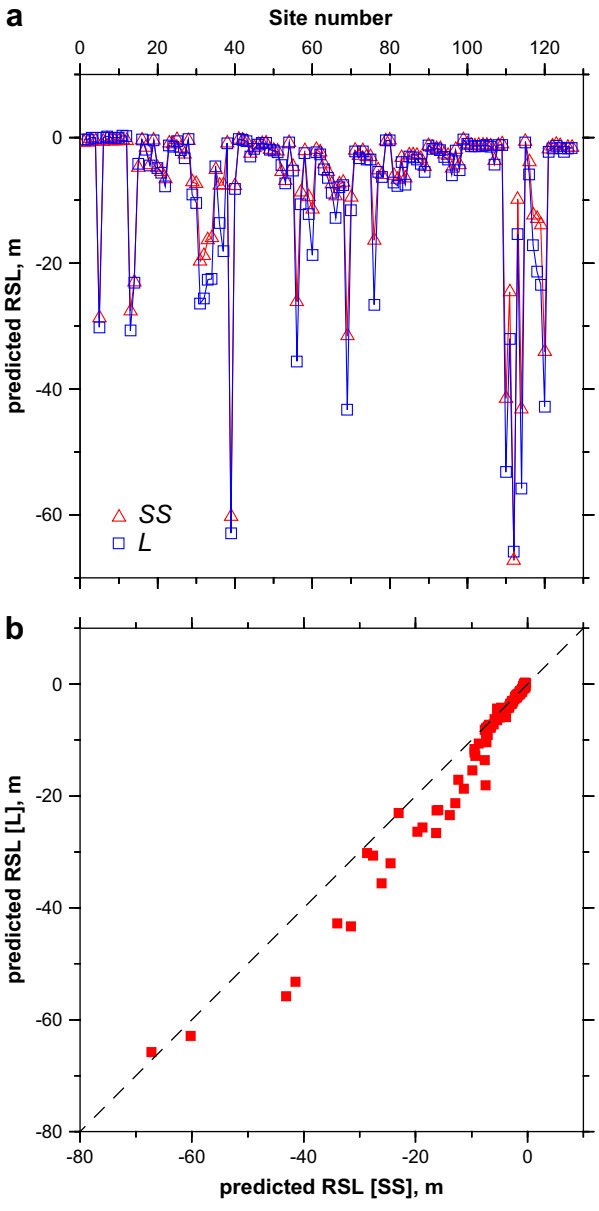

Fig. 8. Comparison between RSL predictions based on the isostatic models SS of Spada and Stocchi (2007) and KL of Lambeck et al. (2004a). Numerical values of RSL are obtained by Table 1 (entries I and L, respectively).

Author's personal copy

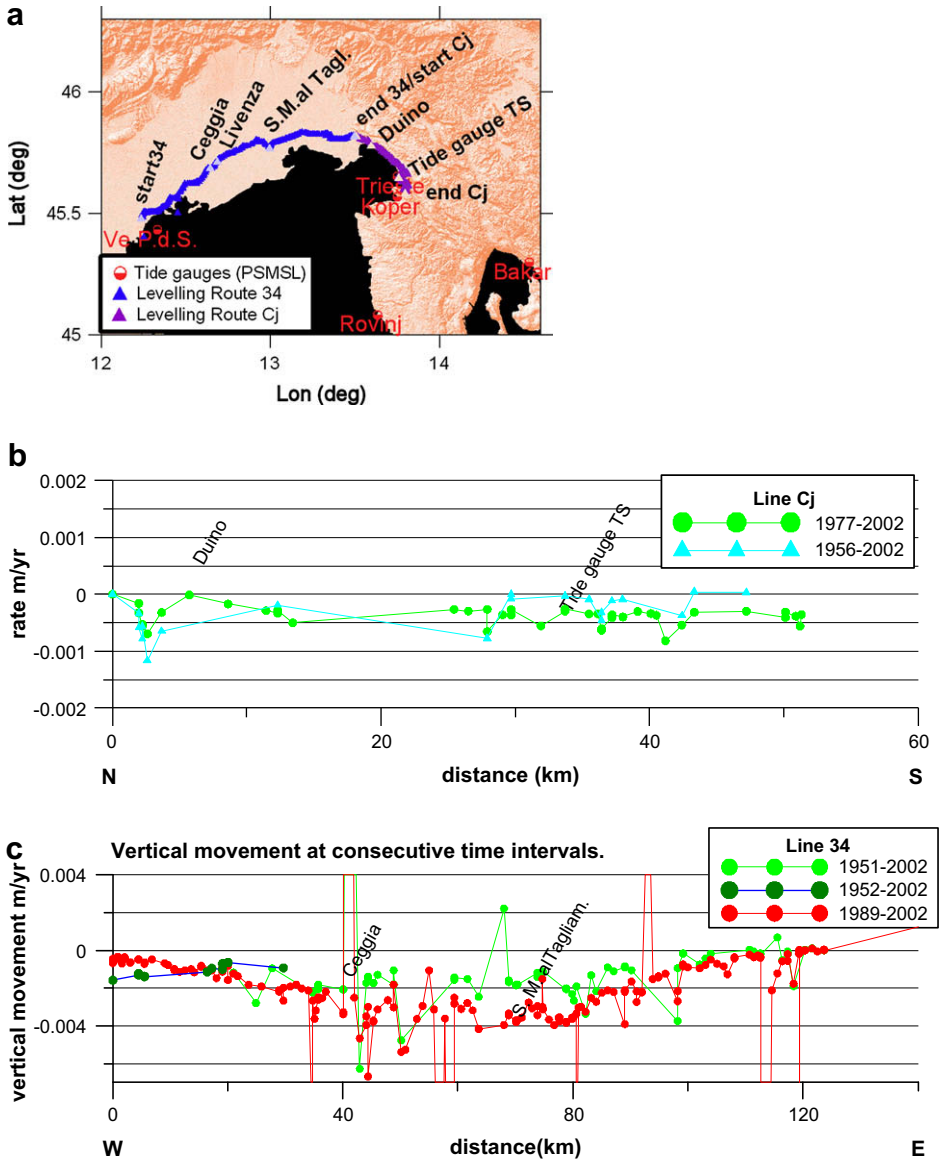

Fig. 9a. Map showing the IGM sites, b Vertical subsidence rates along the IGM levelling route Cj, and c Vertical subsidence rates along the IGM levelling route 34.

relatively nearby northern Italy may differ also for direct effect of ice unloading.

6. Instrumental rates

The values determined for the northern Adriatic have been derived from the relative sea-level variations observed with tide gauges and with the evaluation of repeated precision levelling measurements. The two data series considered, the tide gauges and the repeated levelling measurements, have one great advantage with respect to continuous GPS measurements and the satellite altimetric observations, the relatively great time span available. For the northern Adriatic, repeated levelling campaigns cover a time interval of over 50 years of measurements, and the tide gauges in two stations (Venice and Trieste) an interval of over 100 years. In contrast, the high precision satellite altimetric observations (e.g. Topex/Poseidon and Jason 1) are available since 1992, covering thus 15 years (e.g. Fu and Cazenave, 2001).

The repeated levelling routes have been measured by the I.G.M. (Istituto Geografico Militare). Details on the measuring methods and measuring accuracies are found in Muller (1986). Routes running along the northern Adriatic, from Mestre (mainland of Venice) eastwards towards Trieste (route 34 – Mestre-Ronchi dei Legionari and route Cj – Ronchi dei Legionari-Albaro Vescovà) and along the coast southwards up to the Italian–Slovenian border (see Figs. 4, 6 and 9a) were considered. The two routes have been measured four times in the last half-century (route 34 in 1951/1952, 1968 (only a short segment of the route), 1989 and 2002; route Cj in 1956, 1977, 1989 and 2002).

Calculation of the vertical movement rates along the levelling route was relative to one particular benchmark for both routes, the first benchmark along route Cj, which is measured also for route 34. Fig. 9b and c shows the vertical rates along the two routes, calculated using the two longest available time intervals (Route Cj: 1956–2002 and 1977–2002; Route 34: 1952–2002 and 1968–2002). In principle, the longest time interval would be sufficient, but due to the fact that several of the benchmarks measured in the 1950s were not available in 2002, the next-long time interval is also considered. Route Cj includes one benchmark, which is very near to the Trieste tide gauge stations discussed later in the paper. The vertical rates along the route Cj (Fig. 9b) are relatively small, near zero or slightly negative and do not exceed −1 mm/a. The vertical

Author's personal copy

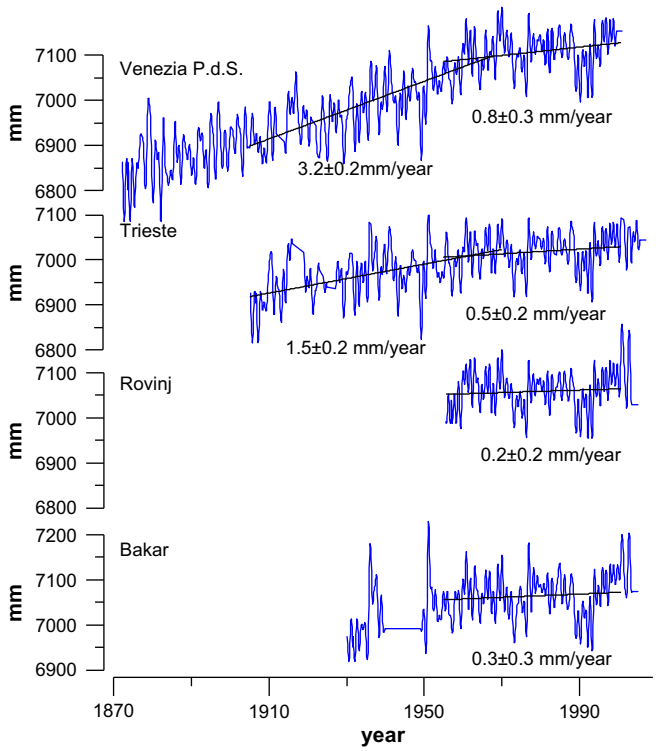

Fig. 10. Differential sea-level rise for a selection of tide gauge station in the northern Adriatic.

rates observed along the east-west trending levelling route 34 ranging from Mestre eastwards for 120 km are shown in Fig. 9c. The vertical rates have been calculated relative to the easternmost benchmark, which connects this route to the southward trending route Cj. The rates shown were calculated for the two longest available time intervals (1989–2002 and 1951/1952–2002). The rates are consistently negative and reach a *plateau* value of −4 mm/a. The area between Ceggia (km 47 of the route) and S. Michele al Tagliamento (km 82 of the route) have the greatest subsidence. The localised peak with number CS52 is a benchmark on a bridge, over the Livenza River.

Another way to obtain relative movement rates is by analysing the differential rates of sea-level change observed with tide gauges. For the Northern Adriatic the PSMSL (Permanent Service for Mean Sea level, PSMSL 2008) stations can be used, which comprise Venice, Trieste, Rovinj, and Bakar. Several other stations can be found in the database, but due to the shortness of the time series the latter are not included in this study.

The two longest series, covering the time span of over 100 years, are Trieste (PSMSL code 280061) and Venice (PSMSL codes 270051 and 270054). The two stations Rovinj (PSMSL code 280006) and Bakar (PSMSL code 280011) are available over a time window of over 50 years. The time span common to all four records extends from 1955 to 2006. As seen in Fig. 10, the years 2000–2002 in the case of Bakar and Rovinj are characterised by two large-amplitude yearly signals, which perturb the analysis. The analysis is therefore limited to the interval 1955–2000.6 (the time variable is given in years with decimals, indicating the fraction of the year).

The time series is modified by least squares fitting with a linear function and a yearly and half-yearly oscillation. Table 3 summarises the results: the Venice station has a greater sea-level rise (0.8 ± 0.3 mm/a) with respect to Trieste station (0.5 ± 0.3 mm/a). The latter shows a greater rate with respect to the Rovinj (0.3 ± 0.3 mm/a) and Bakar (0.2 ± 0.3 mm/a) stations.

Table 3
Rates of sea-level increase for a selection of tide gauge stations in the northern Adriatic.

Station-name and PSMSL code	Time interval	Trend (mm/yr)	Trend error (mm/yr)
Trieste – 270061	1905–2007	1.2	0.08
Trieste – 270061	1905–1970	1.5	0.16
Trieste – 270061	1955–2000.6	0.5	0.24
Rovinj – 28006	1955–2000.6	0.2	0.24
Bakar – 280011	1955–2000.6	0.3	0.26
Venezia – 270051 and 270054	1905–2001	2.5	0.09
Venezia – 270051 and 270054	1905–1970	3.2	0.16
Venezia – 270051 and 270054	1955–2000.6	0.8	0.25

The second area considered is Sicily–Calabria, in Southern Italy, with a comparative study of the available tide gauges. The data have been retrieved from the PSMSL and the APAT (Agenzia per la Protezione dell'Ambiente e per i servizi Tecnici) database (APAT, 2008). The first interval is 1897–1922, which covers the year 1908, when Sicily was struck by a destructive earthquake of $M = 7.0$ (Bottari et al., 1992) that destroyed the city of Messina.

The tide gauge records from PSMSL are available for the stations Palermo, Messina and Catania for the time interval 1897–1922 (Fig. 11). The original records with monthly sampling are shown for stations Palermo and Catania, whereas the time series of the Messina record is relative to the Palermo tide gauge. The good correlation between the Catania and the Palermo time series is evident, and the high-frequency content of the Messina signal is greatly reduced by subtracting the Palermo time series. The Messina record reveals three episodes of sea-level change, which are a slow lowering of 5 cm in the 12–18 months preceding the event, a coseismic level increase of 43.3 cm, which is recorded between the start and end of the 5 months-long interruption of the data, and a subsequent post-seismic sea-level increase with initial rate of 70 mm/a in 1909, decaying to zero values in 1922.

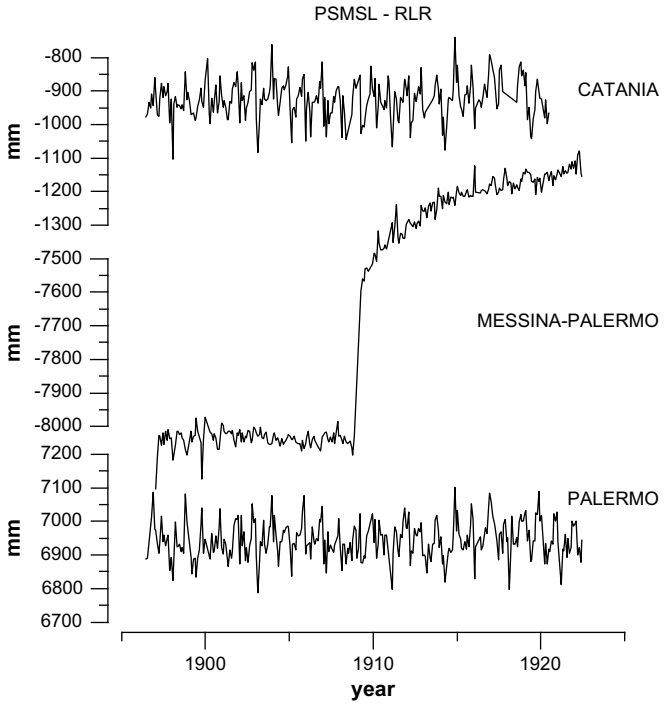

Fig. 11. Differential sea-level rise in Messina station due to the 1908 $M = 7$ seismic event respect to the stations Palermo and Catania.

Author's personal copy

For the more recent years, tide gauge records from the APAT with hourly sampling rate exist for the years 1973–1983 and 1992–2008. The most recent records (1992–2008) are affected by several interruptions, which hamper reliable analysis of the level rates.

Another station of great interest is Reggio Calabria, located on the opposite side of the Messina Straits, on the tip of the Italian peninsula. The data series for this station is available for the years 1951–1968 (PSMSL) and 1999–2008 (APAT). The station Palermo, used as a reference station in the previous analysis, is available only for the more recent interval, whereas for the older time window only the reference station Genova can be used. The recent period also includes the records of the Genova station (APAT data). The Genova and the Palermo stations are well correlated and show a sea-level increase for both time intervals. The Genova station has a differential rate with respect to the Palermo station (interval 1999–2008) of $+2.1 \pm 0.7$ mm/a, a fact taken into account for the PSMSL rates of Reggio Calabria. Presumably, the higher rate is due to a combined effect of subsidence, differences in the post-glacial isostatic movement and possible local differences in the eustatic sea-level component. The data series are shown in Fig. 12, where it can be seen that the Reggio Calabria series reveals a sea-level drop over both intervals, compared to the sea-level increase in the stations of Palermo or Genova, respectively. A summary of the rates is given in Table 4.

7. Discussion

7.1. Significance of Holocene vertical tectonic rates

Lambeck et al. (2004a) divided the Italian coastline into four broad sectors of Holocene tectonic pattern, but there was no control on the behaviour of the western Adriatic coast and on the northern terminus of the Calabrian arc (Fig. 1). Furthermore, although Sardinia was ostensibly thought stable, details were lacking, particularly in the south. This extended review allows uniform coverage of the Italian territory and thus more tightly constrains the limits of deforming blocks.

Fig. 13 compares the observed with the predicted (Lambeck model) Holocene data for the whole Holocene datasets and yields the amount of tectonic motion. Fig. 14 provides an appraisal of the spatial distribution of vertical displacement rates according to 9 classes, illustrating the areal extent of homogeneous coastline behaviour. In the following discussion we will highlight the dominant Holocene tectonic behaviour within each sector.

7.1.1. Area 1 eastern sector

The predominant "colour" of the tectonic rates in this area is blue, which is indicative of subsidence (Fig. 14) using both models as reference (mean -0.509 and -0.294 for the KL and SS model, respectively). Pleistocene marine sediments do not crop out in the whole NE coast of the Adriatic Sea, pointing to long-term tectonic subsidence. However, for the Gulf of Trieste and southern Croatia coast the position of the MIS 5.5 shoreline is still unknown, and long-term vertical tectonic rates have not been established. At all sites with archaeological markers (sites 1–8), the observed data lie below the predicted values, suggesting subsidence in the last 2 ka at -0.6–0.7 mm/a (Table 1 and Fig. 7). However, in a few cores drilled in the Gulf of Trieste (sites 13 and 14) the tectonic subsidence reaches lower values, or even weak uplift (Table 1). Very recent widespread fossiliferous marine deposits which cover a Roman age pier in Trieste (sites 11–12) crop out at the Lambeck predicted altitude, and thus show apparent stability. This area of relative stability or weak uplift might result from the active growth of an NW–SE trending structural high recently detected across the gulf of Trieste using high resolution seismic profiling (Busetti et al., 2007). On the other hand, the possibility that an undocumented tsunami could have ejected marine sediments (about 1600 BP) above the Roman age pier cannot be discounted.

7.1.2. Area 1 western sector

The northwestern Adriatic coast (Friulian and Venetian plain) shows homogeneous negative movements. Holocene rates based on core analysis (Table 1, Fig. 6) vary from -1.44 and -0.08 mm/a, with a mean of -0.64 and -0.72 mm/a using the KL and the SS model, respectively (Fig. 8). In the area of Venice the study of subsidence has a long tradition due to its key role in the preservation of the ancient city, and the available data allow comparison of the Holocene data presented in this paper with information related to long- to very short-term rates.

Analysis of well stratigraphies documents an average Quaternary subsidence rate of -0.7–1.0 mm/a (Carminati et al., 2003; Barbieri et al., 2007), whereas slighty higher values (~ 1.3 mm/a) have been inferred for the post-LGM from stratigraphic data (Bortolami et al., 1985). Relatively high values (up to ~ 1.9 mm/a) have been estimated for the last century due to human-induced sinking (Serandrei-Barbero et al., 2001; Camuffo and Sturaro, 2004; Carbognin et al., 2004). Carminati et al. (2003) and Ferranti et al. (2006) proposed that a significant part of Po Plain subsidence is related to the north-eastward retreat of the Adriatic subduction, which opposes to the regional orogenic uplift. In contrast, recent satellite measures highlight a fairly stable situation, largely related to positive rebound occurred after the stop of deep-water withdrawal in the mainland of Venice (Teatini et al., 2005).

The mean subsidence rate estimated for the last 600 ka from the VENICE-1 core record (Kent et al., 2002) is -0.36 mm/a. This value is considerably lower when compared with the Holocene and upper Pleistocene rates, the latter integrated with new data presented in this paper. The more reasonable explanation is that the mid Pleistocene rates averaged over many cycles of quiescence and rapid motion, and thus cannot be readily compared to the short-term rates, which could witness a phase of rapid tectonic subsidence and human influence. A more reliable marker for comparison is thus represented by the MIS 5.5 marker, also thanks to the wide distribution of the basal MS 5.5 unconformity and the fairly easy recognition of the overlying lagoonal\paralic sediments in cores. The MIS 5.5 data from the same VENICE-1 core provides a rate of -0.69 mm/a (Ferranti et al., 2006), a value comparable to that (-0.62 mm/a) determined when the base of the MIS 5 trangression for the Venetian Plain is integrated in the calculation (Table 2, sites 204, 205, 206).

The new information coming from cores containing MIS 5 marine deposits on the NW Adriatic coast (Friulian and eastern Venetian plain, Table 2, Fig. 6), where the average subsidence ranges between -0.69 and -0.42 mm/a, can be used to predict the depth at which marine sediments related to MIS 5 or MIS 7 highstand are expected in the well log. For this purpose, a mean value of 0.5 mm/a has been taken as the subsidence rate of a "simulated well" for the northern margin of the lagoon of Venice (Fig. 16).

Due to the low gradient of the northern Adriatic, the coastline position reached during different marine highstands strongly conditioned the landward transgression and the occurrence of paralic deposits in the stratigraphy of the analyzed cores. In the simulated well, the MIS 5.5 marine sediments reached up to $+6$ m a.s.l. and, due to the modelled 0.5 mm/a subsidence, they had already been downlifted of ~ 11 m at the peak of MIS 5.3 transgression (102.5 ka), when the sea level stood at -21 m below the present and could not flood the well position. Using the same reasoning, the marine sediment of the MIS 5.5 highstand should have reached -15 m below the present at the peak of MIS 5.1 highstand (81.5 ka). With the -19 m below present, the MIS 5.1 sea level could have partly reworked the base of MIS 5.5 paralic deposits, but it could not have affected the top of MIS 5.5 (Fig. 16).

Author's personal copy

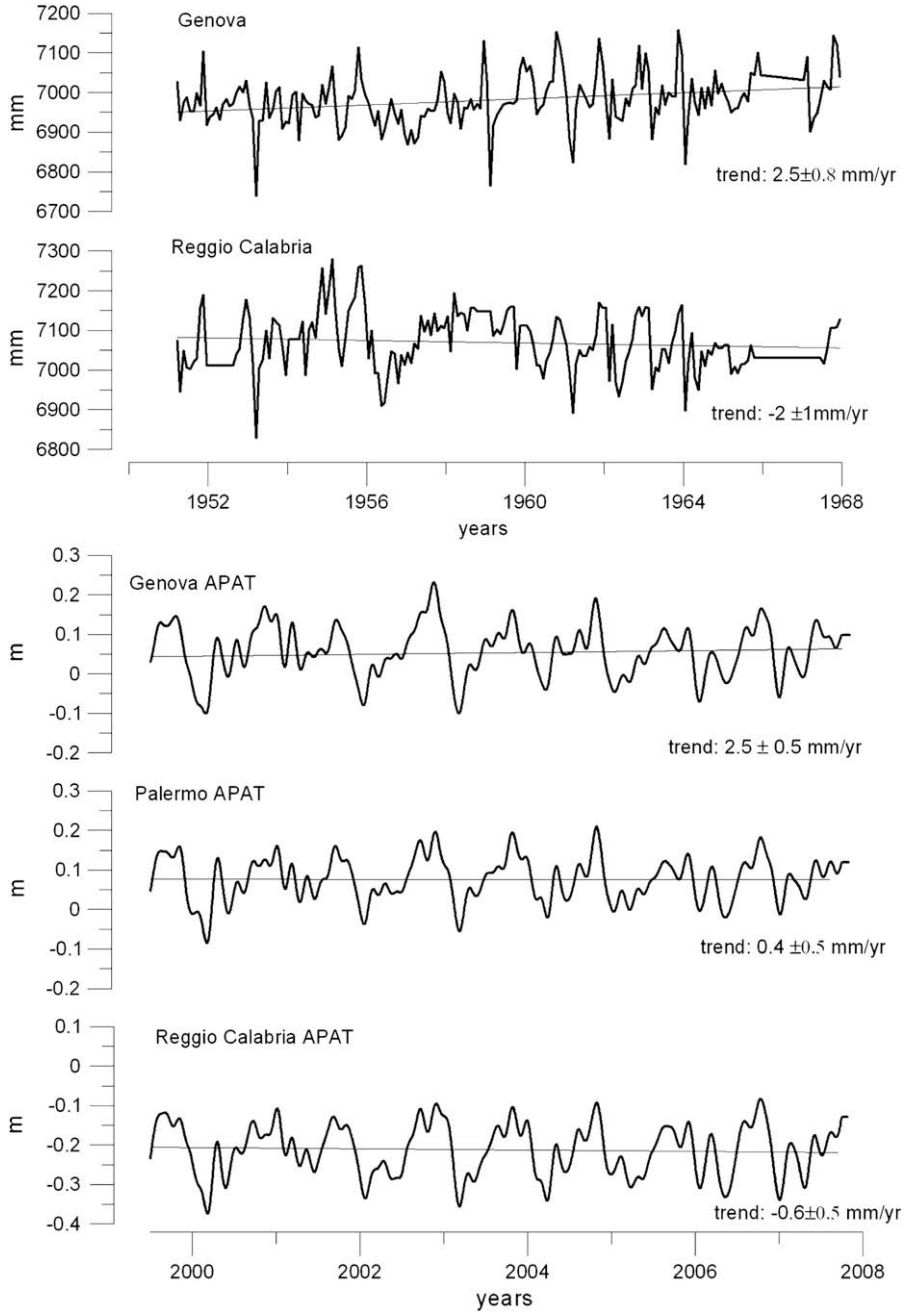

Fig. 12. Sea-level falling in Reggio Calabria station due to tectonic uplift: comparison of sea-level observations with respect to Palermo and Genova stations.

Similarly, the sediment related to sea-level position during MIS 6.5 (166 ka), MIS 7.1 (197 ka), MIS 7.3 (216.5 ka) and MIS 7.5 (230 ka) reached respectively a maximum elevation of −49 m, −10 m, −4 m and −10 m a.s.l.; with an average subsidence rate of −0.5 mm/a, these deposits had already reached a considerably higher depth than the base of the MIS 5.5 marine sediments (Fig. 16). Using this result and taking into account the bathymetry of north Adriatic Sea, younger or older transgression could not erode,

Table 4
Rates of sea-level increase for a selection of tide gauge stations in Sicily and Calabria.

Station-name and PSMSL code	Data-availability	Time interval for drift calculation	Trend (mm/yr)	Trend error (mm/yr)
Messina 260001	1897–1923	Messina earthquake	–	–
Messina APAT	1973–1983	no reference station	–	–
	1992–2008	interruptions	–	–
Palermo 260011	1896–1922	1896–1922	+0.6	0.4
Palermo APAT	1999–2008	1999–2008	+0.4	0.5
Reggio Calabria 250061	1951–1968	1951–1968	−2	1
Reggio Calabria APAT	1999–2008	1999–2008	−0.6	0.5
Genova 260011	1884–1998	1951–1968	2.5	1
Genova Apat	1999–2008	1999–2008	2.5	0.5

Author's personal copy

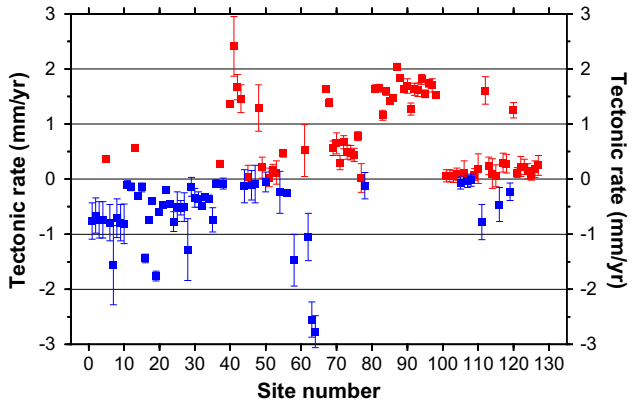

Fig. 13. Tectonic rates with error bars.

or add sediments to, the MIS 5.5 marine deposits whereas they could have partly reworked its top. Thus the thickness of Pleistocene paralic deposits encountered in the wells between 80 and 40 m represents the complete sedimentary cycle recorded during the MIS 5.5 highstand.

The higher Holocene tectonic subsidence with respect to the MIS 5.5 may be partly attributed to sediment compaction, which does not contribute to the long-term rate. East of Venice, Holocene lagoonal sediments older than 6 ka show tectonic rates lower than 0.6 mm/a, similar to the long-term subsidence after an initial compaction. Thus, −0.6 mm/a may be taken as the regional subsidence rate in this area.

7.1.3. Area 2

Two contrasting outputs for the Holocene tectonic rates result using the SS vs the KL model for the Romagna region. With the KL model, Holocene average subsidence rates (∼0.3 mm/a) are lower than the Late Pleistocene rates. In contrast, the SS model yields an average subsidence rate of ∼1 mm/a, similar to the long-term value (Fig. 5; Ferranti et al., 2006). This difference stems from the different ice-volumes included in the two models. Although the idea that Late Pleistocene and Holocene subsidence rates be similar is appealing, as suggested by the SS model result, boreholes offshore of the Po River mouth indicate stability (Fig. 1). Thus, a slowing down of subsidence as predicted by the KL model might be real.

7.1.4. Area 3

Whereas knowledge of the spatial distribution of Late Pleistocene vertical motion along the eastern Adriatic coast is still embryonic (Ferranti et al., 2006), a larger understanding of recent displacements is provided by the several Holocene markers presented in this review (Fig. 14). On average, a consistent Holocene stability (0.01 mm/a uplift) is indicated by both sets of models, and is broadly consistent with the long-term low rate of deformation of the frontal Apennines (Ferranti et al., 2006). A local departure from this trend is found in northern Gargano, with 1.7 mm/a average Holocene uplift, a pattern related to concentrated coseismic deformation (Mastronuzzi and Sansò, 2003) at a location marking the incipient boundary between two fragments of the Adriatic block (Oldow et al., 2002).

7.1.5. Area 4

In the central part of the Sibari plain, around the archaeological settlement of Sybaris, the subsidence recorded from borehole and outcrop samples is quite variable, and can be very high (Table 1). High subsidence is found using both models in three boreholes at the archaeological site (S15, S16, S18, Table 1).

The largest subsidence (∼4–8 mm/a) characterizes the older (∼6–8 ka) samples (datapoints 56, 58–59, 64–65 from cores S15, S16 and S18). The ∼5 ka samples (datapoints 62–63 from borehole S18) have a lesser, but still high subsidence rate of ∼2.5–3 mm/a. In contrast, samples of ∼2.7–3.1 ka age from boreholes S16 and S18 have relatively less subsidence rates of ∼1–1.5 mm/ar (datapoints 57 and 61 from cores S16 and S18), or even a weak uplift (datapoint 60). The very large subsidence values reflect the combination of tectonics and sediment compaction (Cucci, 2004; Pagliarulo, 2006). It appears that subsidence rates have slowed during the Holocene and attained a 1–1.5 mm/a value just before the settling of Sybaris. Sample 66, which post-dates the historical occupation, yields a negative rate of ∼0.2–0.25 mm/a (depending on the model), and confirms the slowing Late Holocene subsidence trend.

Datapoints 54–55 from borehole S1, outside the archaeological site, have a much lesser subsidence rate, pointing to a closely spaced spatial variability in deformation/compaction. Ages from this core, however, provide contrasting results when the SS (from large subsidence to weak uplift) and KL (homogeneous subsidence at ∼0.3–0.5 mm/ar) models are considered (Table 1). Using the more stable KL model for these older (∼5 and 9 ka) ages, there is an ostensible consistency with the recent most rate from the archaeological park, suggesting that compaction had ceased during historical settlment, when the regional tectonic signal at ∼0.2–0.4 mm/ar prevailed.

Although the region around the ancient town experienced long-term uplift (Cucci and Cinti, 1998; Cucci, 2004), which during Late Pleistocene varied between 0.6 and 1.9 mm/a (Santoro et al., 2009), local centres of Holocene subsidence are consistent with active synclinal fold growth and backthrusting in this part of the Southern Apennines (Ferranti et al., in press).

7.1.6. Area 5

Following the review of Antonioli et al. (2006), an update of the Holocene relative sea-level change along the north-eastern Sicily and south-western Calabria coasts (Figs. 7 and 14) is presented based on precise measures and radiometric dating of raised shorelines (Ferranti et al., 2007; unpublished). The Late Holocene uplift rate reaches maximum values of 2.4 mm/a around Taormina (Antonioli et al., 2006) and of 2 mm/a on the eastern side of the Messina Straits (Ferranti et al., 2007). The analysis indicates that vertical displacement in the Messina Straits and Taormina area resulted from the combination of steady and episodic motion, the latter attributed to coseismic slip (De Guidi et al., 2003; Ferranti et al., 2007) on normal faults, which are inferred to run immediately offshore this coast (Monaco and Tortorici, 2000). Detailed analysis on the eastern site of the Messina Straits shows a large stretch of coast (sites 81–94) with very high uplift rate values.

A lower total value of ∼1.4 mm/a Late Holocene uplift rate has been estimated for the Sicilian side of the Messina Straits, where the Ganzirri site (79) is located on the footwall of minor normal faults bounding the basin (Ferranti et al., 2008b). Further west in the Milazzo area (site 80), the large Holocene uplift rate of 1.6 mm/a probably embeds the contribution from an NNW–SSE striking transpressive belt that has caused the growth of a large contractional structure since the Middle Pleistocene (Argnani et al., 2007). Moving northeast on the Tyrrhenian coast of Calabria, new age determinations (sites 97 and 98) at Capo Vaticano (Ferranti and Antonioli, unpublished work) confirm the 1.5–1.6 mm/a uplift rate previously determined by Antonioli et al. (2006). As discussed by Antonioli et al. (2006), the Holocene rates are faster than the 125 ka rates, a fact attributed to clustered Holocene fault activity (Ferranti et al., 2007).

In south-eastern Sicily (Fig. 7), Holocene sea-level indicators are submerged because of slower rates of tectonic uplift. Data on relative sea-level change have been obtained by analysis of boreholes carried out in the most depressed coastal sectors and by

Author's personal copy

Fig. 14. The Holocene sites described in this paper with long-term geological motions calculated using the KL model.

measures of submerged archaeological markers and of speleothems collected in submerged karstic caves. The comparison of all these data with the sea-level rise curve yields a tectonic uplift rate of about 0.5–0.8 mm/a for the Catania-Siracusa coastal area (sites 71–78), whereas the southernmost sector of south-eastern Sicily (Vendicari, sites 69–70) can be considered tectonically stable. The southward decreasing Holocene uplift pattern (Fig. 14) broadly confirms the spatial trend previously evidenced in Late Pleistocene uplift (Ferranti et al., 2006). These data are consistent with a general southward decrease of both the regional uplift and the remote effect of the active normal fault system located in the Ionian offshore between Catania and Siracusa, at the bottom of the Malta Escarpment (Bianca et al., 1999; Argnani and Bonazzi, 2005).

In the Sicily Channel (Figs. 4 and 14), radiocarbon dating on samples of corals and vermetids places tight age constraints on the raised shorelines of Pantelleria Island, the emerged upper part of a large volcanic edifice developed since 300 ka (Civetta et al., 1988; Mahood and Hildreth, 1986). The modality of vertical deformation, characterised by episodic uplift events, and uplift rates up to 5 mm/a averaged over the last millennium (sites 67–68), suggests that the vertical deformation was caused by inflation processes related to magmatic intrusion along feeding fissures.

7.1.7. Area 6

Asat Pantelleria, extraordinary large Holocene vertical motions of ~5–13 mm/a are documented in the world-famous site of Pozzuoli

Author's personal copy

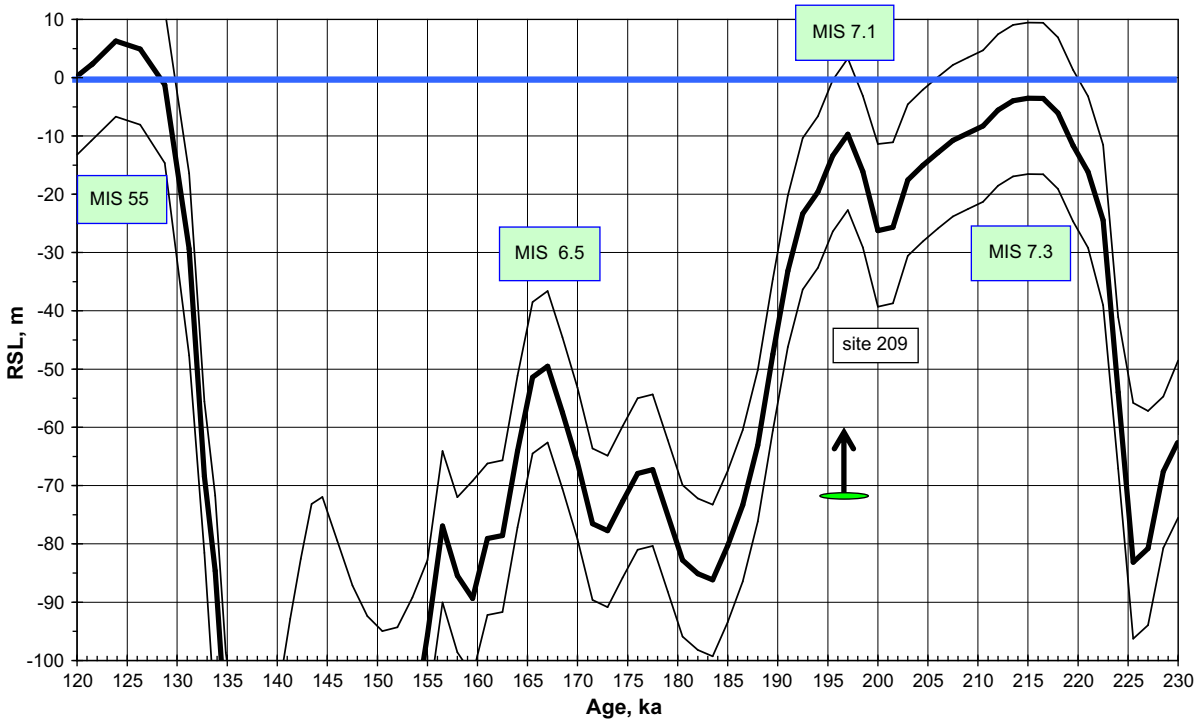

Fig. 15. Waelbroeck sea-level curve and the new U\Th TIMS age from the ENEA core.

(99–100) and are attributed to shallow volcanic sources (Morhange et al., 2006). This uplift patch is laterally confined since the adjacent Naples coastal plain has suffered long- and short-term subsidence controlled by regional tectonic and volcanic processes, with an apparent Holocene decrease in subsidence (Ferranti et al., 2006).

Further north, substantial stability (average displacement rates of 0.032 and −0.013 in the KL and SS models) is testified on the Latium and southern Tuscany coast (sites 101–109; Figs. 4 and 14) by the position of archaeological markers, like fishtanks, well connected with sea level (Lambeck et al., 2004b). Although this area suffered a weak (up to ~0.1–0.2 mm/a) Late Pleistocene uplift attributed to volcanic effects (Bordoni and Valensise, 1998; Ferranti et al., 2006), the very recent shutting of volcanic processes (Barberi et al., 1994) might be the prime factor promoting Holocene stability.

7.1.8. Area 7

The Italian Quaternarist Alessandro Blanc (1936) recovered a sediment core in the Versilia plain that included more than 50 m of Holocene marine deposits. He provided ^{14}C ages for the lagoonal shells between −5 and −50 m, which confirmed a Holocene period of deposition. That original study produced one of the first Italian sea-level rise curves, and Blanc introduced the geological name "*Versiliano*", which is still used today, to refer to the Holocene marine transgression stratotype in the Mediterranean region (Federici, 1993). More recently, Antonioli et al. (1999) provided a new core (ENEA core, 90 m long) from the Versilia plain that, through detailed analysis, confirmed the shape of the marine Holocene transgression curve with greater precision, by identifying a deposit containing the colonial coral *C. coespitosa* at the bottom of the core (between −73 and −67 m). Coral samples were dated using α-counting U-Th dating and yielded ages of 131 and 129 ka with large error bars (Antonioli et al., 1999).

The new MC-ICP-MS U-Th ages reported herein for *Cladocora* specimens from the ENEA core (sites 208–209) allow calculation of precise subsidence rates in this area. The older corals provide an age of 195.7 ± 1.6 ka (at −72.8 m); this indicates growth during the marine transgression of MIS 7.1. The MIS 7.1 transgression was also detected in a submerged stalagmite from the nearby Argentarola cave (Bard et al., 2002; Antonioli et al., 2004b). The base of the core was interpreted as an alternation between backshore and foreshore environments, with an inferred water table elevation at about −10 m.

Comparison of the 195.7 ka age with the Waelbroeck et al. (2002) sea-level curve (Fig. 15) considering, 1: the U-Th error bar, 2: the palaeo-water table −10 m, 3: the minimum highstand during MIS 7.1 of sea level of −18 m (Antonioli et al., 2004b), infers a subsidence of about 50 m over 196 ka (a low rate of about −0.25 mm/a). This is in agreement with the outcrop of MIS 5.5 inner margin adjacent to the ENEA core (Nisi et al., 2003) and with tectonic stability during Holocene marine transgression (Lambeck et al., 2004a).

Concerning Core M1 that crosses Holocene marine deposits and a pre-Holocene transgressive successions in the Arno plain, an average Holocene subsidence of −0.5/−1.5 mm/a was found using the SS and KL models, respectively (Figs. 4 and 14). Similar results are found for the other cores. The marine sediments at the core bottom have a last interglacial age, in agreement with Aguzzi et al. (2007). It is thus concluded that, unlike the nearby Versilia plain to the north, the Arno plain is a tectonically active sector.

7.1.9. Area 8

Predicted and observed Holocene sea-level data show a broad agreement on the whole coast particularly when archaeological markers for the last 2.5 ka are used (Figs. 4 and 14). Stability or weak, but detectable uplift (0.1–0.3 mm/a) is documented by several markers in southern and western Sardinia (sites 116–119 and 125–126). Some discrepancies are noted in southern Sardinia within the Cagliari core, and are probably due to sediment compaction (Orrù et al., 2004), but given the large age uncertainty from this site (datapoints 120–124), a more robust control is needed. Nevertheless, the minor vertical motion might embed a tectonic signal, as contemporary transpression is documented in southern Sardinia by GPS velocities (Ferranti et al., 2008b). The very low deformation of the MIS 5.5 marker (Ferranti et al., 2006) confirms that large cumulative displacements are unexpected.

Author's personal copy

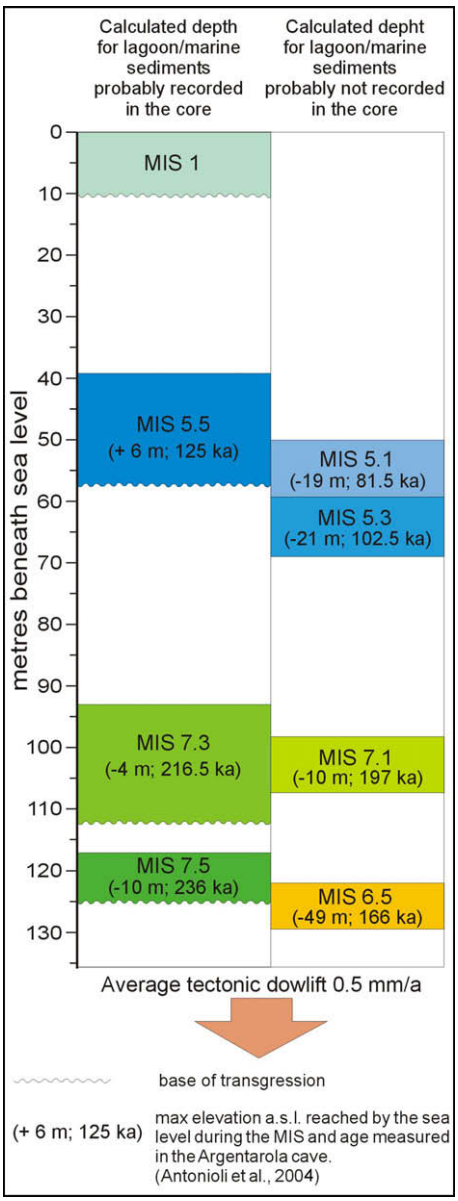

Fig. 16. The "simulated well" for the eastern sector of the Venetian Plain between Tagliamento River and the eastern margin of Venice lagoon using a tectonic rate of −0.5 mm\y.

Elsewhere in the island, the low variability of the MIS 5.5 marker altitude at 7 ± 2 m allows consideration of the Sardinian coasts as an eustatic reference for all the Mediterranean region (Lambeck et al., 2004a; Ferranti et al., 2006). In contrast, along the Orosei Gulf (eastern Sardinia) a characteristic and well-conserved tidal notch is found, whose altitude increases in height from 7.6 in the south to 11.5 m in the north within 30 km and shows an evident northward tilting, attributed to ongoing volcanic processes on the continental margin (Ferranti et al., 2006). Mariani et al. (in press) modelled this deformation as the result of recent volcanic load and overpressure linked to an offshore batholith/laccolith.

7.2. Comparison between the Kurt Lambeck and Spada–Stocchi model results

In this paper different models (Spada–Stocchi SS, Kurt Lambeck KL) were compared using the same observational data. Results indicate (Fig. 8) that the SS model predicts higher tectonic rates. For periods older than 6 ka cal. BP in some cores (e.g. Catania e Cagliari cores), the SS model enhances subsidence when the KL model shows uplift, also in areas where the long-term data confirms uplift. On the contrary, tectonic rates predicted from the SS model in the Venetian and Romagna Plains when compared with longer term data seem to be more realistic.

7.3. Significance of instrumental rates

For the NE Adriatic, the instrumental vertical crustal rates were studied using a different methodology, differentiating the vertical movement rates for couples of stations. This is applied to two different types of datasets, tide gauges and levelling. The vertical crustal rates were calculated with respect to the vertical movement of one reference station, and thus are relative rates. The difficulty in determining absolute rates is inherent to the fact that an absolute reference system is necessary, which is unavailable for the historical data. The only truly absolute vertical movement rates can be obtained with the repeated measurement of the absolute gravity field using an absolute gravimeter. For the Italian coastline such repeated measurements are unavailable, although absolute gravity stations along the coastline do exist, for example the Trieste absolute station. The GPS measured height values are near to absolute, but rely on the reference stations chosen for the GPS solution. The crustal vertical movement rates determined from the difference of the satellite altimetrically derived sea level with that observed with a tide gauge is also near to absolute but depends on the reference stations that were used to determine the precise satellite orbit.

The differential analysis of the tide gauge observations is also a means to determine vertical crustal movement rates averaged over relatively long time windows, reaching several decades. The method consists in determining the differences in the rate of sea-level rise recorded in stations that can be assumed to be subject to the same eustatic rise.

The repeated levelling shows that the area along the EW-trending Ronchi-Mestre line is subsiding with values that are consistently greater (−4 mm/a) than those found along the route Cj reaching Trieste (Fig. 10). The levelling data for the NE region of Italy indicate that anthropogenic subsidence played a significant role. Most probably it was due to extraction of water for agricultural and industrial purposes (Carminati and Martinelli, 2002). The differential analysis of the tide gauges seems to confirm the observation of a slight relative subsidence of the Trieste station obtained from levelling with respect to the reference station. The Venice tide gauge time series shows a greater rate (3.2 ± 0.2 mm/a) in sea-level rise with respect to Trieste (1.5 ± 0.2 mm/a) for the interval 1905–1970. This has been attributed (Pirazzoli, 1991; Tiezzi and Marchettini, 1997; Woodworth, 2003) to enhanced subsidence due to water extraction, which ceased in 1970. It is interesting that also the Trieste station, too distant to be affected by water withdrawal, also shows a decrease in the rate of the long-term sea-level rise at about 1970. The reason for the Trieste rate-reduction is unknown, and could be common also to other Mediterranean stations for which a deceleration of the rate has been observed after 1960 (e.g. Woodworth, 2003 and references therein).

The instrumental rates for Sicily–Calabria included a time interval covering the destructive Messina earthquake of 1908. The level variations observed covering the Messina event are very interesting, as they can be divided into three episodes, which presumably are connected to the earthquake: a possible pre-seismic uplift of 5 cm in the 12–18 months preceding the event, the coseismic subsidence of 43.3 cm, and a subsequent post-seismic subsidence with an initial rate of 70 mm/ar in 1909, decaying to zero values in 1922. The lack of subsequent data does not allow to estimate the full duration of the post-seismic movement, or to

Author's personal copy

determine whether in 1922 it came to an end. The total subsidence, composed of the coseismic and post-seismic movements, amounts to, at least, 77 cm. The pre-seismic uplift cannot be proven unequivocally, but the difference between the two tide gauges indicates a possible downward bending of the curve, preceding the clear coseismic signal. The signal is proposed as a working hypohesis for future works that intend to model the entire deformation, including the pre-seismic, coseismic and post-seismic phases. For the more recent times, interest is focused on the comparison of the tide gauge records of Reggio Calabria to the ones of Genova (1951–1968) and Palermo (1999–2008). Due to the shortness of the time series (17 years and 9 years, respectively), the errors on the differential rates are large, but are indicative of the fact that Reggio Calabria is presently uplifting by a rate of 1 ± 0.7 mm/a relative to the Palermo station. Comparison with the Genova station (interval 1951–1968) reveals a differential rate of 4 ± 1.3 mm/a, which corrected by the rate of Genova with respect to Palermo ($+2.1 \pm 0.7$ mm/a), leads to an estimated uplift of Reggio Calabria relative to Palermo of 1.9 ± 1.5 mm/a. The two estimates are compatible, if errors on the rate-determination are taken into account.

8. Conclusions

Using two different models for the glacio-hydro-isostatic contribution to the post-LGM relative sea-level rise, which appears to have alternating merits when different time-frames and regions are considered, it was possible to estimate the Holocene tectonic displacement rates in several sectors of the Italian coastline, and provide a refined estimation of the broad costal tectonic pattern proposed by Lambeck et al. (2004a). Using an updated appraisal of the MIS 5.5 marker elevation distribution, the Holocene estimate can be compared to indications provided by the long-term rates proposed by Ferranti et al. (2006), and, at selected locations, to contemporary rates derived from instrumental data.

It is confirmed the generalized subsidence of the northern Adriatic coast, which in the Venetian plain occurs at ~0.64–0.7 mm/a, a mean value consistent with the 0.62 mm/a subsidence rate established on the MIS 5.5 marker. In the south, along the Romagna foredeep, the mean of subsidence varies between 0.3 mm/a and 1.0 mm/a, depending on the use of either the KL or SS model, respectively.

Further south, apparent stability is found in the western Adriatic area, except for the northern Gargano, where this coast is crossed by tectonic lineaments that mark a regional geodynamic boundary (e.g. Oldow et al., 2002), and for the Murge (Puglia), where a weak subsidence at up to −0.1 mm/ar is suggested by archaeological markers.

In the southern Apennines, it was possible to investigate only a localised centre of subsidence in Sibari, on the Ionian coast of northern Calabria, where several sources including mainly sediment compaction conspire to produce a high-rate (mean 2.6–3.0 mm/a), negative motion. A refined picture of the large uplift occurring in southern Calabria and Eastern Sicily confirms earlier observations (Antonioli et al., 2006; Ferranti et al., 2007) of substantial increment (125%) of the Holocene respect to the Late Pleistocene uplift rate. An additional point from this paper is the significant Holocene uplift rate in south-eastern Sicily (Siracusa area), which illustrates in more detail the spatial extent of the regional uplift of the Calabrian arc.

A substantial stability is attained along both sides of the Tyrrhenian Sea thanks mainly to a wealth of accurate archaeological markers of Roman, Etruscan and Phoenician age (back to ~3.5 ka), supplemented by borehole data. Following the long-term trend, Sardinia is stable, but marker elevation provides a possible hint to embryonic deformations in the southern part of the island, which matches recently published geodetic evidence of deformation (Ferranti et al., 2008a)

Except for the strong, localised uplift recorded in the active volcanic area of the Phlegrean fields in Campania, stability also is attained in Latium, southern Tuscany and Liguria. Subsidence is found in northern Tuscany but different amounts are indicated by corrections drawn from the two ice-models. New precise U\Th ages in northern Tuscany clarify that tectonic displacement ceased by the MIS 5.5, a fact confirmed for the Holocene by the ENEA core. Further south in the Arno valley, contrasting results are obtained using the two ice-models, but in both cases the deep deposits indicate a subsidence in agreement with the presence of MIS 5.5 at −102 m (Table 2). In addition to the long- vs short-term comparison, instrumental data have allowed comparison, albeit at spot location, the contemporary with the Late Holocene displacement patterns. There is a full consistency in the generalized subsidence of the northern Adriatic region and in the uplift of southern Calabria, although accuracies are by far worse than those stipulated for the Holocene markers. To this end, the Holocene markers are still the more accurate tool to estimate the very recent tectonic behaviour of coastal areas in Italy.

Acknowledgments

We thank Marco Anzidei, Rita Auriemma, Emanuela Solinas and Paolo Orrù for discussion and assistance in abstracting Holocene and MIS 5.5 data. Eugenio Carminati and Steve Kershaw for a useful review. The research was partially funded by VECTOR (*VulnErability of the Italian coastal area and marine Ecosystems to Climatic changes and Their rOle in the Mediterranean caRbon cycles*), by MIUR (Ministero dell' Universita', dell'Istruzione, e della Ricerca, PRIN 2006) "Il ruolo del riaggiustamento isostatico postglaciale nelle variazioni del livello marino globale e mediterraneo: nuovi vincoli geofisici, geologici, ed archeologici", and by the Italian CARG Map project, Regione Veneto.

References

APAT, 2008. Agenzia per la Protezione dell'Ambiente e per i servizi Tecnici. http://www.apat.gov.it/.

Aguzzi, M., Amorosi, A., Castorina, F., Ricci Lucchi, M., Sarti, G., Vaiani, S.C., 2006. Stratigraphic architecture and aquifer systems in the eastern Valdarno Basin, Tuscany. GeoActa 5, 39–60.

Aguzzi, M., Amorosi, A., Colalongo, M.L., Ricci Lucchi, M., Rossi, V., Sarti, G., Vaiani, S.C., 2007. Late Quaternary climatic evolution of the Arno coastal plain (Western Tuscany, Italy) from subsurface data. Sedimentary Geology 202, 211–229.

Amorosi, A., 2008. Delineating aquifer geometry within a sequence stratigraphic framework: evidence from the Quaternary of the Po River Basin, Northern Italy. In: Amorosi, A., Haq, B.U., Sabato, L. (Eds.), Advances in Application of Sequence Stratigraphy in Italy, vol. 1. GeoActa Special Publication, pp. 1–14.

Amorosi, A., Colalongo, M.L., 2005. The linkage between alluvial and coeval nearshore marine successions: evidence from the Late Quaternary record of the Po River Plain, Italy. In: Blum, M.D., Marriott, S.B., Leclair, S.F. (Eds.), Fluvial Sedimentology VII, vol. 35. Special Publication of the International Association of Sedimentologists, pp. 257–275.

Amorosi, A., Colalongo, M.L., Fiorini, F., Fusco, F., Pasini, G., Vaiani, S.C., Sarti, G., 2004. Palaeogeographic and palaeoclimatic evolution of the Po Plain from 150-ky core records. Global and Planetary Change 40, 55–78.

Amorosi, A., Centineo, M.C., Colalongo, M.L., Fiorini, F., 2005. Millennial-scale depositional cycles from the Holocene of the Po Plain, Italy. Marine Geology 222, 7–18.

Amorosi, A., Colalongo, M.L., Dinelli, E., Lucchini, F., Vaiani, S.C., 2007. Cyclic variations in sediment provenance from late Pleistocene deposits of the eastern Po Plain, Italy. GSA Special Paper. In: Arribas, J., Critelli, S., Johnsson, M.J. (Eds.), Sedimentary Provenance and Petrogenesis: Perspectives from Petrography and Geochemistry, vol. 420, pp. 13–24.

Amorosi, A., Sarti, G., Rossi, V., Fontana, V., 2008a. Anatomy and sequence stratigraphy of the late Quaternary Arno valley fill (Tuscany, Italy). In: Amorosi, A., Haq, B.U., Sabato, L. (Eds.), Advances in Application of Sequence Stratigraphy in Italy, vol. 1. GeoActa Special Publication, pp. 55–66.

Amorosi, A., Dinelli, E., Rossi, V., Vaiani, S.C., Sacchetto, M., 2008b. Late Quaternary palaeoenvironmental evolution of the Adriatic coastal plain and the onset of Po River Delta. Palaeogeography, Palaeoclimatology, Palaeoecology 268, 80–90.

Author's personal copy

Amorosi, A., Fontana, A., Antonioli, F., Primon, S., Bondesan, A., 2008c. Post-LGM sedimentation and Holocene shoreline evolution in the NW Adriatic coastal area. GeoActa 7, 41–67.

Amorosi, A., Ricci Lucchi, M., Rossi, V., Sarti G., 2009. Climatic signature of millenial-scale parasequences from Lateglacial-Holocene transgressive deposits of Arno valley fill (Tuscany, Italy). Palaeogeography, Palaeoclimatology, Palaeoecology 273(1–2), 142–152.

Antonioli, F., Leoni, G., 1998. Siti Archeologici e Loro Utilizzazione Quali Indicatori per lo Studio delle Variazioni Recenti del livello del Mare. Il Quaternario, Italian Journal of Quaternary Sciences 1/98, 122–139.

Antonioli, F., Improta, S., Nisi, M.F., Puglisi, C., Verrubbi, V., 1999. Nuovi dati sulla trasgressione olocenica e la subsidenza della piana versiliese (Toscana nord-occidentale). Ferrara. In: Proceedings of the Conference "Le Pianure: Conoscenza e Salvaguardia. Il contributo delle scienze della terra", pp. 214–218.

Antonioli, F., Silenz,i, S., Frisia, S., 2001. Tyrrhenian Holocene palaeoclimate trends from spelean serpulids. Quaternary Science Reviews 20/15, 1661–1670.

Antonioli, F., Dai Pra, G., Segre, A.G., Sylos Labini, S., 2004a. New data on late Holocene uplift-rate in Calabria and Messina Straits area, Italy. Quaternaria Nova 8, 71–84.

Antonioli, F., Bard, E., Silenzi, S., Potter, E.K., Improta, S., 2004b. 215 KYR history of sea level based on submerged speleothems. Global and Planetary Change 43, 57–68.

Antonioli, F., Carulli, G.B., Furlani, S., Auriemma, R., Marocco, R., 2004c. The enigma of submerged marine notches in northern Adriatic Sea. Quaternaria VIII, 27–36.

Antonioli, F., Ferranti, L., Lambeck, K., Kershaw, S., Verrubbi, V., Dai Pra, G., 2006. Late Pleistocene to Holocene record of changing uplift rates in southern Calabria and northeastern Sicily (southern Italy, Central Mediterranean Sea). Tectonophysics 422, 23–40.

Antonioli, F., Anzidei, M., Lambeck, K., Auriemma, R., Gaddi, D., Furlani, S., Orrù, P., Solinas, E., Gaspari, A., Karinja, S., Kovačić, V., Surace, L., 2007. Sea level change during Holocene from Sardinia and northeastern Adriatic (Central Mediterranean sea) from archaeological and geomorphological data. Quaternary Science Reviews 26, 2463–2486.

Argnani, A., Bernini, M., Di Dio, G.M., Papani, G., Rogledi, S., 1997. Stratigraphic record of crustal scale tectonics in the Quaternary of the Northern Apennines (Italy). Il Quaternario, Italian Journal of Quaternary Sciences 10, 595–602.

Argnani, A., Bonazzi, C., 2005. Malta Escarpment fault zone offshore eastern Sicily: pliocene-quaternary tectonic evolution based on new multichannel seismic data. Tectonics 24, doi:10.1029/2004TC001656 TC 4009.

Argnani, A., Serpelloni, S., Bonazzi, C., 2007. Pattern of deformation around the central Aeolian Islands: evidence from multichannel seismics and GPS data. Terranova, doi:10.1111/j.1365-3121.2007.00753.x.

Auriemma, R., Mastronuzzi, G., Sansò, P., 2004. Middle to late Holocene relative sea level changes recorded on the coast of Puglia (Italy). Geomorphologie 1, 19–34.

Auriemma, R., Mastronuzzi, G., Sansò, S., Zongolo, F., 2005. The harbour of the mansio ad Speluncas (Brindisi, Italy): a key to the lecture of sea level changes in the past 3500 years? In: Marcet I Barbe, R., Brebbia, C.A., Olivella, J. (Eds.), Maritime Heritage and Modern Ports. Wessex Istitute of Technology Press, Southampton, UK, pp. 5–14.

Barberi, F., Buonasorte, G., Cioni, R., Fiordelisi, A., Foresi, L., Iaccarino, S., Laurenzi, M.A., Sbrana, A., Vernia, L., Villa, I.M., 1994. Plio-Pleistocene geological evolution of the geothermal area of Tuscany and Latium. Memorie Descrittive della Carta Geologica d'Italia 49, 77–134.

Barbieri, C., Di Giulio, A., Massari, F., Asioli, A., Bonato, M., Mancin, N., 2007. Natural subsidence of the Venice area during the last 60 Myr. Basin Research 19, 105–123.

Bard, E., Antonioli, F., Silenzi, S., 2002. Sea-level during the penultimate interglacial period based on submerged stalagmite from Argentarola Cave (Italy). Earth and Planetary Science Letters 196 (3–4), 135–146.

Beccaluva, L., Brotzu, P., Macciotta, G., Morbidelli, L., Serri, G., Traversa, G., 1989. Cainozoic tectono-magmatic evolution and inferred mantle sources in the Sardo-Tyrrhenian area. In: Boriani, A., Bonafede, M., Piccardo, G.B., Vai, G.B. (Eds.), The Lithosphere in Italy. Advances in Science Research, Accademia Nazionale dei Lincei, pp. 229–248. Rome.

Bianca, M., Monaco, C., Tortorici, L., Cernobori, L., 1999. Quaternary normal faulting in southeastern Sicily (Italy): a seismic source for the 1693 large earthquake. Geophysical Journal International 139, 370–394.

Blanc, A.C., 1936. La stratigtaphyie de la plaine costiere de la basse Versilia (italie) et la transgression flandriene en Mediterrane. In: Rev de Geograpys et geol, vol. 9. Dynam, 2 pp.

Boccaletti, M., Cello, G., Tortorici, L., 1987. Transtensional tectonics in the Sicily Channel. Journal of Structural Geology 9, 869–876.

Bonardi, G., Cavazza, W., Perrone, V., Rossi, S., 2001. Calabria–Peloritani terrane and northern ionian sea. In: Vai, G.B., Martini, I.P. (Eds.), Anatomy of an Orogen: The Apennines and Adjacent Mediterranean Basins. Kluwer Academic Publishers, Dordrecht, pp. 287–306.

Bondesan, A., Mozzi, P., Primon, S., Zamboni, C., 2002. Antiche acque e antiche genti: l'indagine geomorfologica tra passato e presente. In: Ghedini, F., Bondesan, A., Busana, M.A. (Eds.), La tenuta di Ca' Tron, pp. 15–74. Cierre, Verona.

Bondesan, A., Meneghel, M., Miola, A., Valnetini, G., 2003. Paleoenvironmental reconstruction from LGM to historical time in lower coastal plain of the Piave River. Preliminary pollen analysis on a 20 m core of lagoon and fluvial sediments. Il Quaternario 16 (1b), 183–192.

Bondesan, A., Finzi, E., Fontana, A., Francese, R., Magri, S., Mozzi, P., Primon, S., Zamboni, C., 2004. La Via Annia a Ca' Tron: nuovi contributi della geomorfologia, della geofisica e del telerilevamento. In: Busana, M.S., Ghedini, F. (Eds.), La via Annia e le sue infrastrutture, Atti delle Giornate di Studio (Ca' Tron, Roncade, 6–7 novembre 2003). Grafiche Antiga, Cornuda (TV), pp. 109–146.

Bondesan, M., Cibin, U., Colalongo, M.L., Pugliese, N., Stefani, M., Tsakiridis, E., Vaiani, S.C., Vincenzi, S., 2006. Benthic communities and sedimentary facies recording late Quaternary environmental fluctuations in a Po Delta subsurface succession (Northern Italy). In: Coccioni, R., Lirer, F., Marsili, A. (Eds.), Proceedings of the Second and Third Italian Meeting of Environmental Micropaleontology, vol. 11. The Grzybowski Foundation Special Publication, pp. 21–31.

Bordoni, P., Valensise, G., 1998. Deformation of the 125 ka marine terrace in Italy: tectonic implications. Special Publication. In: Stewart, I.S., Vita-Finzi, C. (Eds.), Coastal Tectonics, vol. 146. Geological Society, London, pp. 71–110.

Bortolami, G., Carbognin, L., Gatto, P., 1985. The Natural Subsidence in the Lagoon of Venice, Italy, vol. 151. IAHS Publication, pp. 777–784.

Bottari, A., Carveni, P., Lo Giudice, E., Nikonov, A., Rasa, R., 1992. Anomalous crustal movements prior to great earthquakes as derived from tide-gauge records; the Messina, 1908, I = XI, earthquake case history. Tectonophysics 202, 269–275.

Braitenberg, C., Nagy, I., Romeo, G., Taccetti, Q., 2005. The very broad-band data acquisition of the long-base tiltmeters of Grotta Gigante (Trieste, Italy). Journal of Geodynamics 41, 164–174.

Burollet, P.F., Mugniot, G.M., Sweeney, P., 1978. The geology of the Pelagian Block: the margins and basins of Southern Tunisia and Tripolitania. In: Nairn, A., Kanes, W., Stelhi, F.G. (Eds.), The Ocean Basins and Margins. Plenum Press, New York, pp. 331–339.

Burrus, J., 1984. Contribution to a geodynamic synthesis of the Provencal basin (north-western Mediterranean). Marine Geology 55, 247–269.

Busetti, M., Gordini, E., Baradello, L., Cova, A., Caburlotto, A., Deponte, M., Nieto, D., Tomini, I., 2007. The morphological and seismic stratigraphic characterization of the Grado and Marano lagoon (northern Adriatic). In: Convegno Nazionale "GeoItalia 2007", Rimini 12–14 sett. 2007, vol. 2. Epitome, pp. 48–50.

Caldara, M., Simone, O., 2005. Coastal changes in the eastern Tavoliere Plain (Puglia, Italy) during the Late Holocene: natural or anthropic? Quaternary Science Reviews 24, 2137–2145.

Caldara, M., Pennetta, L., Simone, O., 2002. Holocene evolution of the Salpi Lagoon (Puglia, Italy). Journal of Coastal Research SI 36, 124–133.

Camuffo, D., Sturaro, G., 2004. Use of proxy-documentary and instrumental data to assess the risk factors leading to sea flooding in Venice. Global and Planetary Change 40, 93–103.

Canali, G., Capraro, L., Donnici, S., Rizzetto, F., Serandrei-Barbero, R., Tosi, L., 2007. Vegetational and environmental changes in the eastern Venetian coastal plain (Northern Italy) over the past 80,000 years. Palaeogeography, Palaeoclimatology, Palaeoecology 253, 300–316.

Cantini, P., Testa, G., Zanchetta, G., Cavallini, R., 2001. The Plio-Pleistocene evolution of extensional tectonics in Northern Tuscany, as constrained by new gravimetric data from the Montecarlo basin (Lower Arno Valley, Italy). Tectonophisics 330, 25–43.

Carbognin, L., Teatini, P., Tosi, L., 2004. Eustacy and land subsidence in the Venice Lagoon at the beginning of the new millennium. Journal of Marine System 51 (1–4), 345–353.

Carminati, E., Giunchi, C., Argnani, A., Sabadini, R., Fernandez, M., 1999. Plio-quaternary vertical motion of the Northern Apennines: insights from dynamic modeling. Tectonics 18, 703–718.

Carminati, E., Martinelli, G., 2002. Subsidence rates in the Po plain (Northern Italy: the relative impact of Natural and Anthropogenic causation. Engineering Geology 66, 241–255.

Carminati, E., Doglioni, C., Scrocca, D., 2003. Apennines subduction-related subsidence of Venice (Italy). Geophysical Research Letters 30 (13), 1717.

Catalano, S., De Guidi, G., 2003. Late quaternary uplift of northeastern Sicily: relation with the active normal faulting deformation. Journal of Geodynamics 36, 445–467.

Chelli, A., Federici, P., Pappalardo, M., 2005. Geomorphological and archaeological evidence of Roman times shoreline in the La Spezia gulf. Geografia Fisica e Dinamica Quaternaria Supplemento VII, 97–103.

Cherchi, A., Montandert, L., 1982. Oligo-Miocene rift of Sardinia and the early history of the Western Mediterranean basin. Nature 298, 736–739.

Civetta, L., Cornette, Y., Gillot, P.Y., Orsi, G., 1988. The eruptive history of Pantelleria (Sicily Channel) in the last 50 ka. Bulletin of Volcanology 50, 47–57.

CMT Catalogue, 1976–2006. http://www.seismology.harvard.edu/CMTsearch.html.

Correggiari, A., Roveri, M., Trincardi, F., 1996. Late Pleistocene and Holocene evolution of the North Adriatic Sea. Il Quaternario, Italian Journal of Quaternary Sciences 9, 697–704.

Covelli, S., Fontolan, G., Faganeli, J., Ogrinc, N., 2006. Anthropogenic markers in the Holocene stratigraphic sequence of the Gulf of Trieste (northern Adriatic Sea). Marine Geology 230 (1–2), 29–51.

CPTI Gruppo di Lavoro, 2004. Catalogo Parametrico dei Terremoti Italiani, versione 2004 707 *(CPTI04)*. INGV, Bologna. http://emidius.mi.ingv.it/CPTI/.

Cucchi, F., Pirini Radrizzani, C., Pugliese, N., 1989. The carbonate stratigraphic sequence of the Karst of Trieste (Italy). Memorie della Società Geologica Italiana 40 (1987), 35–44.

Cucci, L., Cinti, F.R., 1998. Regional uplift and local tectonic deformation recorded by the Quaternary marine terraces on the Ionian coast of northern Calabria (southern Italy). Tectonophysics 292, 67–83.

Cucci, L., 2004. Raised marine terraces in the Northern Calabrian Arc (Southern Italy): a ~600 kyr-long geological record of regional uplift. Annals of Geophysics 47, 1391–1406.

D'Agostino, N., Selvaggi, G., 2004. Crustal motion along the Eurasia-Nubia plate boundary In the Calabrian Arc and Sicily and active extension in the Messina Straits from GPS measurements. Journal of Geophysical Research 109, B11402, doi:10.1029/2004JB002998.

Author's personal copy

Degrassi, A., 1957. I porti romani dell'Istria, vol. LVII. AMSI, pp. 24–81.
De Guidi, G., Catalano, S., Monaco, C., Tortorici, L., 2003. Morphological evidence of Holocene coseismic deformation in the Taormina region (NE Sicily). Journal of Geodynamics 36, 193–211.
de Guidi, G., Monaco, C. Late Holocene vertical deformation along the coast of Pantelleria Island (Sicily Channel, Italy). Quaternary International 206, 158–165.
Doglioni, C., 1991. A proposal of kinematic modelling for W-dipping subductions. Possible applications to the Tyrrhenian-Apennines system. Terra Nova 3, 423–434.
Doglioni, C., Mongelli, F., Pieri, P., 1994. The Puglia uplift (SE Italy): an anomaly in the foreland of the Apenninic subduction due to buckling of a thick continental lithosphere. Tectonics 13, 1309–1321.
Doglioni, C., Innocenti, F., Mariotti, G., 2001. Why Mt Etna? Terra Nova 13, 25–31.
Donnici, S., Serandrei-Barbero, R., 2004. I foraminiferi di ambiente vallivo della Laguna di Venezia. Lavori della Societa' Veneziana di Scienze Naturali 29, 101–108.
Dumas, B., Gueremy, P., Hearty, P.J., Lhenaff, R., Raffy, J., 1988. Morphometric analysis and amino acid geochronology of uplifted shorelines in a tectonic region near Reggio Calabria, South Italy. Palaeogeography, Palaeoclimatology, Palaeoecology 68, 273–289.
Enei, F., 2008. Pyrgi sommersa. Ricognizioni archeologiche subacquee nel porto dell'antica Caere. Museo Civico Archeologico S. Severa, Regione Lazio, pp. 111.
Faccenna, C., Becker, T.W., Lucente, F.P., Jolivet, L., Rossetti, F., 2001. History of subduction and back-arc extension in the Central Mediterranean. Geophysical Journal International 145, 809–820.
Faivre, S., Fouache, E., 2003. Some tectonic influences on the Croatian shoreline evolution in the last 2000 years. Zeitschrift für Geomorphologie 47 (4), 521–537.
Farrell, W.E., Clark, J.A., 1976. On postglacial sea level. Geophysical Journal of the Royal Astronomical Society 46, 647–667.
Federici, P.R., 1993. The Versilian transgression of the Versilia area (Tuscany, Italy) in the light of drillings and radiomentric data. Memorie della Società Geologica Italiana 49, 217–225.
Ferranti, L., Oldow, J.S., 2005a. Latest Miocene to Quaternary horizontal and vertical displacement rates during simultaneous contraction and extension in the Southern Apennines orogen, Italy. Terra Nova 17, 209–214.
Ferranti, L., Oldow, J.S., 2005b. Rates of late Neogene deformation along the southwestern margin of Adria, southern Apennines orogen, Italy. In: Pinter, N., Grenerczy, G., Medak, D., Stein, S., Weber, J.C. (Eds.), The Adria Microplate: GPS Geodesy, Tectonics, and Hazards. NATO Science Series IV, vol. 61. Springer, pp. 93–116.
Ferranti, L., Antonioli, F., Mauz, B., Amorosi, A., Dai Pra, G., Mastronuzzi, G., Monaco, C., Orrù, P., Pappalardo, M., Radtke, U., Renda, P., Romano, P., Sansò, P., Verrubbi, V., 2006. Markers of the last interglacial sea level highstand along the coast of Italy: tectonic implications. Quaternary International 145–146, 30–54.
Ferranti, L., Monaco, C., Antonioli, F., Maschio, L., Kershaw, S., Verrubbi, V., 2007. The contribution of regional uplift and coseismic slip to the vertical crustal motion in the Messina Straits, Southern Italy: evidence from raised Late Holocene shorelines. Journal of Geophysical Research 112, B06401, doi:10.1029/2006JB004473.
Ferranti, L., Oldow, J.S., D'Argenio, B., Catalano, R., Lewis, D., Marsella, E., Avellone, G., Maschio, L., Pappone, G., Pepe, F., Sulli, A., 2008a. Active deformation in Southern Italy, Sicily and southern Sardinia from GPS velocities of the Peri-Tyrrhenian Geodetic Array (PTGA). Bollettino della Società Geologica Italiana 127 (2), 211–223.
Ferranti, L., Monaco, C., Morelli, D., Tonielli, R., Tortorici, L., Badalini, M., 2008b. Morphostructural setting and active faults in the Messina Strait: new evidence from marine geological data. Rendiconti della Società Geologica Italiana 1, 86–88.
Ferranti, L., Mazzella, E., Monaco, C, Morelli, D., Santoro E., in press. Active transpression in the northern Calabria Apennines, southern Italy. Tectonophysics.
Feruglio, E., 1936. Sedimenti marini nel sottosuolo della bassa friulana. Bollettino della Società Geologica Italiana 55 (1), 129–138.
Finetti, I., Morelli, C., 1973. Geophysical exploration of the Mediterranean Sea. Bollettino di Geofisica Teorica e Applicata 15, 263–333.
Firth, C., Stewart, I., McGuire, W.M., Kershaw, S., Vita-Finzi, C., 1996. Coastal elevation changes in eastern Sicily: implications for volcano instability at Mount Etna. In: McGuire, W.M., Jones, A.P., Neuberg, J. (Eds.), Volcano Instability on the Earth and Other Planets, vol. 110. Geological Society, London, pp. 153–167. Special Publication.
Fontana, A., 2006. Evoluzione geomorfologica della bassa pianura friulana e sue relazioni con le dinamiche insediative antiche. In: Monografie Museo Friulano Storia Naturale, vol. 47, Udine, pp. 288 (With enclosed the Geomorphological map of the Friulian low plain, scale 1:50,000).
Fontana, A., Mozzi, P., Bondesan, A., 2008. Alluvial megafans in the Venetian-Friulian Plain(North-eastern Italy): evidence of aggrading and erosive phases during Late Pleistocene and Holocene. Quaternary International 189, 71–90.
Fontolan, G., Schiozzi, L., Colizza, E., Bezzi, A., Melis, R., Pillon, S., Lenaz, D., Marinoni, L., Fonda, G., 2007. New stratigraphic information on Upper Pleistocene in the Venice area: the CH1M core at Malamocco inlet. In: Convegno Nazionale "GeoItalia 2007", Rimini 12–14 sett. 2007, vol. 2. Epitome, 67 pp.
Fouache, E., Faivre, S., Dufaure, J.-J., Kovačić, V., Tassaux, F., 2000. New observation on the evolution of the Croatian shoreline between Poreç and Zadar over the past 2000 years. Zeitschrift fur Geomorphologie 122, 33–46.
Fu, L.-L., Cazenave, A., 2001. Satellite altimetry and earth sciences: a handbook of techniques and applications. In: International Geophysics Series, vol. 69. Academic Press, San Diego, 463 pp.
Furlani, S., Degrassi, V., Auriemma, R., Antonioli, F., Melis, R., Fonda, G., Marocco, R., 2007. Relative Sea level Changes along the Eastern Part of the Gulf of Trieste (Italy). In: Convegno Nazionale "GeoItalia 2007", Rimini 12–14 sett. 2007, vol. 2. Epitome, 59 pp.
Ghisetti, F., 1992. Fault parameters in the Messina Straits (southern Italy) and relations with the seismogenic source. Tectonophysics 210, 117–133.
Goes, S., Giardini, D., Jenny, S., Hollenstein, C., Kahle, H.G., Geiger, A., 2004. A recent tectonic reorganization in the south-central Mediterranean. Earth and Planetary Science Letters 226, 335–345.
Greco, E., Luppino, S., 1999. Ricerche sulla topografia e sull'urbanistica di Sibari-Thuri-Copiae. Annali di archeologia e storia antica 6 (nuova serie), 115–164.
Gringeri, G., Bonfiglio, L., Di Geronimo, I., Mangano, G., Antonioli, F., 2004. Uplifted Holocene littoral deposits in the Milazzo peninsula. Quaternaria Nova VIII, 141–154.
Gvirtzman, Z., Nur, A., 2001. Residual topography, lithospheric structure and sunken slabs in the central Mediterranean. Earth and Planetary Science Letters 187, 117–130.
Jacques, E., Monaco, C., Tapponnier, P., Tortorici, L., Winter, T., 2001. Faulting and earthquake triggering during the 1783 Calabria seismic sequence. Geophysical Journal International 147, 499–516.
Kent, D.V., Rio, D., Massari, F., Kukla, G., Lanci, L., 2002. Emergence of Venice during the Pleistocene. Quaternary Science Reviews 21, 1719–1727.
Lambeck, K., Antonioli, F., Purcell, A., Silenzi, S., 2004a. Sea level change along the Italian coast for the past 10,000 yrs. Quaternary Science Reviews 23, 1567–1598.
Lambeck, K., Anzidei, M., Antonioli, F., Benini, A., Esposito, E., 2004b. Sea level in Roman time in the Central Mediterranean and implications for modern sea level rise. Earth and Planetary Science Letter 224, 563–575.
Lezziero, A., 2002. Indagini paleoambientali nel sottosuolo dell'isola di Burano. In: Quaderni di Insula, vol. 10 Venezia63–70.
Mahood, G.A., Hildreth, W., 1986. Geology of the peralkaline volcano at Pantelleria, Strait of Sicily. Bulletin of Volcanology 48, 143–172.
Malinverno, A., Ryan, W.B.F., 1986. Extension in the Tyrrhenian Sea and shortening in the Apennines as a result of arc migration driven by sinking of the lithosphere. Tectonics 5, 227–245.
Mariani, M., Prato, R., 1992. I bacini neogenici costieri del margine tirrenico: approccio sismico-stratigrafico. Memorie della Società Geologica Italiana 41, 519–531.
Mariani, P., Braitenberg, C., Antonioli F., in press. Sardinia coastal uplift and volcanism. Pure and Applied Geophysics.
Martini, I.P., Sagri, M., Colella, A., 2001. Neogene–quaternary basins of the inner Apennines and Calabrian Arc. In: Vai, G.B., Martini, I.P. (Eds.), Anatomy of an Orogen: the Apennines and Adjacent Mediterranean Basin. Kluwer Academic Publishing, Dordrecht, pp. 375–400.
Massari, F., Rio, D., Serandrei Barbero, R., Asioli, A., Capraro, L., Fornaciari, E., Vergerio, P., 2004. The environment of Venice area in the past two million years. Palaeogeography, Palaeoclimatology, Palaeoecology 202, 273–308.
Mastronuzzi, G., Sansò, P., 2002a. Holocene uplift rates and historical rapid sea-level changes at the Gargano promontory, Italy. Journal of Quaternary Science 17 (5–6), 593–606.
Mastronuzzi, G., Sansò, P., 2002b. Holocene coastal dune development and environmental changes in Puglia (southern Italy). Sedimentary Geology 150, 139–152.
Mastronuzzi, G., Sansò, P. (Eds.), 2003. Quaternary coastal morphology and sea level changes. Field Guide. Puglia 2003, Final Conference – Project IGCP 437 UNESCO – IUGS, Otranto/Taranto – Puglia (Italy) 22–28 September 2003. GIS Coast – Gruppo Informale di Studi Costieri, vol. 5. Research Publication, Brizio srl, Taranto, p. 184.
Mastronuzzi, G., Quinif, Y., Sansò, P., Selleri, G., 2007. Middle-Late Pleistocene polycyclic evolution of a geologically stable coastal area (southern Puglia, Italy). Geomorphology 86, 393–408.
McCulloch, M.T., Mortimer, G., in press. Applications of the 238U-230Th decay series to dating of fossil and modern corals using MC-ICPMS. Australian Journal of Earth Sciences.
Milella, M., Pignatelli, C., Donnaloia, M., Mastronuzzi, G., 2006. Past sea-level in Egnatia (Italy) from archaeological and hydrogeological data. II Quaternario, Italian Journal of Quaternary Sciences 19 (2), 251–258.
Miyauchi, T., Dai Pra, G., Sylos Labini, S., 1994. Geochronology of Pleistocene marine terraces and regional tectonics in Tyrrhenian coast of South Calabria, Italy. II Quaternario, Italian Journal of Quaternary Sciences 7, 17–34.
Molinari, F.C., Boldrini, G., Severi, P., Dugoni, G., Rapti Caputo, D., Martinelli, G., 2007. Risorse idriche sotterranee della Provincia di Ferrara. In: Dugoni, G., Pignone, R. (Eds.), Risorse idriche sotterranee della Provincia di Ferrara, pp. 7–61.
Monaco, C., Tortorici, L., 2000. Active faulting in the Calabrian arc and eastern Sicily. Journal of Geodynamics 29, 407–424.
Monaco, C., Tortorici, L., 2007. Active faulting and related tsunami in eastern Sicily and south-western Calabria. Bollettino di Geofisica Teorica e Applicata 48 (2), 163–184.
Monaco, C., Tapponier, P., Tortorici, L., Gillot, P.Y., 1997. Late quaternary slip rates on the Acireale-Piedimonte normal faults and tectonic origin of Mt. Etna (Sicily). Earth and Planetary Science Letters 147, 125–139.
Monaco, C., Antonioli, F., De Guidi, G., Lambeck, K., Tortorici, L., Verrubbi, V., 2004. Tectonic uplift and sea-level change during the Holocene in the Catania Plain (eastern Sicily). Quaternaria Nova 8, 171–186.
Montone, P., Mariucci, M.T., Pondrelli, S., Amato, A., 2004. An improved stress map for Italy and surrounding regions (central Mediterranean). Journal of Geophysical Research 109, B10410, doi:10.1029/2003JB002703.
Morhange, C., Marriner, N., Laborel, J., Todesco, M., 2006. Rapid sea-level movements and noneruptive crustal deformations in the Phlegrean Fields caldera, Italy. Geology 34 (2), 93–96.

Author's personal copy

Mozzi, P., Bini, C., Zilocchi, L., Becattini, R., Mariotti Lippi, M., 2003. Stratigraphy, palaeopedology and palinology of Late Pleistocene and Holocene deposits in the landward sector of the Lagoon of Venice (Italy), in relation to the "caranto" level. Il Quaternario, Italian Journal of Quaternary Sciences 16 (1b), 193–210.
Muller, G., 1986. Appunti di livellazione. Istituto Geografico Militare, Firenze, 92 pp.
Muttoni, G., Carcano, C., Garzanti, E., Ghielmi, M., Piccin, A., Pini, R., Rogledi, S., Sciunnach, D., 2003. Onset of major Pleistocene glaciations in the Alps. Geology 31 (11), 989–992.
Nisi, M.F., Antonioli, F., Dai Pra, G., Leoni, G., Silenzi, S., 2003. Coastal Deformation between the Versilia and the Garigliano plains (Italy) derived from the elevations of the Last Interglacial stage. Journal of Quaternary Science 18, 709–721.
Ogorelec, B., Faganeli, J., Misic, M., Cermelj, B., 1997. Reconstruction of paleoenvironment in the Bay of Koper (Gulf of Trieste, northern Adriatic). Annales 11, 187–200.
Oldow, J.S., Ferranti, L., Lewis, D.S., Campbell, J.K., D'Argenio, B., Catalano, R., Pappone, G., Carmignani, L., Conti, P., Aiken, C.L.V., 2002. Active fragmentation of Adria, the north African promontory, central Mediterranean orogen. Geology 30, 779–782.
Ori, G.G., 1993. Continental depositional systems of the Quaternary of the Po Plain (northern Italy). Sedimentary Geology 83, 1–14.
Orrù, P.E., Antonioli, F., Lambeck, K., Verrubbi, V., Lecca, C., Pintus, C., Porcu, A., 2004. Holocene sea level change of the Cagliari. Quaternaria Nova 8, 193–212.
Pagliarulo, R., 2006. Coastal changes and the environmental evolution of the archaeological site of Sybaris (Southern Italy). Geografia Fisica e Dinamica del Quaternario 29 (1), 51–60.
Pagliarulo, R., Cotecchia, F., Coop, M.R., Cherubini, C., 1995. Studio litostratigrafico e geotecnico della Piana di Sibari con riferimento all'evoluzione morfologica e ambientale del sito archeologico. Geologia Applicata e Idrogeologia 30, 375–391.
Paladino, A., Troiano, G., 1989. Calabria Citeriore. Archeologia in provincia di Cosenza (Galasso Editore), pp. 192.
Parlagreco, I., Antonioli, F., Devoti, S., Leoni, G., Montagna, P., Screpanti, A., Silenzi, S., Verrubbi, V, in press. Depositional setting of the sedimentary sequence filling the lower trunk of the Sangro Valley (Abruzzo, Italy). GeoActa Special Publication 2.
Pascucci, V., 2005. Neogene evolution of the Viareggio Basin, Northern Tuscany (Italy). GeoActa 4, 123–138.
Peltier, W.R., 2004. Global glacial isostasy and the surface of the ice-age earth: the ICE-5G(VM2) model and GRACE. Annual Review of Earth and Planetary Sciences 32, 111–149.
Pieri, M., Groppi, G., 1981. Subsurface geological structure of the Po Plain, Italy. In: Progetto Finalizzato Geodinamica, Pubblicazione, vol. 414. C.N.R., Roma, pp. 1–23.
Pirazzoli, P.A., 1991. Possible defenses against a sea-level rise in the Venice area, Italy. Journal of Coastal Research 7, 231–248.
Pirazzoli, P.A., Mastronuzzi, G., Saliege, J.F., Sansò, P., 1997. Late Holocene emergence in Calabria, Italy. Marine Geology 141, 61–70.
Pondrelli, S., Morelli, A., Ekström, G., 2004. European–Mediterranean regional centroid moment tensor catalog: solutions for years 2001 and 2002. Physics of the Earth and Planetary Interiors 145, 127–147.
Preti, M., 1999. The Holocene transgression and the land sea interaction south of the Po Delta. Giornale di Geologia 61, 143–159.
Profumo, M.C., 2007 Archeologia della costa: la situazione marchigiana. Preatti congresso Trieste L'archeologia dei paesaggi costieri e le variazioni climatiche 8–10.11.2007. II Progetto Interreg Italia-Slovenia "AltoAdriatico", pp. 49–50.
PSMSL, 2008. Permanent Service for Mean Sea Level. Proudman Oceanographic Laboratory, Liverpool, United Kingdom. http://www.pol.ac.uk/psmsl.
RCMT Catalogue, 1997–2006. http://mednet.ingv.it/events/QRCMT/Welcome.html.
Randisi, A., 2007. Evoluzione morfotettonica tardo-quaternaria della Piana di Sibari, Calabria settentrionale. Tesi di dottorato in Scienza e Ingegneria del Mare, Università Federico II di Napoli, pp. 147.
Regione Emilia-Romagna, ENI – AGIP, 1998. Riserve idriche sotterranee della Regione Emilia-Romagna. S.EL.CA, Firenze.
Regione Lombardia, ENI Divisione AGIP, 2002. Geologia degli acquiferi Padani della Regione Lombardia. S.EL.CA, Firenze.
Rust, D., Kershaw, S., 2000. Holocene tectonic uplift patterns in northeastern Sicily: evidence from marine notches in coastal outcrops. Marine Geology 167, 105–126.
Santoro, E., Mazzella, M.E., Ferranti, L., Randisi, A., Napolitano, E., Rittner, S., Radtke, U., 2009. Raised coastal terraces along the Ionian Sea coast of northern Calabria, Italy, suggest space and time variability of tectonic uplift rates. Quaternary International 206, 78–101.
Sartori, R., Colalongo, M.L., Gabbianelli, G., Bonazzi, C., Carbone, S., Curzi, P.V., Evangelisti, D., Grasso, M., Lentini, F., Rossi, S., Selli, L., 1991. Note stratigrafiche e tettoniche sul rise di Messina (Ionio nord-occidentale). Giornale di Geologia 53, 49–64.
Scandone, R., Bellucci, F., Lirer, L., Rolandi, G., 1991. The structure of the Campanian Plain and the activity of the Neapolitan volcanoes (Italy). Journal of Volcanology and Geothermal Research 48, 1–31.
Scicchitano, G., Monaco, C., Costa, B., Di Stefano, A., Tortorici, L., 2007. Tectonic uplift and sea-level change during the Holocene in eastern Sicily by coastal plain bore-holes data. In: Epitome, FIST Geoitalia 2007, Rimini, 12–14 Settembre 2007, p. 233.
Scicchitano, G., Antonioli, F., Castagnino Berlinghieri, E.F., Dutton, A., Monaco, C., 2008. Submerged archaeological sites along the Ionian coast of south-eastern Sicily (Italy) and implications for the Holocene relative sea level change. Quaternary Research 70, 26–39.
Scrocca, D., Carminati, E., Doglioni, C., Marcantoni, D., 2007. Slab retreat and active shortening along the central-northern Apennines. In: Lacombe, O., Lavé, J., Roure, F., Vergès, J. (Eds.), Thrust Belts and Foreland Basins: From Fold Kinematics to Hydrocarbon Systems. Frontiers in Earth Sciences, pp. 471–487.
Serandrei-Barbero, R., Lezziero, A., Albani, A., Zoppi, U., 2001. Depositi Tardo-Pleistocenici ed Olocenici nel sottosuolo veneziano: paleoambienti e cronologia. II Quaternario, Italian Journal of Quaternary Sciences 14, 9–22.
Serpelloni, E., Anzidei, M., Baldi, P., Casula, G., Galvani, A., 2005. Crustal velocity and strain rate fields in Italy and surrounding regions: new results from the analysis of permanent and nonpermanent GPS networks. Geophysical Journal International 161 (3), 861–880.
Spada, G., Stocchi, P., 2006. The sea level equation. In: Aracne (Ed.), Theory and Numerical Examples, p. 96. Rome.
Spada, G., Stocchi, P., 2007. SELEN: a Fortran 90 program for solving the "sea-level equation". Computers and Geosciences 33 (4), 538–562.
Stewart, I.S., Cundy, A., Kershaw, S., Firth, C., 1997. Holocene coastal uplift in the Taormina area, northeastern Sicily: implications for the southern prolongation of the Calabrian seismogenic belt. Journal of Geodynamics 24, 37–50.
Stocchi, P., Spada, G., in press. Glacio and hydro-isostasy in the Mediterranean Sea: Clark's zones and role of remote ice sheets. Annales Geophysicae.
Teatini, P., Tosi, L., Strozzi, T., Carbognin, L., Wegmüller, U., Rizzetto, F., 2005. Mapping regional land displacements in the Venice coastland by an integrated monitoring system. Remote Sensing of Environment 98, 403–413.
Tiezzi, E., Marchettini, N., 1997. Venezia e il problema delle acque alte. II rischio di danno al patrimonio urbano a causa della crescita relativa del livello del mare. Quaderni Trimestrali Consorzio Venezia Nuova 5/2, 23–45.
Tortorici, L., Monaco, C., Tansi, C., Cocina, O., 1995. Recent and active tectonics in the Calabrian Arc (Southern Italy). Tectonophysics 243, 37–49.
Tortorici, G., Bianca, M., De Guidi, G., Monaco, C., Tortorici, L., 2003. Fault activity and marine terracing in the Capo Vaticano area (southern Calabria) during the Middle-Late Quaternary. Quaternary International 101–102, 269–278.
Tosi, L., Rizzetto, F., Bonardi, M., Donnici, S., Serandrei Barbero, R., Toffoletto, F. (Eds.), 2007. Note illustrative della Carta Geologica alla scala 1:50.000, foglio 128 Venezia. APAT – Regione Veneto, p. 164.
Vannoli, P., Basili, R., Valensise, G., 2004. New geomorphic evidence for anticlinal growth driven by blind-thrust faulting along the northern Marche coastal belt (central Italy). Journal of Seismology 8, 297–312.
Velić, I., Tišljar, J., Matičec, D., Vlahović, I., 2000. Introduzione alla geologia dell'Histria. In: 80° Riunione estiva della Società Geologica Italiana, Trieste, 6–8 settembre 2000, pp. 237–245.
Waelbroeck, C., Labeyrie, L., Michel, E., Duplessy, J.C., Lambeck, K., McManus, J.F., Balbon, E., Labracherie, M., 2002. Sea-level and deep water temperature changes derived from benthic foraminifera isotopic records. Quaternary Science Reviews 21, 295–305.
Westaway, R., 1993. Quaternary uplift of Southern Italy. Journal of Geophysical Research 98, 21741–21772.
Woodworth, C., 2003. Some comments on the long sea level records from the northern Mediterranean. Journal of Coastal Research 19, 212–217.
Wortel, M.J.R., Spakman, W., 2000. Subduction and slab detachment in the Mediterranean–Carpathian region. Science 290, 1910–1917.
Zanferrari, A., Avigliano, A., Fontana, A., Paiero, G., in press. Carta Geologica d'Italia, Foglio 086 san vito al Tagliamento, scala 1:50.000. APAT, Regione Friuli Venezia Giulia, 1 foglio, pp. 160.
Župančič, M., 1985. Koper/Cesta JLA – Renesančno mestno obzidje (Renaissance Town Wall). Arheološki Vestnik 36, 188–189.